Journal of Power Sources 377 (2018) 161–188

Contents lists available at ScienceDirect

Journal of Power Sources

journal homepage: www.elsevier.com/locate/jpowsour

Review article

Investigating the error sources of the online state of charge estimation methods for lithium-ion batteries in electric vehicles

Yuejiu Zheng[a,b,*], Minggao Ouyang[b,**], Xuebing Han[b], Languang Lu[b], Jianqiu Li[b]

[a] College of Mechanical Engineering, University of Shanghai for Science and Technology, Shanghai 200093, PR China
[b] State Key Laboratory of Automotive Safety and Energy, Tsinghua University, Beijing 100084, PR China

HIGHLIGHTS

- SOC estimation methods are reviewed with general merits and demerits.
- New perspective with focus on error analysis of SOC estimation methods is proposed.
- Using error flow charts to analyze SOC error sources from models to algorithms.
- Choosing more reliable and applicable SOC estimation methods is discussed.
- Future development of the promising online SOC estimation methods is suggested.

ARTICLE INFO

Keywords:
State of charge
Estimation error
Lithium-ion battery
Electric vehicles
Battery management system

ABSTRACT

Sate of charge (SOC) estimation is generally acknowledged as one of the most important functions in battery management system for lithium-ion batteries in new energy vehicles. Though every effort is made for various online SOC estimation methods to reliably increase the estimation accuracy as much as possible within the limited on-chip resources, little literature discusses the error sources for those SOC estimation methods. This paper firstly reviews the commonly studied SOC estimation methods from a conventional classification. A novel perspective focusing on the error analysis of the SOC estimation methods is proposed. SOC estimation methods are analyzed from the views of the measured values, models, algorithms and state parameters. Subsequently, the error flow charts are proposed to analyze the error sources from the signal measurement to the models and algorithms for the widely used online SOC estimation methods in new energy vehicles. Finally, with the consideration of the working conditions, choosing more reliable and applicable SOC estimation methods is discussed, and the future development of the promising online SOC estimation methods is suggested.

1. Introduction

With the increasing focus on the environmental protection and energy conservation, new energy vehicles (NEVs) have been extensively investigated during the past decade. Among various types of NEVs, hybrid electric vehicles (HEVs), Plug-in hybrid electric vehicles (PHEVs), battery electric vehicles (BEVs) and fuel cell electric vehicles (FCEVs) are the most popular [1,2]. They all implement the battery-motor system as the auxiliary or the main power source (HEVs, PHEVs and FCEVs) or the unique power source (BEVs) [1]. Lithium-ion batteries (LiBs) are now the most promising batteries to construct the battery-motor system owing to their favorable performances in energy density, lifespan and energy efficiency. Battery management system (BMS) is essentially required to keep LiB packs working safely and efficiently [3].

Sate of charge (SOC) estimation is generally acknowledged as one of the most important functions in BMS and is thus widely studied by academia and industry. However, a consensus has not been reached on the definition of SOC [4]. SOC is generally defined as the ratio between the available capacity and the reference capacity [3–6]. The reference capacity commonly refers to the current maximum capacity the battery can release at a constant current rate and a specific ambient temperature as the manufactory suggests. Hence, the reference capacity is almost invariant if the time scale is small and battery ageing is accordingly ignored. Unfortunately, when LiBs work in various ambient temperatures and with different current rates, we get different available

* Corresponding author. College of Mechanical Engineering, University of Shanghai for Science and Technology, Shanghai 200093, PR China.
** Corresponding author.
E-mail addresses: yuejiu.zheng@gmail.com (Y. Zheng), ouymg@tsinghua.edu.cn (M. Ouyang).

https://doi.org/10.1016/j.jpowsour.2017.11.094
Received 5 August 2017; Received in revised form 16 October 2017; Accepted 30 November 2017
0378-7753/ © 2017 Elsevier B.V. All rights reserved.

capacities [7]. If the above definition is used, SOC could be different when the current rate and the ambient temperature change.

Nevertheless, because SOC represents a charge "state", the working condition theoretically has no influence on SOC if LiBs are not charged or discharged. It means that if the battery SOC is 50% at room temperature, it should remain 50% at −10 °C. It also implies that when a LiB cannot deliver power at −10 °C, its SOC could be greater than 0. This is not weird because one may confuse the concepts between SOC and state of function (SOF, also known as state of power, SOP) which indicates the power can be released from the battery at the current situation.

We believe SOC definition having no relevance to the working conditions could be more reasonable. From the battery point of view, the main reaction at the negative electrode is

$$\mathrm{Li}_x\,\mathrm{N} \underset{\text{Charge}}{\overset{\text{Discharge}}{\rightleftarrows}} x\mathrm{Li}^+ + x\mathrm{e}^- + \mathrm{N} \tag{1}$$

where N is the active negative electrode material and x represents Li amount in the negative electrode. Similarly, the main reaction at the positive electrode is

$$y\mathrm{Li}^+ + y\mathrm{e}^- + \mathrm{P} \underset{\text{Charge}}{\overset{\text{Discharge}}{\rightleftarrows}} \mathrm{Li}_y\mathrm{P} \tag{2}$$

where P is the active positive electrode material and y represents Li amount in the positive electrode. The change of Li amount in the positive electrode is proportional to that in the negative electrode. Therefore, the Li amount in the negative electrode x can be used to measure battery SOC [8,9]. For the electrodes, the Li amount should be in the range that no Li deposition happens due a high Li amount x in the negative electrode (noted as $x_{\max}$), and also no positive electrode distortion due to a high Li amount y in the positive electrode (which means a low Li amount x in the negative electrode, noted as $x_{\min}$) [10]. The reference battery capacity can be defined as the electric charge of the electrons released from $x_{\max}$ to $x_{\min}$ in equation (1). And when the Li amount is x, SOC can then be calculated as

$$SOC = \frac{x - x_{\min}}{x_{\max} - x_{\min}} \tag{3}$$

Equation (3) also suggests that the exact SOC definition from the battery point of view has no relevance to the environment, but is directly related to the Li amount in the negative/positive electrode.

However, we are not able to measure the Li amount, neither can we exactly know the maximum and minimum Li amount. Though the Doyle-Fuller-Newman model can be used to estimate Li amount, it is usually too complicated for online applications. Fortunately, this model points out that, for the same battery system, when the LiB is discharged to the cut-off voltage at a specific condition (such as 1/3C[1] at 25 °C, and given sufficient time for a stable polarization in the LiB), the distribution of the lithium concentration on the positive and negative electrodes is almost unchanged. It means that the Li amount in the negative electrode is approximately constant when it reaches the cut-off voltage with a constant current discharge of 1/3 C at 25 °C. The Li amount can then be considered as the minimum value $x_{\min}$ allowed by the manufacturers. When the LiB is charged, the similar result happens and the Li amount reaches the maximum value $x_{\max}$. Therefore, from the engineering point of view, the rated capacity is the capacity when the Li amount increases from $x_{\min}$ to $x_{\max}$ in the negative electrode. Hence, the Li amount from x to $x_{\min}$ in the negative electrode can also represent the capacity discharged to the cut-off voltage with a constant current discharge of 1/3 C at 25 °C. Correspondingly, SOC should be defined as the ratio between the available capacity at the standard discharge and the reference capacity. The "available capacity" in the SOC definition should be defined as the capacity discharged to the cut-off voltage with a constant current discharge of 1/3 C at 25 °C rather than an "available capacity" that may vary with temperature and current.

Accurate SOC estimation in NEVs has many advantages:

(1) Parameters of the LiB modeling change with SOC. An accurate SOC can provide accurate parameters according to the SOC-parameter look-up tables, and thereby the model can better simulate the LiB.
(2) For all types of NEV battery systems, accurate SOC estimation can prevent the battery from over-charge and discharge, and therefore ensures the battery system safety, extends battery life and makes use of the limited energy more efficiently.
(3) For BEVs and PHEVs in pure electric drive mode, accurate SOC estimation can support the accurate estimation of the driving range.
(4) For BEVs and PHEVs, better charging strategy, which may improve battery life, and efficient vehicle-to-grid strategies [11] could be developed with the knowledge of the accurate SOC.
(5) For FCEVs, HEVs and PHEVs in hybrid mode, accurate SOC estimation can be used for a more reasonable vehicle energy management strategy, which improves the efficiency of other power sources.
(6) SOC estimation of the single cells is an important indicator for balancing strategies, and an accurate SOC obviously makes balancing strategies work more effectively.

SOC cannot be directly measured, but we may calculate it according to its definition. For example, SOC can be calculated according to equation (3), if the coulometric titration technique is used to determine the Li amount x in the negative electrode. Nonetheless, this method will destroy the LiB. The available capacity can also be obtained at the standard discharge and then SOC can be calculated. This method is simple and reliable, but it destroys the original SOC and neither is it practical in real applications. As a result, plenty of SOC estimation methods were invented, and they were reviewed and compared in a few references [3–6,12–18].

Zhang et al. [13] had an early review on the SOC estimation methods, where six estimation methods were discussed, including fuzzy logic (FL), artificial neural network (ANN), extended Kalman filter (EKF) and so on. Waag et al. [5] classified the respective approaches in various groups with the focus on the strengths and weaknesses for the use in online BMS applications. They suggested that approaches still had to be extended and qualified further to be able to deal with aged batteries and under real conditions. Lu et al. [3] reviewed different SOC estimation algorithms with their advantages and disadvantages. They suggested that the Ampere-hour counting (AHC) method with correction by open circuit voltage (OCV) and SOC calibration was suitable for BEVs and PHEVs. The AHC combined with the algorithm of the adaptive control theory was suggested to be the most suitable method for HEVs. Kalawoun et al. [6] presented a review of methods and models used for SOC estimation. They introduced a novel classification of the existing SOC estimation methods. They believed SOC estimator based on directly measured input variables did not take into account the sensor noises. They also indicated methods based on closed-loop processing, like the Kalman filter (KF) and controller, were promising candidates, but the main difficulty of these methods was the parameter identification. Finally, they suggested that the machine learning techniques could provide an ideal SOC model. Cuma et al. [14] reviewed SOC estimation methods for different battery systems, including NiMH, lead acid, lithium polymer and lithium-ion batteries. They categorized the estimation methods into five groups, and listed their average errors indicated in publications. Li et al. [15] compared the Luenberger observer, EKF and sigma point Kalman filter (SPKF) for SOC estimation. Barillas et al. [16] further added the sliding-mode observer (SMO) for the comparison of SOC estimation. System performances in terms of the accuracy, estimation robustness against temperature uncertainty and sensor drift were discussed. Nejad et al. [17] presented a systematic review for lumped-parameter equivalent circuit models (ECMs) for

[1] 1/X C current rate indicates X hours for a complete discharge.

$LiFePO_4$ (LFP) and $LiNi_xCo_yMn_{1-x-y}$ (NCM) cells and thereafter analyzed SOC estimation errors with dual-EKF algorithm combined with the ECMs. They concluded that Resistance-Capacitance (RC) models had an outstanding SOC estimation accuracy and the RC model with one time constant combined with a dynamic hysteresis model would enhance SOC estimation for LFP cells. Campestrini et al. [18] reviewed and compared 18 different KF family based SOC estimation methods in various working loads and found that the estimation results were quite similar with different KF family algorithms. Interesting topics have been reviewed and discussed by Li et al. [4] on SOC estimation recently. They suggested that SOC estimation by AHC method was essential, and ECMs might be more appropriate in practice than the electrochemical models at present. A recent review by Hannan et al. [12] suggested that further research on SOC estimation methods should be investigated over conventional methods under the effect of aging, hysteresis, different discharge rate and temperature. They also believed that an appropriate model is required for adaptive filter algorithms under various model uncertainties and disturbances in the system.

Every effort is made for various online SOC estimation methods to reliably increase the estimation accuracy as much as possible within the limited on-chip resources. Therefore, a comprehensive review of the error sources for those SOC estimation methods is essentially required. However, the current reviews mainly focused on the introduction of the SOC estimation methods with their advantages and disadvantages, lacking a detailed analysis of the error sources. Though many references on the SOC estimation methods gave definite SOC errors under their specific scenarios [15,16,19–36], the results are mostly achieved in the laboratories and in a relatively short time interval. Before the practical errors of their SOC estimation methods could be claimed, they should be further tested in real vehicle applications, which have much worse working condition and experience a very long period.

We try to discuss the errors sources of the SOC estimation methods considering real working conditions in electric vehicles (EVs) in this review paper. A novel perspective focusing on the error analysis of the SOC estimation methods is proposed. The error flow chart (EFC) is initiated to analyze the error sources from the signal measurement to the models and algorithms for the widely used online SOC estimation methods in EVs. We further discuss about choosing more reliable and applicable SOC estimation methods for different vehicle applications. The topic about the future development of the promising online SOC estimation methods is also included.

The remainder of the paper proceeds as follows. The commonly studied SOC estimation methods are reviewed in Chapter 2. A novel perspective for the error analysis of the SOC estimation methods is proposed and the technical routes are outlined in Chapter 3. EFCs are initiated to analyze the error sources for the current online SOC estimation methods in Chapter 4. Choosing more reliable and applicable SOC estimation methods and the future development of the promising online SOC estimation methods are discussed in Chapter 5. Ultimately, some conclusions are summarized in Chapter 6.

2. Commonly studied SOC estimation methods

In this chapter, we review the commonly studied SOC estimation methods in view of the traditional classification of these methods. It will help readers better understand the current situation of the SOC estimation methods.

2.1. OCV based estimation

The battery electromotive force (EMF) is the electrode potential difference between two electrodes when they are in the reversible equilibrium state. The theoretical value of the EMF is calculated according to the thermodynamics. While OCV is the stable electrode potential difference in the open circuit state. Therefore, OCV is theoretically smaller than EMF. Though there is perceivable difference, they are very small and therefore we usually do not distinguish between OCV and EMF.

EMF is monotonically related to the Li amount of the positive and negative electrode, and therefore we may infer that OCV is also monotonically related to SOC. And this relationship can be approximately maintained to a large extent with the cycle life or temperature changes [37], though we will find in a later chapter that the small change of SOC-OCV relationship with the cycle life or temperature has contributions on the SOC error. It is also important that the SOC-OCV curve is perfectly consistent for the same batch of LiBs, which allows us to use the experimental curves for online applications. In addition, OCV hysteresis can usually be neglected at moderate and high temperatures [5]. Hence, OCV based SOC estimation is a considerably feasible method for online applications. The only exception is LiBs with LFP or similar cathodes, which have a very flat SOC-OCV curve and a significant OCV hysteresis phenomenon [38–45]. As a result, OCV based SOC estimation in the SOC range of the flat SOC-OCV curve is not reliable when LFP cathode is used in LiBs [21].

Two measures are required for the OCV based SOC estimation: a reliable SOC-OCV curve and achieving an accurate OCV. Although, the SOC-OCV curve is relatively stable for the LiBs, it changes with the cycle life [40,46–48] and temperature [49–52]. Therefore, to have a reliable SOC-OCV relationship, we may need extensive experiments at different cycle life and temperature. While using such a reliable SOC-OCV relationship could still be a problem if the online state of health (SOH, indicating LiB lifetime) is not well estimated.

Achieving an accurate OCV is also the key issue for OCV based estimation. In order to obtain a stable electrode potential, LiBs need to rest for a sufficiently long time, which commonly depends on the temperature and SOC [4,12]. At low temperature, it may take more than 2 h to have a stable potential due to the slow diffusion [12]. Hence, OCV based estimation is only used in the particular working condition – a sufficiently long time rest, e.g. 3 h could be a suitable rest time for most working conditions, according to our experience and as well as refs [38,39]. In NEV applications, each time the NEV is activated with the BMS powered up and before the main contactor is closed, there could be a chance to determine whether the LiB packs have a sufficient rest and thereafter to achieve the OCV.

We cannot directly measure the voltage as the OCV if there is no sufficient rest time. Nonetheless, OCV can be estimated by some empirical models or combining with theoretical analysis [53–55]. However, some OCV estimation models are not well applicable to SOH or temperature change [56,57]. Waag et al. [58] established an adaptive method to estimate OCV for online applications. Nevertheless, OCV based estimation cannot be applied in dynamic working conditions. To work in dynamic working conditions, OCV identification by ECM etc. is a possible choice. In the following Section 2.4, the ECM based methods intrinsically estimate the SOC by explicitly identifying the OCV or implicitly using the SOC-OCV curves.

Direct OCV based SOC estimation has a very low computational complexity and a relatively high accuracy, but the method is restricted by the working conditions. Hence, it is ordinarily used as a calibration technology. By OCV estimation, especially OCV estimation using ECM, OCV based SOC estimation can be extended to dynamic working conditions. However, the accuracy is surely not as good as that of the direct OCV based SOC estimation.

Direct OCV based estimation is a basic SOC estimation method. Readers may refer to Section 4.1 for more discussion on the error analysis.

2.2. Ampere-hour counting estimation

AHC or ampere-hour integral estimation is directly derived from the definition of SOC, it is calculated as

$$SOC = SOC_0 - \frac{1}{C_N}\int_{t_0}^{t} \eta I \cdot d\tau \quad (4)$$

where: SOC_0 is the initial SOC at time t_0; C_N is the nominal capacity; η stands for the coulombic efficiency (CE); CE of the commercial LiBs is usually very close to 1 [59]; I is the current, negative for charge and positive for discharge here.

AHC estimation has a very low computational complexity and thus is widely used for online SOC estimation [60]. The accuracy could be acceptable by improving the AHC method, such as regular calibration of the initial SOC and capacity, and adjustment of the current sensor drift [61] and so on. However, it is generally considered that the main disadvantage of AHC estimation is still its estimation accuracy. The initial SOC, self-discharge rate, CE, errors of the current sensor and the capacity of the LiB are all the error sources for AHC estimation. AHC estimated SOC without calibration for a long time is not reliable.

Because AHC estimation is widely used and concerned, readers may refer to Section 4.2 for more discussion on the error source analysis for AHC estimation.

2.3. Impedance and internal resistance based estimation

If SOC, SOH and temperature are fixed for a LiB, the impedance is considered to be the intrinsic electric characteristic which describes the LiB voltage response under any current excitation. Online electrical impedance spectroscopy (EIS) measurement could be very difficult, because additional signal generators for various frequencies of sinusoidal alternating current may be required [62–65]. While fast Fourier transformation (FFT) analysis and other similar methods for current excitation analysis need additional computation [66,67]. Besides, high-frequency sampling and data storage are essentially required for high-frequency signal analysis, which undoubtedly increases the cost.

Even if the impedance is obtained, the relationship between the impedance and SOC is not as stable as the SOC-OCV relationship. The major problems are as follows:

(1) The impedance change is not sensitive to SOC change in some SOC range, and there could be a nonmonotonic relationship between the impedance and SOC;
(2) The impedance change is more sensitive to temperature change rather than SOC change [68–70], and the compensation of temperature influence becomes difficult as a result;
(3) The impedance changes a lot with SOH [68,71–74], and therefore, compensation of the ageing effect must be considered;
(4) According to ref. [68], the impedance may change with the current and historical working condition;
(5) Online measurement of the impedance will involve the contact impedance [75];
(6) The impedance difference between LiB cells is hard to evaluate [76].

The internal resistance based estimation can be considered as a special case of the impedance based estimation. Compared to the impedance, the internal resistance is easier to be obtained, but the demerits also include the above six issues. Besides, because the internal resistance can be considered as one value in the EIS at a fixed frequency, the first issue list above becomes more serious as the internal resistance is basically unchanged in the SOC range of 20%–90% for a lot of LiBs.

Generally speaking, the impedance and internal resistance based SOC estimation is not accurate to be used in vehicle applications.

2.4. ECM based estimation

ECM family is currently the most widely used models for online vehicle applications. ECMs mostly utilize resistances and RCs to simulate the electrical characteristics for LiBs. An ideal ECM should be able to simulate a real LiB voltage under any current excitation. While, in practice, some features of the LiBs cannot be well represented by circuit elements, such as the hysteresis effect or the Warburg effect [77]. Pure mathematical models such as the first order hysteresis [44,45] or the fractional-order model [24,78–81] are consequently used to further improve the voltage simulation accuracy.

Two technical routes are taken to estimate SOC using ECM. The first method is a straightforward one: SOC is directly estimated by ECM parameter identification [31,82–86]. The most common ECM parameter for SOC estimation is the OCV, while other ECM parameters, such as the resistances, are seldom used. The reasons have been described in Sections 2.1 and 2.3. The second method firstly uses a predetermined SOC to achieve OCV and thereafter estimates the LiB voltage by ECM. By comparing the model voltage and the measured one, a new SOC is then modified. The optimal estimation discussed in Section 2.7 is usually required for this method. The above two approaches all implement SOC-OCV relationship in the ECMs to estimate SOC. Therefore, the SOC-OCV relationship could be very important not only in OCV based estimation. The influence of the SOC-OCV relationship will further be analyzed in Section 4.1.

SOC could be estimated in dynamic working conditions without complicated calculations using ECM. If the model parameters have been determined, SOC can also be estimated in the stationary conditions such as constant current charge and discharge. However, there are two major issues need to be solved for ECM based SOC estimation. The first and also the most important problem lies in the determination of the model parameters. Experiments at different ageing and temperatures should be carried out in order to achieve model parameters. However, even the model parameters are achieved at different SOH, as the online SOH is difficult to determine, the model parameters are still hard to be exactly matched for the real applications. The use of the adaptive model may enhance the model accuracy, but it increases model complexity [87,88]. As a result, ECM should not be too complicated, or the online parameter identification will be very difficult [30,86]. Online parameter identification requires additional CPU (Central Processing Unit) load and more storage space [89], and furthermore, the online data accuracy and synchronization also need to be addressed [90]. Besides, if the current is stationary, the adaptive model cannot be used to identify the model parameters due to no current excitation, which limits its scope of applications. The second problem is also challenging: the voltage accuracy from the conventional ECMs in the low SOC range [8,34,36,91] is relatively low.

2.5. Electrochemical model based estimation

ECM can be considered as a gray box model. It cannot describe the electrochemical and physical characteristics of the LiBs, but acts as an analogy model. The electrochemical model has some partial differential equations, which are built on mass transfer, chemical dynamics and thermodynamics [92–94]. It can well simulate various electrochemical phenomena for LiBs, and is considered as a white box model [95]. However, the solutions to the partial differential equations are always too complicated for online applications. Besides, due to the large number of model parameters, many of them are from the experimental results [92,96,97], which will lead to the same issue as ECM parameters - the model parameters are needed to be matched according to SOH while SOH is difficult to be accurately estimated. Besides, there are many parameters to be identified, which may lead to a possible overfitting. Therefore, adequately reducing the estimation parameters of an electrochemical was reported in Ref. [98].

Estimating the Li amount or the average Li concentration in the positive or negative electrodes is the key in the electrochemical model based SOC estimation method [99–104]. SOC can be directly calculated according to the definition using the Li amount identification in the negative or positive electrodes from the electrochemical model

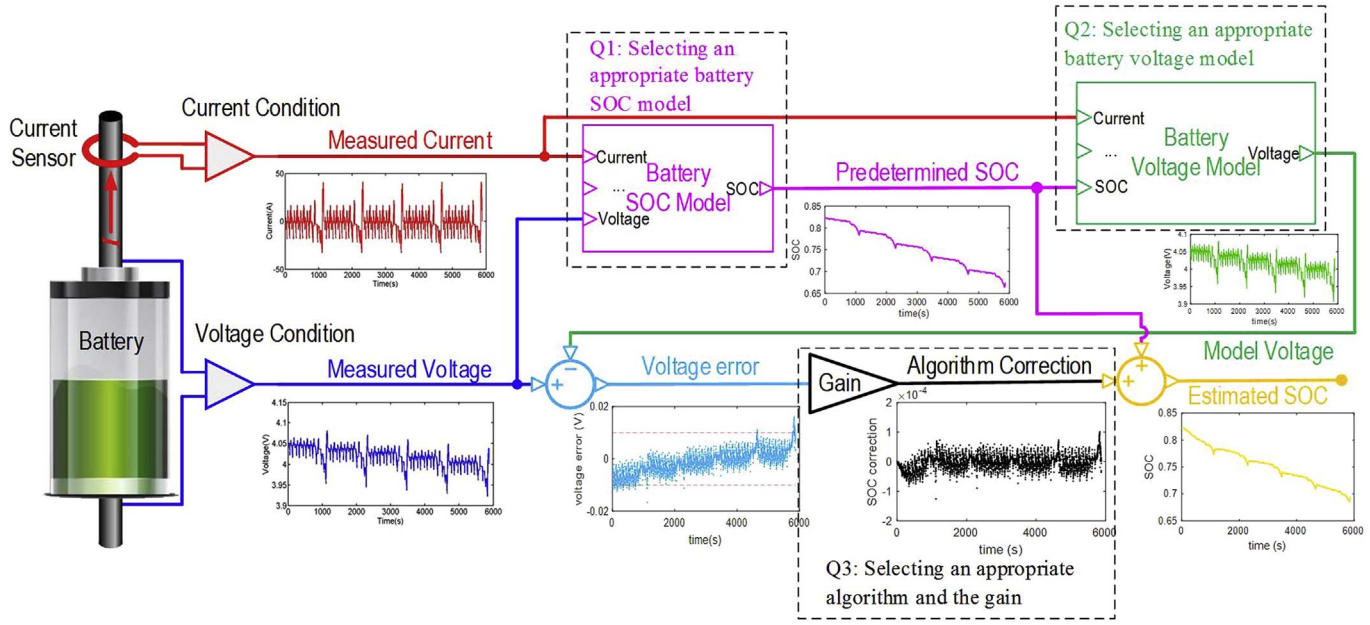

Fig. 1. Flow chart of the modern control theory based SOC estimation.

[101,103]. Another approach is similar to the ECM based method. It firstly uses a predetermined SOC to achieve the model voltage by the electrochemical model, and by comparing to the measured voltage, a new SOC is then modified [100,102,104].

While if the SOH is considered, we should further investigate the Li amount when the SOC is zero and 100%. Therefore, partial differential equations considering side reactions need to be added in the electrochemical model, which will further enhance the model complexity [105].

In general, the electrochemical model can theoretically obtain the most accurate SOC estimation from the original SOC definition. The model is suitable for off-line design and performance analysis for LiBs. However, due to the complexity of the electrochemical model and as well as the dozens of the model parameters, it is too difficult to be used for online SOC estimation.

2.6. Machine learning based estimation

Thanks to the rapid progress in computer science, battery models based on machine learning are becoming a hot topic for SOC estimation as an alternative to ECMs and electrochemical models. Battery models based on machine learning are all black-box models that can be generally described by:

$$z_t = f(r_t, \mathbf{w}) \tag{5}$$

where z_t is the model output, and r_t the model input, and $\mathbf{w}$ the model parameters to be estimated. The model output could be SOC if the battery voltage is the input, and vice versa. The input can additionally include the current, temperature, impedance etc.

Two phases are needed before the models based on machine learning are used: the construction of the training dataset phase and the learning phase [6,26,106]. Currently the training data are collected in laboratories where the environment is quite mild: the current and voltage sensors are very precise, and the temperature is usually moderate and the batteries are not aged [6,107]. Some used the simulated data [108]. SOC is required as the input or output value, and it is usually calculated using the AHC method under such mild environment. The model parameters are then estimated based on the collected data during the learning phase [109]. The optimal model parameter estimation is usually based on an estimation criterion such as minimum variance, maximum likelihood, maximum a posteriori or least squares (LS) estimation.

ANN [110,111], support vector regression (SVR) [108,112,113] and Bayesian network [100] are the typical machine learning methods for SOC estimation. One may refer to ref. [6] for more details of the ANN and SVR methods.

The key merits of the machine learning based models are their universality: the types of the batteries do not need to be concerned. However, as shown above, the models based on machine learning strongly depend on the training dataset. While the training data are mostly collected in the in a laboratory with the moderate environment in order to achieve precise SOC by the AHC method [106,114]. As a result, the training data are unable to represent the real-world working conditions when the temperature, battery ageing, sensor noises are considered [107,115].

To improve the accuracy of battery models based on machine learning under various working conditions, ideas of online learning were proposed for SOC estimation [6]. Nevertheless, online collecting the data and online training and tuning the models require enormous hardware resources from the CPU and memory, which are quite precious for vehicle applications. Besides, over-fitting and robustness need to be carefully examined. A more serious problem is the absence of a reliable SOC as a part of the training dataset. We can achieve the precise SOC by the AHC method in the experiment, while it is almost impossible for us to get a reliable online SOC qualified for the training and tuning the models.

2.7. Modern control theory based estimation

SOC could be a direct or indirect output value in ECMs, electrochemical models and battery models based on machine learning. For example, by OCV identification, SOC is indirectly estimated from ECM [31,82–86,116]; in the electrochemical model, SOC is calculated by the Li amount identification [101,103,117]; SOC can be direct output in the battery models based on machine learning [118–120]. LS [31,121], linear parameter varying (LPV) [21], and metaheuristic algorithms like genetic [122], particle swarm [123,124] optimizations and so on can be used to achieve the above parameter identification in their respective models. The LS estimation can be further extended to recursive LS in order to be implemented for online applications [31,83–86].

To improve the accuracy and decrease the noises of model based SOC estimation, modern control theory can provide another way for

SOC estimation. The idea is firstly to use a predetermined SOC as an input for the models mentioned above. The models will output the simulated voltage at the predetermined SOC. By comparing the model voltage and measured voltage, a new SOC is then modified. A flow chart of the modern control theory based estimation is shown in Fig. 1. As suggested in the flow chart, three topics are basically required to be discussed. The first one is how to estimate a predetermined SOC using the battery SOC model. The second one is which model we should choose for the battery voltage model. The third one is how to determine the gain to update the SOC.

In the first topic, the battery SOC model requires SOC as an output to be a part of the state equation. As long as the model is a different configuration from the battery voltage model, all the above models can be used as the battery SOC model. For example, battery models based on machine learning with SOC as output can also give a predetermined SOC. However, because the online real-time computation load should always be concerned and the predetermined SOC is not accurately required, AHC is used as the battery SOC model without exception. Another consideration of choosing AHC as the battery SOC model is that the difference between the measured voltage and the model voltage from the battery voltage model is commonly a high-frequency signal, choosing a low-frequency predetermined SOC by the AHC method will help to denoise the SOC estimation. Therefore, we may see that a low calculation load and a relatively stationary predetermined SOC are the two principal requirements for selecting the battery SOC model. It seems no doubt that the AHC method is a very good choice.

Using the predetermined SOC, along with other state parameters from other state equations, the model voltage is estimated by the battery voltage model. We have a number of models to choose for the battery voltage model, e.g. ECMs [19,20,32,41,86,122,125–130], electrochemical models [100,131–134] and battery models based on machine learning [22,26,109,113,135]. Considering the online calculation load, most literature selected ECMs as the battery voltage model [41,86,122,125–130].

By comparing the model voltage and measured voltage, a new SOC can be modified by using an appropriate feedback gain. While the gain is determined by the algorithm. One of the simplest algorithms is the Luenberger observer [19,104,136–138]. A better choice for a more appropriate feedback gain is the KF family algorithms [139,140]. KF can only be used in the linear models, but most LiB models have significant nonlinear characteristics. As a result, EKF could be a suitable candidate. The computational complexity of the EKF is small, and the result is relatively reliable. Therefore, EKF becomes the most widely used and studied algorithm for SOC estimation. The core idea of the EKF algorithm is determining the optimal filter gain by evaluating the model and measurement noises. While literature suggested that EKF might lack robustness and might not guarantee the optimal feedback gain due to the linearization of the nonlinear LiB systems [140–143]. Thus, SPKF [140,141] including central difference Kalman filter (CDKF) [142] and unscented Kalman filter (UKF) [29,35,51,143] is used for SOC estimation. Although the computational complexity is increased, SPKF is proved to have higher robustness and better feedback gain in optimal estimation for the nonlinear models. It should be noted that some special battery voltage models such as models including fractional-order elements, a fractional-order KF must be applied [24,78,144].

The KF family algorithms need information about the model and measurement noises. The values of these noises are usually arbitrarily set or tuned in the literature [122,128,145]. The adaptive EKF (AEKF) [146–148] can be used to estimate the model and measurement noises in order to solve the problem. Besides, model and measurement noises are supposed to be Gaussian for EKF. In fact, most noises in real applications cannot be Gaussian, and this fact always has a negative influence on the convergence behavior and accuracy of the filter.

Particle filter (PF) [132,149–153], SMO [25,80,111,154–157], Sequential Monte Carlo (SMC) [27,158] and H-infinity observer [115,159–164] do not need to know the model and measurement noises, neither do they care whether the noises are Gaussian. Accordingly, these filters and observers can theoretically further improve the quality of the feedback gain, resulting in better SOC estimation. Nevertheless, the above filters and observers have higher computational complexity.

The accuracy of the modern control theory based SOC estimation is highly related to the accuracy of the battery voltage model. Parameters of the battery voltage model change with LiB ageing and temperature. If the model parameters were not updated, the SOC estimation accuracy would decrease no matter which algorithms are used. For the KF family, considering the change of model parameters over the battery lifetime, joint or dual-KF family algorithms can be employed [33,165]. Nevertheless, taking into account the robustness of the algorithm, the model usually is constrained to be relatively simple, and the model parameters which can be updated are commonly limited to be battery capacities [166] or internal resistances. Ref. [167] demonstrated an interesting dual-KF which implemented KF and UKF for estimating RC parameters. Ref. [87] used an on-board parameter updating method which however did not rely on the joint or dual-KF method.

In conclusion of the modern control theory based SOC estimation method, using AHC method as the battery SOC model and ECM as the battery voltage model, and with the EKF algorithm for the feedback gain, the estimation method could be quite reliable at an acceptable computational complexity for online applications. Thus, it has become a widely studied and implemented SOC estimation method. Readers may refer to Section 4.3 for more discussion on the error analysis.

3. Novel classification for SOC estimation methods

Varieties of literature reviews have classified the SOC estimation methods as seen in Refs. [3–6,12–18]. We have also adopted the traditional classification to introduce these estimation methods in Chapter 2. The traditional classification is conducive to the individual investigations on the specific SOC estimation methods in detail. However, we may see that SOC estimation methods in the traditional classification have much repeatability: these methods do not have a mutually exclusive relationship but merely from a different perspective. To analyze the error sources of the SOC estimation methods, a novel perspective which adopts the step-by-step classification of the estimation methods is proposed. By the combination of the step-by-step classification, the commonly studied SOC estimation methods can be analyzed from a perspective focusing on the error sources.

As shown in Fig. 2(A), we consider that every SOC estimation methods are composed of four parts, namely, measured values, models, estimation algorithms and state parameters. Any SOC estimation method uses one or more estimation algorithms to estimate state parameters in the models with the measured values, and finally directly or indirectly obtains the SOC. The names of the SOC estimation methods in Chapter 2 are merely signs which have been placed extra emphasis on their respective measured values, models, estimation algorithms or state parameters. The following sections reintroduce the SOC estimation methods from the views of the measured values, models, estimation algorithms and state parameters, mainly focusing on the error source analysis with additionally consideration of the feasibility for online SOC estimation.

3.1. Measured values

The mainly used measured values are the current and LiB terminal voltage. Another commonly measured value in BMS is the temperature, which has great effects on model parameters, but cannot be used to directly estimate the SOC. Other measured values such as the magnetic field intensity [168], mechanical stress [169,170] or ultrasound velocity [171,172] might also be used for SOC estimation in some researches for special use. However, the feasibility is poor because

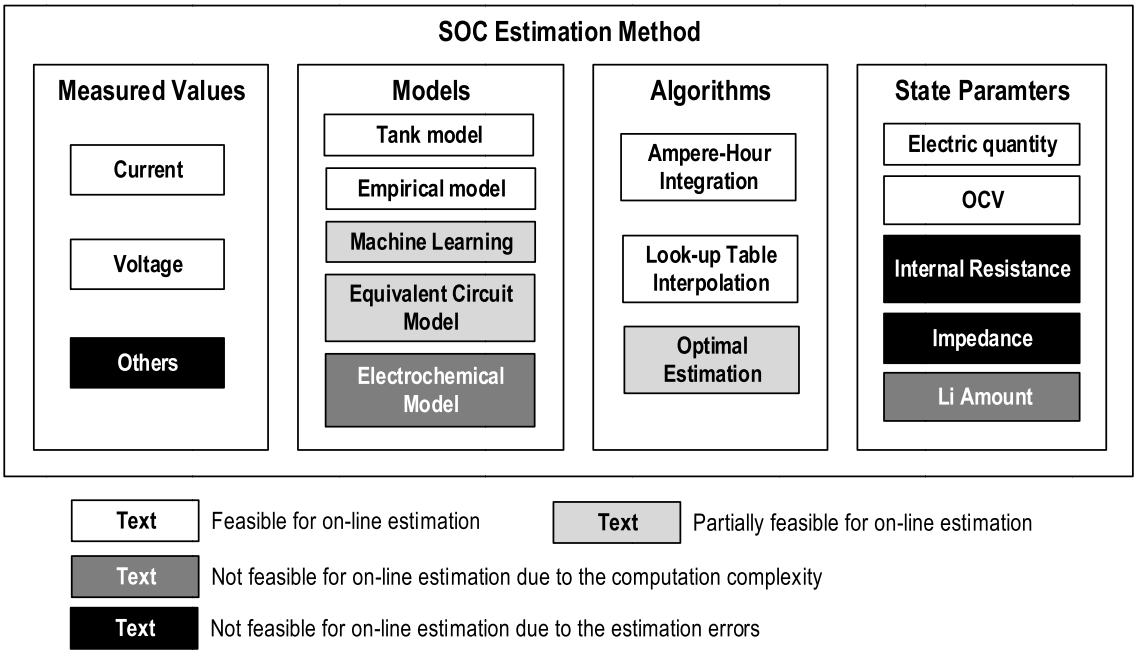

(A) Novel perspective with focus on the error analysis of the SOC estimation methods

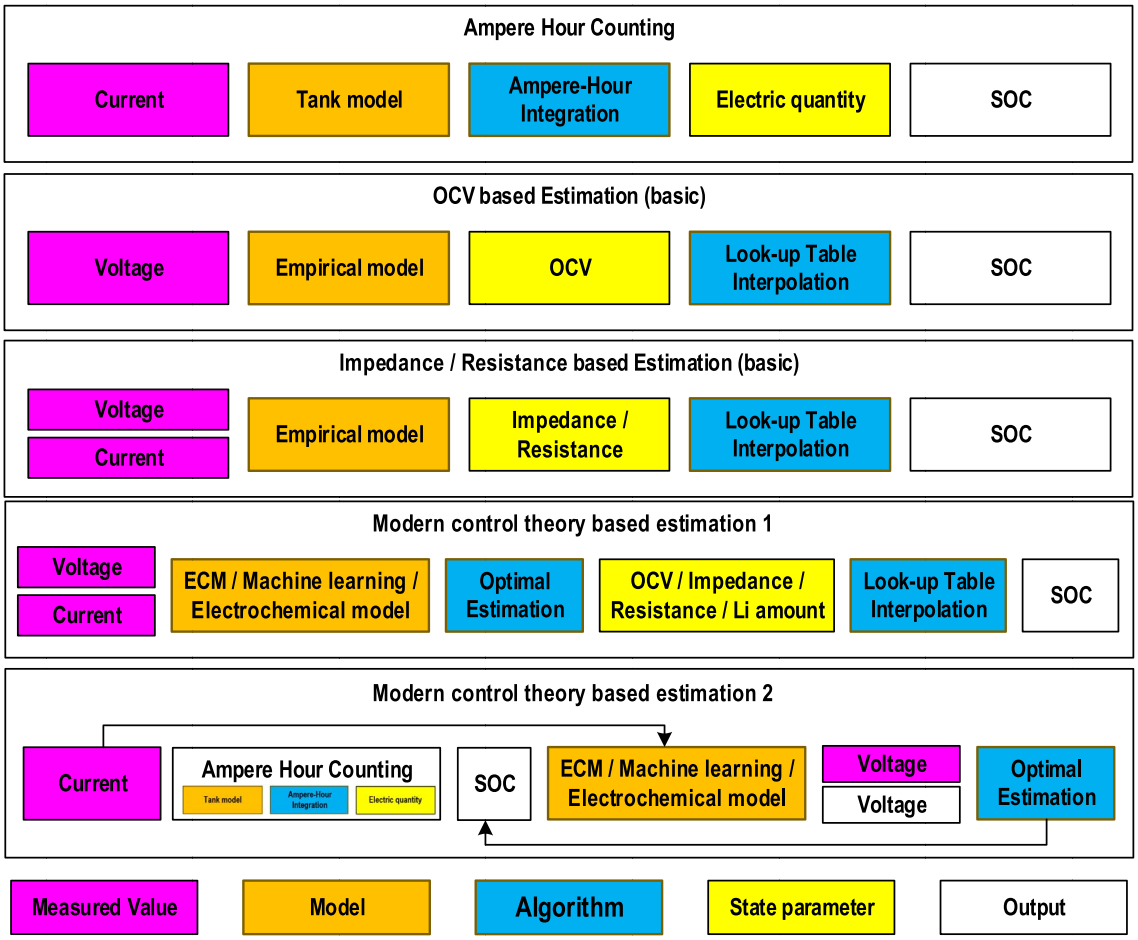

(B) Technical routes of the commonly studied SOC estimation methods

Fig. 2. Classification of the SOC estimation methods (A) Novel perspective with focus on the error analysis (B) Technical routes.

additional sensors are required. Besides, the accuracy is also in doubt. Because the current and voltage are the mainly used measured values, most SOC estimation methods can be classified into three categories: current based, voltage based and current-voltage based estimation.

Current based estimation mainly refers to the AHC method, and voltage based estimation is the OCV based estimation. Nevertheless, SOC estimation based on the current or voltage alone is usually not feasible. The voltage signal is required to offer assistance to the current-based method, i.e. in AHC estimation, the initial SOC determination usually requires the voltage signal to achieve the OCV. A more reliable method to achieve the initial SOC for BEVs is to use the full charge calibration,[2] which also use the voltage signal to determine the full charge state. The voltage based estimation must ensure that the current is zero for some time in order to obtain the OCV. The SOC estimation methods in Sections 2.1 and 2.2 are in fact named after the measured values. Exceptionally, Chun et al. [173] proposed a current sensor-less method by the high- and low-pass filters to estimate SOC. This method completely abandons the current signal, which is suitable for a redundant SOC estimation when the current sensor failure occurs, but it sacrifices the estimation accuracy. In addition, when the current signal has high frequency components, i.e. in dynamic work conditions, this method seems not applicable.

Most SOC estimation methods are current-voltage based: almost all of the battery voltage models use the current as one of the inputs and the voltage as the output. The current is used to forecast a predetermined SOC in modern control theory based estimation as shown in Fig. 1, and as the input for the battery voltage model to estimate the voltage. Subsequently, the estimated voltage is compared to the measured voltage.

The errors from the voltage and current measurement will directly affect the accuracy of all SOC estimation methods. Thus, analyzing the voltage and current measurement errors is very important to the analysis of the SOC estimation errors. Chapter 4 will further investigate the influences of the voltage and current measurement errors on SOC estimation.

3.2. Models

SOC estimation methods can be divided into five categories in view of the battery models, namely, tank model, empirical model, machine learning model, ECM and electrochemical model based estimation.

3.2.1. Tank model

The water tank model is very intuitive and easy to understand, but it is quite special. The model takes the water tank as an analogue for the battery energy storage: the size of the tank is the battery capacity; water in the tank stands for the electric quantity in the battery; the water flow in and out is the charging and discharging current; the ratio of the water and the tank is the battery SOC; and the flow meter is considered as the current sensor. The AHC estimation is intrinsically based on the tank model to calculate the SOC. Because the AHC estimation is very simple to be understood, direct calculation for SOC without involving the tank model is quite normal, though the tank model is only used in the AHC estimation.

Improvements to the tank model include reshaping the tank, so that the water height is analogous to the battery voltage [46] or adding a tap for water leakage to simulate the self-discharge of the battery. The battery capacity decline can also be analogized by gradually decreasing the tank capacity. In addition, in the dual tank model, each electrode can be considered as a tank and the Li amount is the water in the tank [46]. This model can better and more intrinsically simulate the LiB voltage, energy storage and capacity loss because LiBs are mainly composed of the positive and negative electrodes.

The tank model is tailored for the AHC estimation and is currently the most widely used SOC estimation model for online applications.

3.2.2. Empirical model

The empirical model could be a relationship between SOC and relevant state parameters, which is based on the experimental results. The most commonly used empirical model is the empirical model for SOC-OCV curve. As we indicated in Section 2.1, because the SOC-OCV curve is relatively stable, this empirical model becomes an important SOC estimation method. The relationship between the impedance/internal resistance and SOC can also be used to establish empirical models. Nevertheless, as we stated in Section 2.3, the drawbacks of these empirical models hinder their online utilization.

Investigation on other empirical models for SOC estimation has not formed a systemic method. Refs. [53–57] established the empirical model for the relationship between the OCV and the measured voltage. We [174] previously proposed the uniform charging voltage curves to estimate cell SOC and capacity which is also an empirical model.

Most empirical models have a relatively low calculation load and therefore is suitable to be applied for online SOC estimation. While the drawbacks are also obvious: some empirical models such as the OCV based model or constant charging based empirical models, cannot be used for real-time estimation due to the restriction of the working condition; others may suffer from the estimation accuracy which highly depends on the SOH, cell variation and temperature.

3.2.3. Machine learning model

Machine learning models may actually be considered as high-level empirical models, the “experience” of which is from the rules established by the machine itself and eventually forms a number of complex empirical maps. We have previously in Section 2.6 discussed the machine learning model. An online tuning machine learning model requires an accurate SOC as a reference and additionally too much hardware resources from CPU and memory, which are impossible for vehicle applications. While general machine learning models have the similar problems that the empirical models are facing. If the training data set is not comprehensive, the machine learning models may produce additional errors with the changing SOH, cell variation and temperature.

3.2.4. ECM

We have discussed the ECM based SOC estimation method in Section 2.4. The voltage accuracy and computational complexity of the ECMs are the two indicators to evaluate the ECMs. There is commonly a trade-off relationship between the indicators [175]. Hu et al. [176] collected several commonly used ECMs in the literature, including the Rint model (simple model), the first-order RC model, the first-order RC model with one-state hysteresis, the second-order RC model, the second-order RC model with one-state hysteresis and other types. They indicated that the first-order RC model with one-state hysteresis is suitable for LFP cells, and the first-order RC model is basically accurate enough for NCM cells.

Complex ECMs (such as high order models) have a significant increase in complexity and therefore is difficult to be used for online applications. Besides, in real applications, model accuracy highly depends on model parameters. A complex ECM usually has more model parameters. The possibility of the parameter mismatch can lead to poor accuracy. By abandoning the higher order ECMs, the model accuracy is still acceptable because simpler models with fewer model parameters may be better fitted. Besides, the calculation load is lowered, and therefore simpler ECM can be widely used in vehicle applications.

3.2.5. Electrochemical model

As described in Section 2.5, the electrochemical model is too complex to be solved for online applications. In addition, due to a large

[2] Full discharge calibration may also be feasible, but BEVs seldom discharge to the discharge cut off voltage.

number of the model parameters to be fitted, over-fitting may happen. Therefore, even though the theoretical accuracy is high, the electrochemical model may not be advantageous for online applications because of not only the calculation load but also a possible poor accuracy in real applications due to the poor parameter fitting.

3.3. Algorithms

Models and algorithms are often confused in the traditional classification of the SOC estimation methods. Models are actually the description for the characteristics of the concrete object, while algorithms are a set of solutions to abstract problems. Therefore, models for SOC estimation are descriptions for LiBs, but algorithms and LiBs have no relationship. Algorithms are essentially used to estimate the state parameters in the LiB models and further obtains SOC. Good algorithms can reduce the SOC estimation errors for the models, while the calculation load is not dramatically increased.

Algorithms for SOC estimation can be generally divided into three categories: ampere-hour integration, look-up table interpolation and optimal estimation algorithms. The ampere-hour integration is tailored for the tank model, and is specially used for the AHC estimation. It estimates the SOC by integrating the electric quantity. The current noise will have very little influence on the SOC errors because the effect of the integration will vanish the current noise [177]. Look-up table interpolation is mainly used for the empirical model. It has very low computational load, but the estimation accuracy almost all depends on the empirical model. Look-up table interpolation has little influence on the estimation accuracy.

The optimal estimation methods are divided into two types. When SOC is not used as a state parameter in the model, such as OCV as a state parameter in ECM, or Li concentration as in the electrochemical model, LS or the global optimization algorithms may be used to achieve the optimal estimation of the state parameters. By applying the optimal estimation, SOC estimation error caused by the model noise could be minimized.

When SOC is one of the state parameters in the model, the basic framework of the algorithm in Fig. 1 could be used. Different algorithms have different feedback gains. As introduced in Section 2.7, the algorithms could be the Luenberger observer, KF family, PF family, SMO, H-infinity observers or other nonlinear observers [134,178–180]. These algorithms essentially fuse the SOC estimated by the battery SOC model and the battery voltage model acknowledged SOC.[3] Hence, the obtained SOC is generally able to take into account the respective advantages of the battery SOC model and the battery voltage model, and these algorithms are therefore widely recognized.

3.4. State parameters

Electric quantity, OCV, impedance, internal resistance, and Li amount in the positive or negative electrode are the state parameters related to SOC estimation. Some of them are only used for the respective models, e.g. electric quantity is only used as a state parameter in the tank model and Li amount in electrochemical models. Other state parameters can correspond to a variety of models, such as OCV, internal resistance and impedance, which can be used in empirical models, machine learning models, ECMs and electrochemical models.

In the case of a known capacity, it is simple and effective to calculate the SOC by integrating the electric quantity, which is why the AHC estimation is widely used. OCV is used as the critical state parameter in the OCV based estimation. Because this state parameter is quite stable with SOC against ageing, temperature and cell variation, SOC could be well estimated by look-up table interpolation if the OCV is reliably estimated. As shown in Section 2.3, the internal resistance or the impedance is not as stable as the OCV with SOC. Hence, we do not recommend the internal resistance or the impedance as state parameters for SOC estimation, unless new methods or new LiBs types may solve the aforementioned issues. Li amount is only used in the electrochemical models, so using it as a state parameter to estimate SOC in fact means using the electrochemical model that has been discussed in the aforementioned sections.

3.5. Technical routes of the SOC estimation methods

According to the above step-by-step classification for SOC estimation methods, various types of SOC estimation methods can theoretically be combined by one or more measured values, models, algorithms and state parameters. Some of these combinations may not be practical, such as combining ECM and the Li amount. And others are still under investigation in small scale, such as a combination of the tank and machine learning models with the optimal estimation [107]. Nevertheless, the technical routes of the SOC estimation methods in Chapter 2 can be easily analyzed using the step-by-step classification as shown in Fig. 2 (B).

The current is the key measured value in the AHC estimation. Taking the tank model as the model and the ampere-hour integration as the algorithm, the electric quantity is achieved and finally SOC is obtained. The estimation errors are mainly from the current measurement and modeling of the tank model. The tank model and the ampere-hour integration are responsible for the computational complexity, which is clear to be very low.

In the basic OCV based estimation, voltage becomes the key measured value. Using the OCV empirical model to achieve OCV as the state parameter, with the look-up table interpolation as the algorithm, SOC can be achieved. The estimation errors are mainly from the voltage measurement, the OCV empirical model, and as well as the SOC-OCV look-up table interpolation. The OCV empirical model and the look-up table interpolation are responsible for the computational complexity. Therefore, the method has a low computational complexity.

The basic impedance/internal resistance based estimation is similar to the basic OCV based estimation. It uses the current and voltage as the measured values. With the impedance/internal resistance empirical model to achieve the impedance/internal resistance as the state parameter, SOC can be finally achieved with the look-up table interpolation. The SOC accuracy is influenced by the voltage and current errors and the impedance/internal resistance empirical model, and as well as the look-up table interpolation. However, due to the low reliability of the SOC- impedance/internal resistance look-up table, the error of the SOC estimation is relatively large, though the computational complexity of the basic impedance/internal resistance based estimation is low.

Modern control theory based estimation includes two technical routes. The first technical route uses the voltage and current as the measured values; ECM, machine learning or model or other models as the model; LS, genetic or other algorithms as the optimal estimation algorithm to directly calculate OCV, internal resistance, impedance or Li amount; and finally the method estimates SOC by the look-up table interpolation. The error sources of this method are principally the models and the measured values. The optimal estimation algorithms and the look-up table interpolation could also contribute additional errors. The computational complexity is mainly from the model and algorithm complexity. Especially when the global optimal solution is required, the algorithms, such as genetic algorithm, could be quite complicated and therefore cannot be used in the vehicle applications.

The second technical route also has the current and voltage as the measured values. The current plays two roles: one is used to have a forecast SOC in the battery SOC model, which is commonly the tank model with the AHC method; the other is for the battery voltage model to have a model voltage. By comparing the model voltage and the

[3] If SOC used as the input for the battery voltage model and the model output voltage is exactly the same as the measured voltage, the SOC is then called as the model acknowledged SOC here.

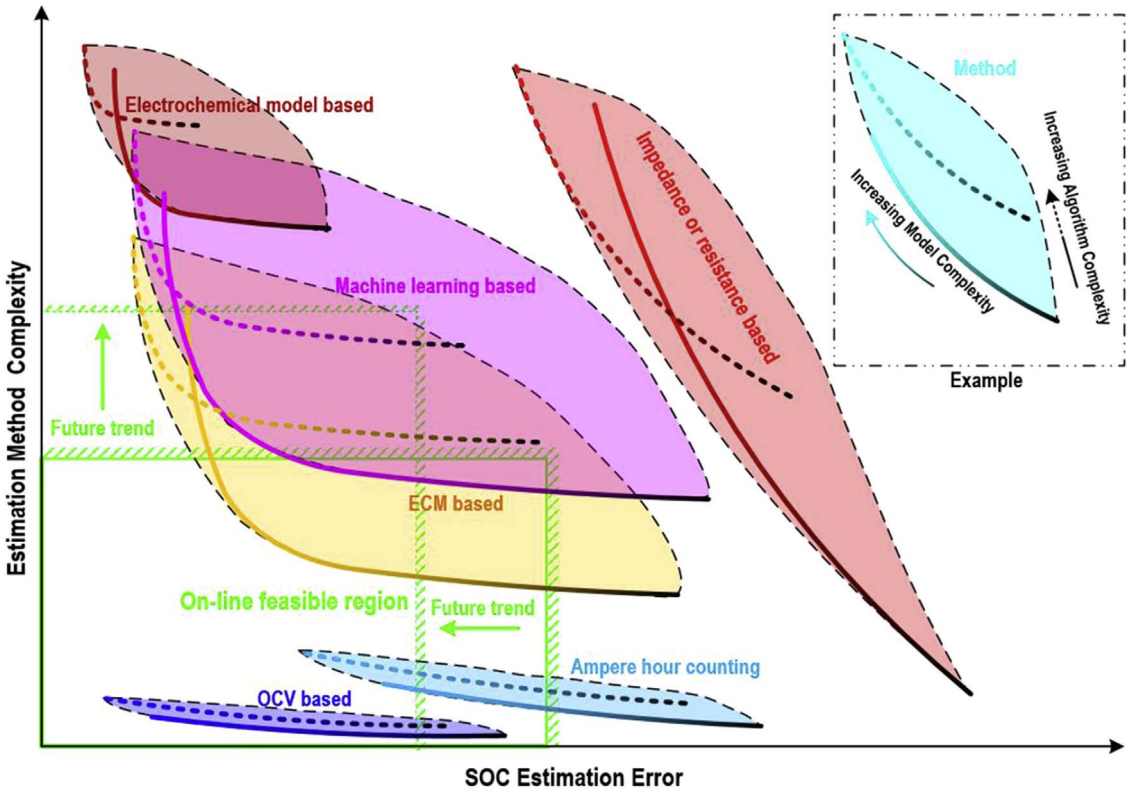

Fig. 3. Estimation error and computational complexity for the commonly studied SOC estimation methods.

measured voltage, the forecast SOC is modified with a feedback gain according to the optimal estimation algorithm. Because the forecast SOC is always modified, the accuracy of the forecast SOC by the battery SOC model has little influence on the final estimated SOC. However, the current used as the model input, with the model together, will affect the model voltage. Because the forecast SOC is modified according to the feedback gain and the difference between the measured and estimated voltage, the effect of the measured voltage on the SOC accuracy is also large. The complexity of achieving the predetermined SOC using the battery SOC model is negligible in contrast with the battery voltage model and the optimal algorithm. Comparing to the global optimal algorithm in the first technical route, the algorithm used to calculate the feedback coefficient is relatively simple and could be applied for online applications.

3.6. The accuracy and complexity of the commonly studied SOC estimation methods

According to the aforementioned analysis, the estimation error and computational complexity of the commonly studied SOC estimation methods are approximately demonstrated in Fig. 3. The abscissa is the SOC estimation error, and the ordinate is the computational complexity of the estimation methods. An example shown in the cyan theme color in the black dashed dotted rectangle depicts how to read the information about the method. Curves in the black to cyan gradients indicate the overall estimation error and computational complexity by increasing the model complexity with the same algorithm. The solid to dashed curves represent the effect of increasing the algorithm complexity on the error and the overall complexity of the SOC estimation method. The cyan area surrounded by the black dotted closed curve is the error and the overall complexity of the SOC estimation method under various types of models and algorithms. Because the errors and computational complexity of the current SOC estimation methods have not been quantitatively studied, the area can only represent the relative errors and complexity of the various SOC estimation methods.

The green rectangle is the online feasible region for SOC estimation methods. The hardware resources of the BMS limit the computational complexity of the methods, and the SOC estimation accuracy demanded by the vehicle applications limits the estimation error of the methods.

Six SOC estimation families are given in Fig. 3. The AHC estimation family in the cyan theme color has very low computational complexity. Improvements to the tank model or the ampere-hour integration algorithm, such as using a precise capacity, coulomb efficiency and self-discharge, add little computational complexity, while they will effectively decrease the estimation error.

The OCV based estimation in the blue theme color has a very similar shape to the AHC estimation family. Because of the look-up table interpolation, The OCV based estimation commonly has the lowest computational complexity. With an accurate SOC-OCV, the error is smaller than the AHC method, which is the reason that the OCV based estimation can be used for SOC calibration for the AHC method. However, although the area of the basic OCV based estimation is in the online feasible region, it can only be used in special circumstances and cannot estimate SOC in real time. Therefore, it is commonly used as an auxiliary estimation method.

The red theme color represents the resistance/impedance based estimation family. Because the resistance/impedance as a state parameter has a weak relationship with the SOC, the estimation error is easy to be too large for online applications even the complexity of the model and algorithm is drastically increased. It results in a large distance between the red area and online feasible region. Hence, we do not recommend the resistance/impedance based estimation family to be used for online SOC estimation at the current state.

The ECM based estimation family as shown in the yellow theme color has a certain choice of the models and algorithms in the online feasible region. Generally, SOC estimation combining a simple ECM and the simple EKF algorithm can meet the requirement of online estimation. According to [176], it can be deduced that, with the same

algorithm, increasing the model complexity will quickly reduce the estimation error when the model is simple, but it will not gain much if the model complexity is already high. However, when the model is too simple, even highly complicated algorithms are used, the error is reduced to a less extent. Therefore, it is worth discussing how to choose a better ECM and algorithm to have a higher SOC accuracy within a limited computational complexity.

The machine learning based estimation family in the pink theme color generally has higher model complexity compared to the ECM based estimation family. Some simple machine learning models combined with simple algorithms are expected to be applied for SOC estimation in BMS. With the increasing computational capabilities of the BMS, the machine learning based estimation family will have a more flexible choice of the models and algorithms. However, further improving the accuracy of this method through the online learning is still a big problem.

The electrochemical model based estimation family in the dark red theme color has a satisfactory accuracy with well-fitted parameters. Most problems of this family are concentrated on the model complexity and the parameter fitting [92,96]. Therefore, the focus of this method is not to further improve the SOC accuracy but to reduce the model complexity [181], such as done in Refs. [96,102,104,117,182–185], so as to have the opportunity to be applied online in the future when the computational capabilities of the BMS further increase. However, one need to note that model reduction is known to cause an estimation bias, and the SOC estimation error would be generated with a reduced-order model as demonstrated by Ref. [186].

In summary, there are mainly three SOC estimation families, which are currently applicable for online applications: AHC estimation method, basic OCV based estimation method and ECM based estimation method with relatively simple ECMs and algorithms.

4. Error source analysis for online SOC estimation methods

Although some references claimed that the accuracy of their SOC estimation methods might reach as high as 1% [26,30,35,86,187,188], these results were cases under the experimental conditions. This paper does not use certain cases under the experimental conditions to discuss the error sources of the SOC estimation methods. Instead, we consider the general error sources of the SOC estimation methods under the vehicle working condition, which has limited CPU, low measurement accuracy, wide-range temperature, violent current and full SOH range. Worse conditions may occur, such as the low sampling frequency, network latency, EMI (Electro Magnetic Interference) and so on.

In Chapter 3, we have analyzed the accuracy and complexity of the commonly studied SOC estimation methods and suggested three online applicable SOC estimation families. The basic OCV based estimation method and the AHC estimation method are currently most widely used methods in BMSs, and the ECM based estimation method with a simple ECM of first-order or second-order RC and EKF (simple ECM + KF family based estimation) is becoming the widely demonstrated and applied SOC estimation method in BMSs. However, research on the error sources regarding these three methods is seldom discussed. Therefore, this paper will analyze the SOC errors of these three online SOC estimation methods, adopting the step-by-step classification in Chapter 3.

4.1. OCV based estimation

The OCV based estimation has been introduced in the aforementioned sections. The key point of the method is to estimate the OCV. Estimation of the OCV in the basic OCV based SOC estimation includes two technical routes: by direct measurement and by empirical model estimation. The basic OCV based SOC estimation family has the same routine to estimate the SOC after obtaining the OCV, and therefore could be universally analyzed.

4.1.1. Errors in OCV estimation

One of the most widely used SOC estimation methods in NEVs is to use a directly measured voltage value as the OCV to calibrate the SOC. However, it is essential to satisfy the condition that the LiB needs to rest for a sufficiently long time in order to use the measured voltage directly as the OCV. Three hours or more is generally acknowledged a sufficiently long rest time [38,39,58]. Roscher et al. [38] indicated that voltage change is commonly less than 1 mV after 3 h rest. However, because the diffusion process mainly dominates the voltage relaxation process, when the LiB is almost empty, at low temperatures and after charging or discharging with a high current, additional rest time is required to achieve the real OCV [3,58]. With a sufficiently long rest, little error is found using the measured voltage as the OCV. While without a sufficient voltage relaxation, the error is not negligible. Roscher et al. [38] showed that there was an error of approximately 3 mV when the LiB is rested for half an hour at room temperature.

In addition to the voltage error caused by empirically using the measured voltage as the OCV, all the SOC estimation methods involving the voltage measurement need to discuss the voltage measurement error. Chips for battery voltage management now have a good accuracy of typically less than 2 mV for cell voltages [189–193]. While most BMS producers guaranteed their cell voltage accuracies of 5 mV [3,23,60,194,195], and some claimed as high as 1–2 mV [196,197], which were almost the same accuracy as the battery test benches [47,147,198,199]. The voltage measurement error has two aspects. One is the voltage drift, which describes the mean voltage measurement error in a period, and the other is the voltage measurement noise. The voltage measurement noise usually does not affect the OCV because the voltage is usually sampled for multiple times and then averaged. While the voltage drift does. Cell voltage accuracy usually refers to the voltage drift in the absence of special declaration. Therefore, the voltage measurement drift is usually in the range of 1–5 mV. While the measurement noise is usually considered to be more than 5 mV [16,186,200], and it may change in a different environment, such as the condition of the earthing and EMI. Considering the voltage drift error and the error due to the insufficient rest time, we may roughly estimate the OCV error of the online direct measurement to be probably 5 mV, with an optimistic case of 1–2 mV and a pessimistic case of 7–10 mV.

In case that LiBs cannot be relaxed for a sufficiently long time, the OCV can be estimated using the empirical model using a short time voltage relaxation. Waag et al. [5] had a very good review on the use of empirical models to estimate OCV. The developed model by Waag et al. [58] showed that approximately 10 mV OCV estimation error was an optimal result. Taking into account the voltage measurement error, OCV error by empirical model estimation might be more than 12 mV.

4.1.2. Errors from OCV to SOC

One to one relationship between SOC and OCV is the fundamental for SOC estimation by OCV. If the SOC-OCV tables in BMS are the real relationship between SOC and OCV, no errors happen when the SOC is estimated by OCV. However, the real situation is different. Optimistically, we may believe that the errors of battery test benches can be ignored. Although, the OCV is relatively stable with temperature and ageing, the slight fluctuations do exist [37,201,202]. Temperature effects on OCV curves have been studied in Refs. [49–52]. Fleckenstein et al. [50] showed the temperature coefficient of OCV for the investigated LFP cell. Liu et al. [203] also studied OCV change with temperature at different SOC for LiBs. Their results showed that OCV changed more with temperature at low SOC, while it changed less at high SOC (SOC > 40%). For example, when SOC is zero, temperature change of 10 °C could lead to OCV change of 3 mV, but when SOC is 50%, it could only change about 1 mV for OCV. Though the change is small, if the SOC-OCV table at 25 °C is used, OCV could change 3 mV at −5 or 55 °C when the SOC is around 50%, and even could change 9 mV when the SOC is near zero. Temperature compensation for the OCV is carried out in Refs. [204,205]. We test the discharge OCVs of the LFP

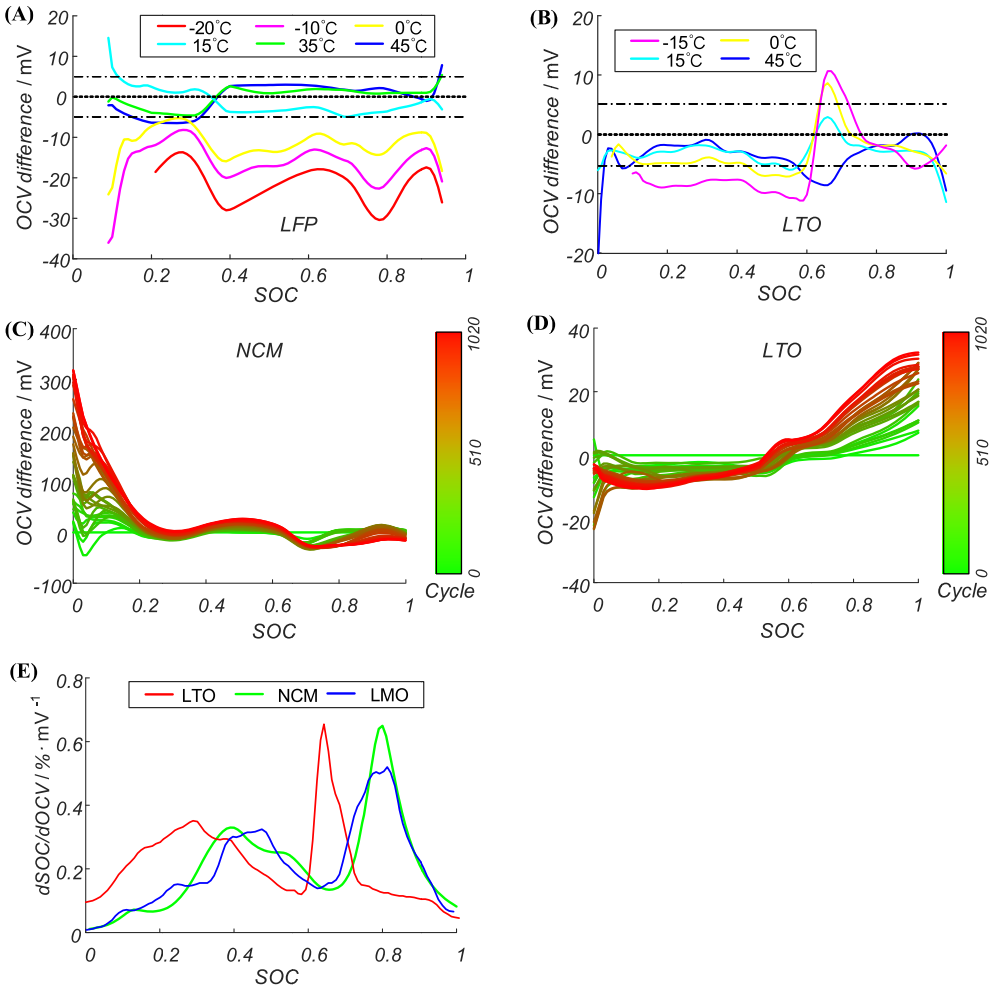

Fig. 4. OCV characteristics under different temperatures and ageing at different SOC. (A) OCV differences at different temperatures for LFP cell; (B) OCV differences at different temperatures for LTO cell; (C) OCV differences at different cycles for NCM cell; (D) OCV differences at different cycles for LTO cell; (E) SOC change per mV at different SOC for three types of cells.

and $Li_4Ti_5O_{12}$ (LTO) cells at different temperatures and compare them with those at 25 °C as shown in Fig. 4(A) and (B) respectively. The differences of the discharge OCVs of the LFP cell from 15 to 45 °C are very small and kept within 5 mV. OCV at 0 °C or lower temperatures will be 15 mV or more different from OCV at 25 °C. Therefore, if the OCV based method is to be applied for SOC estimation, low temperature SOC-OCV tables should be used. OCV differences of the LTO cell in the range of 0–45 °C can be kept within 5 mV as shown in Fig. 4 (B). Even at low temperature of −15 °C, the difference is kept within 10 mV.

The influence of the SOH on OCV is also different at different SOC. Literature [40,46–48] showed that OCV of the LFP cell in the SOC range of 70–80% was greatly influenced by the SOH. The OCV difference between the old and new LFP cells might reach more than 20 mV. OCV differences between the aged cells and the new ones for NCM and LTO cells are displayed in Fig. 4(C) and (D). OCV change with ageing in the low SOC range is very large for NCM cells as shown in Fig. 4(C). The OCV difference could be 100 mV between the new NCM cell and the one after 500 cycles when the SOC is less than 10%. OCV change in the other SOC interval is comparatively small, but it still may reach as high as 20 mV. Therefore, the OCV based SOC estimation for NCM cells must consider the influence of the battery ageing. Fig. 4(D) shows the OCV differences between the aged and new LTO cell. Though OCV difference is still within 20 mV after 1000 cycles in most SOC range, OCV change with the full SOH is still difficult to be guaranteed within a low level, because LTO cells have a long cycle life and the actual life for vehicle applications could be more than 10000 cycles [206–209]. In general, the effect of SOH on OCV is considerable, so the OCV based SOC estimation is required to consider the corresponding modification. However, since SOH estimation is more difficult than SOC estimation, many SOH estimation methods depend on SOC estimation [33,149,188,210,211]. As a result, SOC estimation error may result in SOH estimation error, and SOH estimation error conversely may lead to an inappropriate SOC modification. Nevertheless, we believe that even though the SOC modification considering the SOH effect is not accurate enough, it is better than that takes no measures on SOH effect [201]. Tong et al. [212] demonstrated an interesting work where the SOC-OCV relationship could be updated with the estimated SOH and resulted in an improved SOC accuracy.

In addition, almost all LiBs have hysteresis phenomenon, whereas the hysteresis phenomenon of LFP cells is the most obvious [38–43]. Marongiu et al. [40] comprehensively investigated the temperature, current rate, short-term history and ageing influences on the hysteresis behavior of the LFP cells. Zhu et al. [39] used the Preisach hysteresis model to estimate the hysteresis of the LFP cells to reduce the errors caused by hysteresis. In ECMs, zero-state, one-state hysteresis or other more complex hysteresis model is applied to simulate hysteresis for LiBs [44,45]. The OCV hysteresis error could be reduced by judging the battery state before the rest for the basic OCV based SOC estimation [213].

The above analysis shows that even for the simple OCV based method, if the effects of the temperature, SOH and hysteresis are not well considered in the SOC-OCV tables, the error contributed by the SOC-OCV table is much larger than that of OCV estimation. Although current studies have much research on the temperature, SOH and hysteresis, little literature have reported the comprehensive impact on the OCV tables. Ref. [201] considered the OCV change with ageing and

temperature in SOC estimation by EKF. Ref. [214] modeled the OCV considering the ageing and the temperature for the LFP cell, while the hysteresis is not discussed. Even though the OCV based estimation method considers the SOC-OCV table modification of the temperature, SOH and hysteresis, we might only optimistically assume that the error contributed by the SOC-OCV table is similar to the error of the OCV estimation.

Finally, the OCV error will lead to different SOC error at different SOC for all kinds of LiBs. Refs. [3] and [47] suggested that a voltage error of 1 mV might easily cause 5% SOC error in the SOC range of 40%–60% and 80%–90% for LFP cells. We here additionally compare the SOC-OCV rate curves, which indicate the SOC change per mV, for LTO, NCM and LMO cells as shown in Fig. 4(E). The three curves are similar because the cathode materials are all made of Mn-based complex. Compared to LFP, these three types of LiB cells have smaller SOC change per mV. The average SOC change per mV is around 0.2%. The worst case for LTO is at 65% SOC, and for NCM and LMO at 80%, where the SOC change per mV is about 0.6%. Obviously, if the OCV error is larger than 10 mV, the error of the OCV based SOC estimation might possibly reach 5% when the three types of LiB cells are used around these SOC points.

4.1.3. EFC of the basic OCV based estimation method

According to the above analysis, we can give the EFC for the basic OCV based estimation as shown in Fig. 5(A). The main body of the EFC for the basic OCV based estimation method includes the voltage as the measured value, OCV as the state parameter and the look-up table as the empirical model. The voltage measurement error includes the drift $e_{U,D}$, the noise $e_{U,N}$ and the error due to signal distortion by the sampling frequency $e_{U,SF}$. By multiple averaging, only the voltage drift $e_{U,D}$ has an impact on OCV. Considering the OCV estimation error caused by insufficient rest time e_t, the OCV estimation error $e_{O,E}$ is composed of two parts: $e_{U,D}$ and e_t. While the error of the SOC-OCV curve used in the real applications is caused by the temperature e_T, ageing e_A and hysteresis e_H. Ultimately, the SOC error can be obtained by these voltage errors according to the SOC change per mV at the corresponding SOC.

In an optimistic scenario, the OCV estimation error $e_{O,E}$, which is composed of $e_{U,D}$ and e_t, could be 3 mV. Even if the ageing, temperature and hysteresis are satisfactorily considered, the SOC-OCV curve error could easily be larger than 5 mV when the LiB works in all working conditions and full cycle life. The OCV error of 8 mV for LTO, NCM and LMO cells will lead to an average SOC error of about 1% according to Fig. 4(E). Hence, we may say that, for LTO, NCM and LMO cells in an optimistic scenario, when ageing, temperature and hysteresis are satisfactorily considered, the rest time is sufficient and the voltage measurement error is very small, SOC error by the basic OCV based estimation is approximately 1% when the LiB works in all working conditions and full cycle life. A baseline scenario might be 2% or even more when any of the above conditions are not well satisfied. While for the LFP cell, when it works in all working conditions and full cycle life, it is difficult for the OCV based method to get an error of less than 3% due to the flat SOC-OCV curve of the LFP cell.

The error sources of the OCV based method can be analyzed according to Fig. 5(A). For example, we consider an LTO cell with about 90% SOC after 500 cycles at the ambient temperature of 0 °C. With 3 h rest and the accurate voltage measurement, the OCV estimation error $e_{O,E}$ could be restricted to 2 mV. The error caused by the hysteresis e_H is neglected for LTO at 90% SOC. Without the temperature and ageing modification, the SOC-OCV curve errors from the temperature e_T and the ageing e_A are 2 mV and 10 mV respectively according to Fig. 4(B) and (D). Finally, using 0.1% per mV at 90% SOC in the SOC-OCV rate curve in Fig. 4(E), the SOC estimation error is about 1.4%. If ageing and temperature are considered in the SOC-OCV tables, because the temperature is measurable, the OCV table error e_T could be controlled in 1 mV. Because SOH is hard to be estimated, the SOC-OCV table at 500 cycles may not be successfully used. Instead, the SOC-OCV table at 400 or 600 cycles is likely to be used. If the SOC-OCV table at 400 cycles were used, the error from the ageing e_A is about 3 mV according to Fig. 4(D). Hence, the SOC estimation error is then 0.6%. Therefore, the error for the OCV based estimation at some certain conditions is very small.

4.2. AHC estimation

The AHC estimation can also be described from the measured values, model, algorithm and state parameter. Because the AHC estimation is very simple, direct calculation using equation (4) for SOC without mentioning the model is quite normal. Nevertheless, from the perspective of error source analysis, we need to analyze two major error sources, which are the measured values and the model. The most important measured value is the current. For a battery pack with a cell balancing system, the balancing current should be considered. The error sources of the model include the self-discharge, CE, initial SOC value, battery capacity and so on.

4.2.1. Errors from the measured values

The current is the most important measured value in the AHC estimation. Other measured values include the time and voltage. Although the AHC method is much sensitive to the time measurement error, the time measurement is now usually very accurate in BMS. Hence, the error caused by the time measurement error is negligible.

Full charge calibration or the basic OCV estimation requires the voltage measurement to calculate the SOC. Although the recalibration happens occasionally, its error on the AHC estimation preserves. Therefore, the voltage measurement error is important for the AHC estimation. Considering that the recalibration influences the initial SOC, which is one of the error sources in the model, we will discuss it in the next section.

The current measurement error can be as low as 0.01% for the test benches as claimed by Ref. [35], while the errors of the most current sensors are around 0.1%–1% for online applications [196,215]. However, the current error discussed was general in these references. Similar to the voltage, the current error is also divided into two types: one is the current drift, and the other is the current noise. Few references have discussed the difference between the two types, but the influence is quite different. Experiments in Ref. [28] showed that the current drift might reach a maximum of 1%. Under normal circumstances, due to the temperature and the electromagnetic environment, a drift of 200 mA is possible. Ref. [16] respectively studied the current drift and noise errors of 100 mA for SOC estimation. Because the optimal algorithms were used, the influences of the current drift and noise errors on the SOC error were not obvious (see Section 4.3). Especially for the current noise, ref. [216] showed that a large random white noise of the current has almost no influence on the SOC estimation by EKF in their demonstration. However, if only the AHC method is used, the influences of the current drift and noise are completely different. Our work [177] suggested that the current noise induced SOC error tended to be zero in the long term thanks to the effect of the integration in the AHC estimation. While the current drift is different from the noise: the current drift is accumulated during the integration, which leads to an increasing error with the time in AHC estimation. Therefore, when the current measurement error needs to be discussed, we may focus on the current drift. If the current sensor drift is 100 mA and the NEV runs 8 h per day, the accumulated error is 0.8Ah in one day. For a battery pack of 100Ah in the NEV, the SOC estimation error is 0.8% per day, and quickly reaches 5% in one week.

At the same time, one also needs to notice that the relative accuracy is not guaranteed for small currents due to the large scale of the measurement scope. Commonly, a fixed maximum error is given at a low current, e.g. a maximum error of 20 mA below 20A. This indicates that the relative error in the whole current measurement range is not consistent. The relative error can be significantly large when the current is

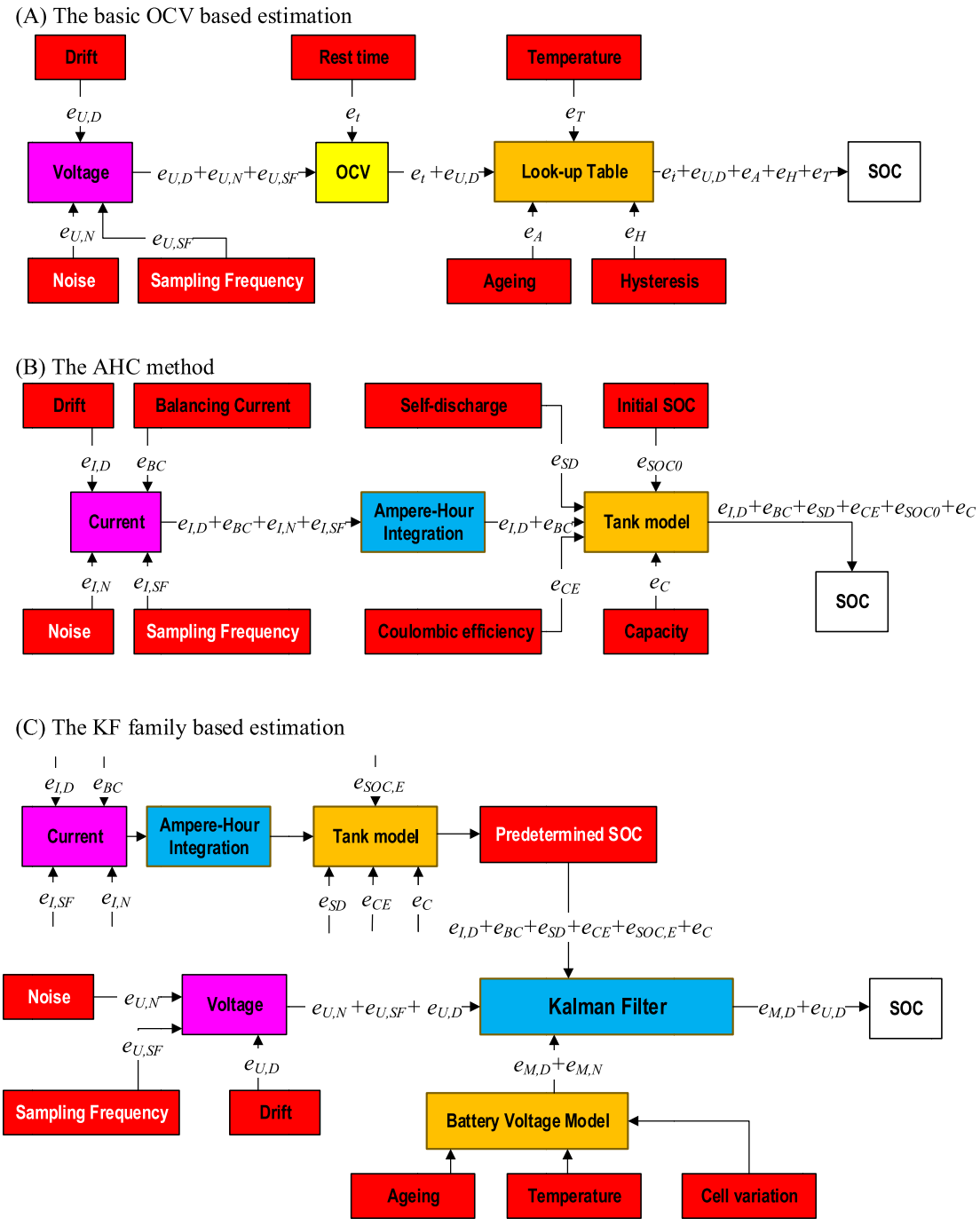

Fig. 5. EFCs for the online SOC estimation methods. (A) The basic OCV based estimation; (B) The AHC method; (C) The KF family based estimation.

very small. Unfortunately, the current is usually small due to the accessory power consumption in the "idle" state for NEVs. If the current sensor cannot detect the small current or there is a large relative error, SOC estimation error is greatly increased using the AHC method. Therefore, for battery packs which often run in a low current condition, if a small-scale current sensor is added to the full-scale current sensor, it can greatly improve the current measurement accuracy and finally extend the recalibration time required for the AHC method.

For a battery pack with a cell balancing system, because the balancing current is not measured by any current sensor, it should be additionally estimated in order to accurately estimate the SOC when the cell balancing is working. However, most balancing systems use the voltage-based equalization [217–221], which is an algorithm targeting the same voltage for all the cells. The balancing current is seldom estimated in such balancing systems. Besides, the non-dissipative cell balancing topologies commonly implement the excitation current, which is hard to be estimated [222]. Even the simple dissipative cell balancing is applied, the balancing current needs to be calculated according to the cell voltage and the duty ratio of the control switch [223]. For most commercialized NEVs with dissipative cell balancing, if the balancing current is ignored, SOC error would be enlarged using the AHC estimation.

Other literature [3,6] mentioned that the current sampling frequency might have an impact on the AHC SOC estimation, because the sampling frequency was too low that the current signal was distorted. In practice, however, the current sampling frequency of the BMS is usually

not too low (typically larger than 1 Hz). Therefore, the current signal distortion can be approximated to the white noise. While the long-term integration of the white noise is zero, and therefore, the typically used sampling frequency has little impact on the AHC SOC estimation. Our research [177] showed that when the sampling frequency became 2 Hz, with respect to the original signal frequency of 4 Hz, the SOC estimation error by the AHC method was not influenced. Yuan et al. [224] showed in their work that SOC errors induced by different sampling frequencies of 1 Hz and 10 Hz are almost the same.

In summary, the current sensor drift and the current measurement error during "idle" state principally influence the AHC estimation SOC error. In addition, the estimation accuracy of the balancing current also greatly affects the AHC estimation SOC error. The SOC deviation of the AHC estimation caused by the current measurement error is often unidirectional and increases with time. With only consideration of a general current drift of 50 mA (including the current sensor drift error, the current measurement error during "idle" state and the estimation error of the balancing current), for an EV with a battery pack of 100Ah that runs 100 h (including driving, charging and idle), the error could be 5%. Therefore, SOC estimation using the AHC method for a long time without recalibration is unreliable.

4.2.2. Errors from the model

The error sources in the tank model include the self-discharge, CE, initial SOC value and battery capacity.

Self-discharge phenomena include irreversible capacity loss (IRCL) and reversible capacity loss (RCL) [10,225,226]. As implied by the name, recharging a cell will not recover IRCL. On the other hand, RCL will be recovered by recharging a cell. RCL has little relevance to cell capacity, while it reduces discharge electric quantity and leads to a lower SOC as a result. Detail mechanisms of RCL remain unclear to date, but it is well recognized that a redox shuttle mechanism principally causes RCL [10,227,228]. The redox shuttle mechanism suggests that RCL happens when soluble oxides generated at cathodes are reduced at anodes. Further studies [229,230] believed that the generated soluble oxides were metastable electron-ion-electrolyte complex, which acted as the redox shuttle and caused RCL. Literature indicates that RCL exists in any LiBs whether the it is stored or cycled in all kinds of lithium-ion systems and it becomes large at high temperatures [226]. Experiments showed that the amounts of IRCL and RCL were comparable [72,231–233] which means RCL is relatively small. Most RCLs of normal LiBs in mass production are currently within 1% SOC per month. Hence, RCL may cause no more than 12% SOC change in one year. Nevertheless, compared to the contribution from the current drift error (5% per 100 running hours), the self-discharge induced SOC error is relatively small. A special case is that when NEVs are left idle for a long time during which BMSs do not work but the self-discharge continues. The self-discharge is then the major influence factor to the SOC error. Fortunately, after a long-term storage of the battery pack, the OCV based SOC estimation could be implemented to recalibrate the SOC, and therefore, this problem caused by the self-discharge could be ignored in real applications. With the progress of current measurement technology [234,235], the self-discharge induced SOC error will approximate the current drift induced SOC error at high temperatures. Thereafter, the self-discharge should be carefully examined. If the self-discharge is neglected or not well estimated, the SOC deviation of the AHC estimation is also unidirectional and increases with time.

For the AHC SOC estimation, inaccurate CE makes a notable contribution to the SOC estimation error [236,237]. Long cycle life and high energy efficiency of the lithium-ion batteries are mainly attributed to their high CEs [238]. CEs of most commercial lithium-ion batteries reach almost 100% [174,238–240]. However, little literature focused on how CEs were measured, not to mention the accuracy of the measurement results. The most important reason is that precise CE is very difficult to be measured [241–243], because the errors of the best current sensors for battery test benches at present are relatively too large for the measurement of precise CE. J. R. Dahn et al. [242,243] reported how precise CE was measured by constructing an expensive device for the first time. They achieved fruitful results for the measured CE versus cycle numbers of different cell types. However, high price discouraged the approach to be widely used even in laboratories. While with conventional battery test benches, suppose the measurement error for both positive and negative current is 0.1%, which is the claimed accuracy by most battery test bench makers, the scene may happen that CE of a cell is measured to be 99.8% while its real CE might be 99.9%. Suppose a cell that has a high CE of 99.9%, but is considered to be 99.8% when the SOC is calculated using equation (4). If no calibration were introduced, the SOC error would be around 10% after 100 full cycles, which is not acceptable for vehicle applications. However, compared to the contribution from the current drift error, the CE induced SOC error is less than 1% in one week with a full charge and discharge per day. CE is similar to the self-discharge on the AHC estimation. An accurate CE is important to AHC SOC estimation in the long term. If CE is not well estimated, the SOC deviation of the AHC estimation is also unidirectional and increases with time.

The initial SOC has a continuous effect on the AHC estimation, and therefore is a very important value. The initial SOC is usually determined by the OCV based estimation or full charge calibration. Compared to the OCV based estimation, the full charge calibration is more accurate because it directly uses the SOC definition. When the LiB can seldom be fully charged, the OCV based estimation may provide a suitable initial SOC to recalibrate the SOC for the AHC method. The error of the OCV based estimation has been discussed in Section 4.1, where the error of the OCV based estimation is quite different under different conditions. Considering a scenario when a LiB is fully charged, we undoubtedly use the fully charged SOC as the initial SOC.[4] After a period, the OCV based estimation is ready to be applied when some conditions are satisfied, such as a sufficiently long rest time. A problem emerges whether we should use the SOC estimated by the OCV based method as the new calibrated SOC or we do nothing but use the previous SOC value as the next initial SOC. Similar questions have never been discussed, and we will later try to discuss this issue in Chapter 5.

According to refs [165,210,244–247], the capacity estimation error might be around 2.5%. Therefore, we estimate that the capacity estimation error may reach 5% or more in all working conditions and full cycle life.[5] Hence, it may have a notable impact on SOC estimation by the AHC method. Nevertheless, the error does not increase with time. The maximum error caused by the capacity estimation error using the AHC method will not exceed the capacity estimation error. In fact, according to equation (4), the error caused by the capacity estimation error is proportional to the net charge (discharge) electric quantity change. For example, when the LiB runs after a number of cycles and reaches a state that the net charge electric quantity is zero, the capacity estimation error has no influence on the SOC estimation error using the AHC method. It means that the SOC estimation by the AHC method for LiBs in HEVs is not influenced by the capacity error, because the SOC is usually maintained within a narrow SOC range and the net charge electric quantity is approximately zero in HEVs [47,248–250]. For BEVs, if the capacity estimation error is e_C, and the SOC difference between the initial and current SOC is ΔSOC, the SOC error caused by the capacity estimation error is then $\Delta SOC \cdot e_C$.

4.2.3. EFC of the AHC estimation method

According to the above analysis, we can give the EFC for the AHC estimation as shown in Fig. 5(B). The errors of the current include the

[4] The fully charged SOC may not be 100%, because charging at different temperature and current rate will result in different SOC when the LiB is charged to the cut-off voltage. However, the fully charged SOC value could be achieved by experiments in advance.

[5] The EOF (end of life) of the LiB for vehicle applications is commonly defined when the SOH reaches 80%. Therefore, if the capacity estimation error reaches 5%, the relative error for the capacity loss estimation is 25%, which is a notable error.

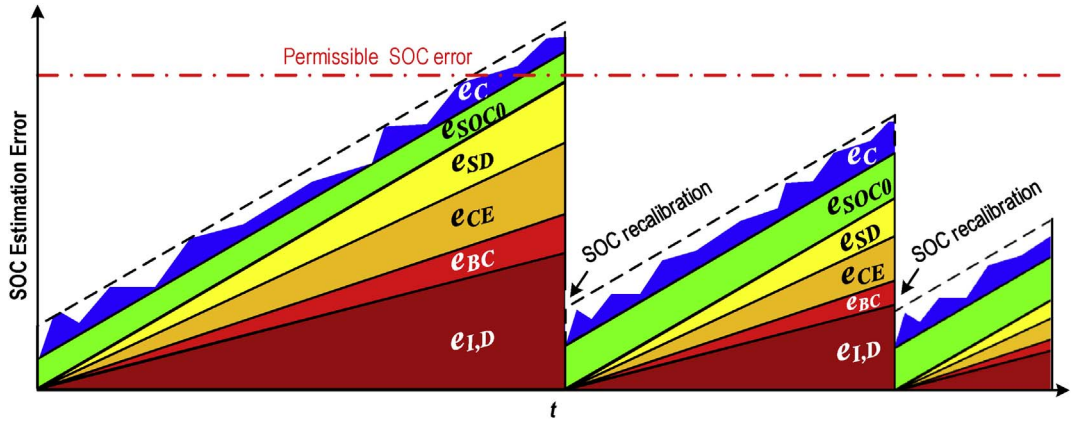

Fig. 6. The SOC estimation error and the error components by the AHC method with time.

current drift $e_{I,D}$ and the current noise $e_{I,N}$. The relative error is enhanced in cases of small current and "idle" state. In addition, the balancing current estimation error e_{BC} and the error due to signal distortion by the sampling frequency $e_{I,SF}$ is also included in the current measurement error. By the ampere-hour integration, the current noise $e_{I,N}$ and the sampling frequency induced current error $e_{I,SF}$ are approximately eliminated, but the current drift $e_{I,D}$ and the balancing current estimation error e_{BC} remain. The SOC error is finally obtained by combining the self-discharge e_{SD}, CE e_{CE}, initial SOC e_{SOC0} and capacity e_C induced errors.

$e_{I,D}$, e_{BC}, e_{SD} and e_{CE} are cumulative with time, but e_{SOC0} and e_C are not cumulative. Therefore, we need to further consider the SOC estimation error by the AHC method with time. Fig. 6 gives a sketch that shows the SOC estimation error and the error components by the AHC method with time. The current induced errors $e_{I,D}$ and e_{BC}, the CE induced error e_{CE} and the self-discharge induced error e_{SD} increase with time. However, the initial SOC induced error e_{SOC0} remains constant with time. The capacity induced error e_C is not related to the time but to the net discharge electric quantity. Because the net discharge electric quantity will not exceed the battery capacity, the capacity induced error e_C is restricted to a limited range ($\Delta SOC \bullet e_C < e_C$). The error components in Fig. 6 are schematic, and the specific proportion depends on the actual situation. According to the aforementioned analysis, $e_{I,D}$ accounts for a large part of the error. e_{BC} has a small part, and if no balancing system is applied, it is should be zero. e_{SD} and e_{CE} are relatively small which are estimated to be about 1/5 of $e_{I,D}$. The red dash dotted line shows the SOC error allowed by online applications. Because $e_{I,D}$ and other errors increase with time, it is easy to exceed the online allowable SOC error. The SOC error before the first recalibration shown in the figure exceeds the online allowable SOC error, because the first recalibration time is too long due to the insufficient rest time for OCV based estimation or unavailable full charge calibration. After the recalibration, all the other error sources induced errors will be forced to zero except for the new initial SOC error e_{SOC0}.

In an optimistic scenario, the current drift $e_{I,D}$ is supposed to be minimized to an average of 10 mA no matter the NEV runs or stops. For a battery of 100Ah, the SOC error caused by the current drift is 0.24% per day. We suppose e_{BC} is zero because no balancing is applied, and e_{SD} and e_{CE} are 1/5 of the current drift $e_{I,D}$. Hence, the cumulative error is then 0.336% per day. If the full charge calibration is used, the initial SOC error e_{SOC0} is considered to be zero. An ideal SOH estimation error is supposed to be 2%. Therefore, in order to keep the SOC error less than 5%, which is commonly required by vehicle applications, the longest recalibration period is about 9 days ((5%–2%)/0.336%). Therefore, even in such an optimistic scenario, SOC error will exceed the permissible error in 10 days without recalibration. In a general scenario, we may say that SOC estimation by the AHC method without recalibration for one week is not reliable for vehicle applications.

4.3. ECM + KF family based estimation

ECM combined with KF (ECM + KF) family based SOC estimation is widely discussed and studied. Plett et al. [139,251,252], Xiong et al. [34,165,253,254], Chen et al. [129,255] and other groups have carried out a lot of research and had fruitful results. While most researches focused on the improvement for algorithms, Hu et al. [176] considered the accuracies of different ECMs. Wang et al. [256] studied the relationship between the model accuracy and SOC estimation and showed that a close positive relationship between them.

We have presented the flow chart of the modern control theory based SOC estimation in Fig. 1. The KF family algorithm, as the one of the most classical approaches, follows the basic principle of prediction plus correction (also known as feedforward and feedback). The AHC is used as a prediction. The correction in KF family based estimation uses the Kalman gain and the difference between the ECM and measured voltages. Regardless of the types of the ECMs or KF algorithms, the prediction and correction can be expressed by the following equation, as long as the AHC method is used as the prediction.

$$\hat{SOC}_{k-1}^{+} \xrightarrow{+\Delta\hat{x}_k^{-}\left(=\frac{\eta I_k \Delta t}{C_k}\right)} \hat{SOC}_k^{-} \xrightarrow{+\Delta\hat{x}_k^{+}(=L_k(U_k-\hat{U}_k^{-}))} \hat{SOC}_k^{+} \tag{6}$$

where, $\hat{SOC}_{k-1}^{+}$ is the estimated SOC at time k-1; $\hat{SOC}_k^{-}$ is the SOC prediction by the AHC method at time k; $\hat{SOC}_k^{+}$ is the estimated SOC at time k after the correction by the KF family algorithm; I_k is the current at time k; C_k is the capacity at time k; Δt is the time interval for each estimation iteration; L_k is the Kalman gain at time k; U_k is the measured voltage at time k and $\hat{U}_k^{-}$ is the ECM voltage at time k when the SOC prediction $\hat{SOC}_k^{-}$ and the current I_k are used as the inputs for the ECM.

Therefore, from the estimated SOC at time k-1 ($\hat{SOC}_{k-1}^{+}$) to k ($\hat{SOC}_k^{+}$), the estimated SOC is modified twice. One is modification from the AHC prediction $\Delta\hat{x}_k^{-}$, and the other is the modification from the Kalman correction $\Delta\hat{x}_k^{+}$. Thus, we can analyze the SOC error sources for the ECM + KF family based estimation by respectively considering the AHC prediction $\Delta\hat{x}_k^{-}$ and the Kalman correction $\Delta\hat{x}_k^{+}$.

4.3.1. Errors from the AHC prediction

The prediction is commonly based on the AHC estimation. According to Fig. 6, the error origins for the AHC prediction can be divided into 3 types. The current drift $e_{I,D}$ and errors from the balancing current estimation e_{BC}, self-discharge e_{SD} and CE e_{CE} have similar effects on SOC errors by AHC estimation, and therefore, they can be generally represented by the current drift error. The other two types are the initial SOC e_{SOC0} and the battery capacity e_C induced errors. To focus on the influence of the prediction error, we assume that the voltage measurement error is zero and the model is completely accurate.

4.3.1.1. Initial SOC induced error e_{SOC0}. All KF family based SOC

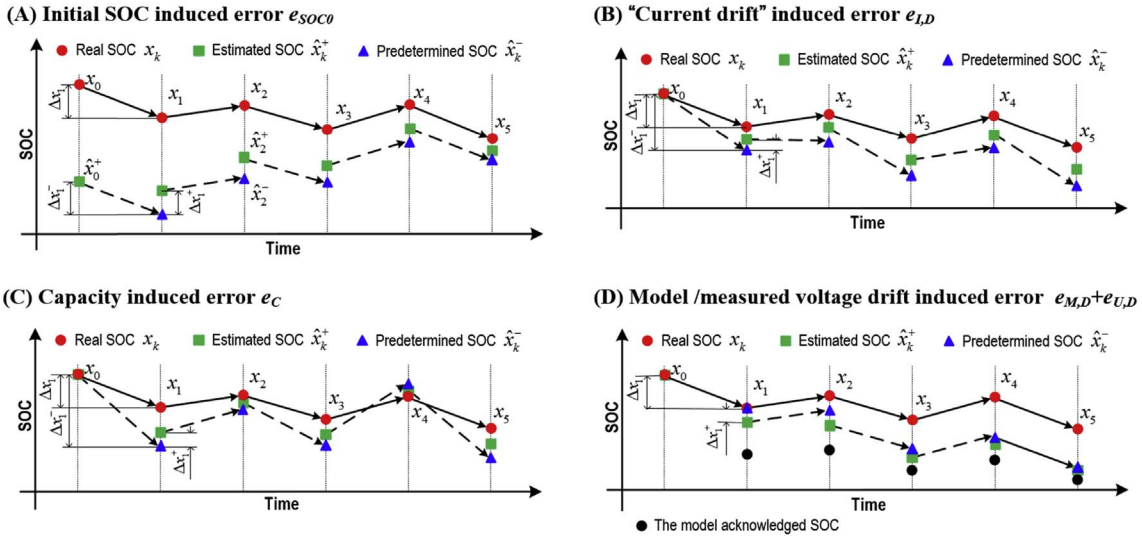

Fig. 7. A schematic diagram for the effects of the error sources on the KF family based SOC estimation (A) Initial SOC induced error e_{SOC0}; (B) "Current drift" induced error $e_{I,D}$; (C) Capacity induced error e_C; (D) Model/measured voltage drift induced error $e_{M,D}+e_{U,D}$.

estimation studies, without exception, showed that the initial SOC induced error e_{SOC0} is eliminated [23,35,44,146,147,155,257–261]. This characteristic has made the KF family based SOC estimation much popular. These studies demonstrated excellent results with large initial SOC errors when the methods were evaluated. Fig. 7(A) schematically depicts the effect of initial SOC induced error e_{SOC0} on the KF family based estimation. The red dot is the real SOC x_k, the estimated SOC $\hat{x}_k^+$ is represented by the green square and the predetermined SOC $\hat{x}_k^-$ is represented by the blue triangle. With the assumption that the measured and model voltages are completely accurate, the model acknowledged SOC is consistent with the real SOC. Fig. 7(A) shows that there is an error between the estimated and real initial SOCs ($\hat{x}_0^+$ and x_0). During the next estimation, because the other errors of the AHC method are not considered, the AHC prediction $\Delta\hat{x}_1^-$ is equal to the real SOC change Δx_1. The error of the predetermined SOC $\hat{x}_1^-$ is equal to the initial error. During the Kalman correction phase, because the model voltage $\hat{U}_1^-$ is different from the measured voltage U_1 with the predetermined SOC $\hat{x}_1^-$ as the input, the Kalman correction $\Delta\hat{x}_1^+$ is generated according to the Kalman family algorithms to lower the influence of the initial SOC error. Hence, the estimated SOC $\hat{x}_1^+$ becomes closer to the real SOC x_1 compared to the estimated and real initial SOCs ($\hat{x}_0^+$ and x_0). Finally, the initial SOC error can be eliminated approximately during the next several iterations.

4.3.1.2. "Current drift" induced error $e_{I,D}$. The errors from the balancing current estimation e_{BC}, self-discharge e_{SD} and CE e_{CE} have similar effects to the current drift on SOC errors by AHC estimation. Hence, we use the current drift to represent these similar error sources. Barillas et al. [16] and He et al. [262] pointed out that good SOC estimation results could be achieved by the KF family algorithm with small current drifts. Fig. 7(B) is a demonstration for the influence of the current drift induced error on SOC estimation by KF family algorithm. The current drift here is arbitrarily assumed to have a discharge attribute.[6] Therefore, the error of the AHC prediction $\Delta\hat{x}_1^-$ is negative.[7] During the Kalman correction phase, because the model voltage $\hat{U}_1^-$ is different from the measured voltage U_1 with the predetermined SOC $\hat{x}_1^-$ as the input, the Kalman correction $\Delta\hat{x}_1^+$ is generated according to the Kalman family algorithms to counteract the error of the AHC prediction $\Delta\hat{x}_1^-$. The estimated SOC $\hat{x}_1^+$ is closer to the real SOC x_1 as a result. However, the Kalman correction $\Delta\hat{x}_1^+$ does not eliminate the error caused by the AHC prediction $\Delta\hat{x}_1^-$, and the new error of the AHC prediction generates during the next prediction. Therefore, SOC estimation error may increase during the first several iterations. Nevertheless, as the error increasing, the Kalman correction $\Delta\hat{x}_k^+$ increases, and finally the Kalman correction $\Delta\hat{x}_k^+$ could completely eliminate the increasing error trend caused by the AHC prediction $\Delta\hat{x}_k^-$. The error of the estimated SOC $\hat{x}_k^+$ becomes stable as a result. Commonly, the error generated by the AHC prediction due to the current drift at one step is small, and if a suitable Kalman gain is used, the stable error of the estimated SOC $\hat{x}_k^+$ could be neglected.

4.3.1.3. The capacity induced error e_C. Fig. 7(C) shows a schematic diagram for the influence of the capacity induced error e_C on SOC estimation by KF family algorithm. The estimated capacity is arbitrarily assumed to be smaller than the actual capacity in this case. When the estimated capacity is larger, similar results could be analyzed. Since the estimated capacity here is less than the actual capacity, the absolute value of the AHC prediction $\Delta\hat{x}_1^-$ is larger than the actual one. Similar as the current drift induced error $e_{I,D}$, when the SOC continues to decrease or increase, the error of the estimated SOC $\hat{x}_k^+$ becomes stable. When the SOC maintains with fluctuations (dynamic charge and discharge) as shown in the figure, the KF family algorithm can reduce the error fluctuation caused by the capacity error. These features make the dual-KF family algorithm feasible to estimate the battery capacity [33,165,166,188,202]. Because the estimated SOC by KF family algorithm is quite accurate regardless of the capacity error, the capacity could be estimated based on the accurate SOC.

Based on the above analysis, it is concluded that the KF family algorithm can well correct the SOC errors caused by the initial SOC, current drift and battery capacity under the assumptions that the voltage measurement error is zero and the model is completely accurate. The error from the initial SOC can be completely eliminated, the error fluctuation induced by the capacity will be reduced, and the current drift induced error is controlled. Therefore, we may say that the AHC prediction in the KF family algorithm affects the convergence of the SOC estimation. The influence on SOC error could be relatively negligible.

4.3.2. Errors from Kalman correction

The Kalman correction in equation (6) includes three parts, the Kalman correction L_k, the measured voltage U_k and the model voltage

[6] A discharge attribute here means the measured current is larger than the real current during the discharge and smaller than the measured current during the charge.

[7] It means the AHC predicted SOC has a larger decrease during the discharge and smaller increase during the charge compared to the real value.

$\hat{U}_k^-$ with the predetermined SOC $S\hat{O}C_k^-$ as the model input. To emphasize on the Kalman correction, the predetermined SOC $S\hat{O}C_k^-$ is assumed to have zero error in this section.

4.3.2.1. Kalman gain L_k. Take the EKF algorithm for example, according to the equations of the EKF gain [139], when the covariance matrix Σ_w increases, the Kalman gain L_k increases, and when the covariance matrix Σ_v increases, the Kalman gain L_k decrease.[8] This means that the Kalman gain principally depends on the covariance matrices Σ_w and Σ_v.When Σ_w increases, the Kalman gain L_k increases, and the predetermined SOC $S\hat{O}C_k^-$ is considered to be less reliable by the EKF algorithm. Hence, the Kalman correction $\Delta\hat{x}_k^+$ will have a larger increase, and the estimated SOC $S\hat{O}C_k^+$ will tend towards the model acknowledged SOC. On the contrary, when Σ_v increases, the Kalman gain L_k decreases, and the battery voltage model is considered to be less reliable. Hence, the Kalman correction $\Delta\hat{x}_k^+$ will only have a small increase, and the estimated SOC $S\hat{O}C_k^+$ will tend towards the predetermined SOC $S\hat{O}C_k^-$. Little literature gave a specific guideline for the determination of the covariance matrices Σ_w and Σ_v. They are seldom determined by the real process noise and measurement noise, which are hard to be measured or evaluated. Instead, the covariance matrices Σ_w and Σ_v are commonly determined by synthetically considering the convergence rate and the effectiveness of the filtering, which is similar to the proportional-integral-derivative (PID) tuning. By using the adaptive EFK (AEFK) for online tuning of the covariance matrices Σ_w and Σ_v according to the model error in Refs. [23,30], a better Kalman gain L_k could be expected which will theoretically result in a better SOC estimation in some local details.

The AHC prediction $\Delta\hat{x}_k^-$ acts as feedforward, and the estimated SOC always tends to the model acknowledged SOC due to the presence of the Kalman gain L_k. Pulse interference like the initial SOC error could be eliminated no matter how small the Kalman gain L_k is. Continuous unidirectional interference such as the current drift induced error could be constrained, and fluctuation interference such as capacity error induced error could be reduced with a suitable Kalman gain. The Kalman gain L_k influences the number of iterations for the estimated SOC to the model acknowledged SOC, which is also considered as the convergence rate of the algorithm. A larger Kalman gain L_k contributes to the fast convergence of the algorithm and helps to tend to the model acknowledged SOC. However, because the battery voltage model is quite dynamic in the dynamic working conditions, a larger Kalman gain L_k will result in larger fluctuation of the estimated SOC, which could be quite different from the real SOC changing in low frequency [177]. Therefore, a well-tuned Kalman gain L_k mainly influences the estimated SOC in some local details that are commonly seen in the convergence rate and filtering effects. Nevertheless, it has very little contribution to the average error and its effect on the SOC error from the view of a large time scale is not very obvious.

4.3.2.2. Measured voltage U_k. We have discussed the voltage measurement accuracy in Section 4.1.1. Similar to the error analysis of the current, the accuracy of the voltage measurement needs to consider the voltage drift, noise and sampling frequency. The voltage noise may change with the system EMI and is difficult to be estimated. Nevertheless, the merit of the KF family algorithm is its strong suppression over the noise. Barillas et al. [16] studied the influence of voltage measurement noise on the SOC estimation error by KF family algorithm. The results showed that the error was almost not influenced from the view of a large time scale. The sampling frequency might have little effect on the SOC estimation error by KF family algorithm, because our study [177] showed that low sampling frequency signal could be considered to have an additional noise compared to the high sampling frequency. However, the voltage drift is different. Because the Kalman correction is $\Delta\hat{x}_k^+ = L_k(U_k - \hat{U}_k^-)$, when there is a voltage drift from the measurement sensor, i.e. $U_k = U_{k,real} + U_{k,drift}$, where $U_{k,real}$ is the real voltage at time k, and $U_{k,drift}$ is the measured voltage drift at time k, the battery voltage model should generate the model voltage $\hat{U}_k^-$ under deviated state variables to compensate the measured voltage drift $U_{k,drift}$. Theoretically, deviations of all the state variables in the battery voltage model are able to cause the model to produce voltage deviation to compensate the measured voltage drift $U_{k,drift}$. For example, in a third-order RC ECM with one-state hysteresis, SOC_k, $U_{1,k}$, $U_{2,k}$, $U_{3,k}$, and h_k are all likely to produce the voltage deviation to compensate $U_{k,drift}$ by deviating themselves. The proportion of the compensating voltage for each state variable depends on the covariance matrix of the process noise Σ_w. In general, literature tends to use a large SOC noise, and keep other state variables with small noises in the process noise [18,201,214,263–266]. Hence, the initial SOC error could be quickly eliminated and the estimated SOC will converge to the model acknowledged value. However, in this condition, when there is a voltage measurement drift error, the compensation voltage produced by the model will principally be contributed by the SOC deviation. For ECMs, the model voltage change due to a slight SOC deviation is mainly from the SOC-OCV curve. When the measured voltage drift is compensated by the SOC deviation in the model, the SOC error is approximately $e_{SOC,U,D} \approx \frac{dSOC}{dOCV}U_{k,drift}$, where $\frac{dSOC}{dOCV}$ is the SOC change per mV as shown in Fig. 4(E). Ref. [267] deduced a similar result theoretically for the LFP cell. In Section 4.1, we point out that the voltage measurement drift will be 1–5 mV, and therefore the error caused by the voltage drift can be calculated. For example, for NCM and LMO cells at SOC of approximately 80%, the SOC change per mV is about 0.6%, and if a voltage measurement drift of 3 mV is assumed, the error is about 1.8%. However, for LFP cells in the SOC range of 40–60%, if there is a voltage measurement drift, the error is difficult to be controlled within 5%.

4.3.2.3. Model voltage $\hat{U}_k^-$. The error of the model voltage $\hat{U}_k^-$ is the main error source for the SOC estimation by the modern control theory based estimation. The model voltage error refers to the voltage difference between the model and the real voltage when the predetermined SOC is accurate. The model voltage error can also be divided into model voltage noise and drift [267]. According to the Kalman correction $\Delta\hat{x}_k^+ = L_k(U_k - \hat{U}_k^-)$, the model voltage error has exactly the same effects on SOC estimation as the measured voltage error. The model voltage noise will not affect the SOC estimation accuracy [267]. The model voltage drift needs to be compensated by deviation of the state variables in the model. SOC deviation contributes the most because the SOC noise is commonly tuned to be the largest in the process noise. Therefore, we have $e_{SOC,M,D} \approx \frac{dSOC}{dOCV}\hat{U}_{k,drift}^-$.

ECMs, machine learning models and electrochemical models can serve as the battery voltage models in the dynamic working conditions. ECM + KF family based SOC estimation is most widely discussed. Several reports used machine learning models combined with KF family based SOC estimation [107,114,135], and electrochemical models combined with KF family based SOC estimation are also seen in Refs. [131,187,268]. Most references used RMSE to evaluate the accuracy of the battery voltage model during the parameter tuning or training phase [17,20,33,36,129,176,256,269–273]. Optimization of the parameters of the battery voltage model using the RMSE as the indicator obviously minimizes the model voltage noise, but it only objectively reduces the model voltage drift to a certain extent. Refs [79,126,270] showed the best average drift of about 5 mV. While parameters change in real applications due to temperature, ageing and cell variations, which will result in a large model voltage drift [274]. Though the voltage drift could be low during the parameter tuning for ECMs, the SOC-OCV curve changes with temperature and ageing, and other parameters vary with cell variations besides temperature and ageing.

[8] Σ_w and Σ_v are covariance matrices of the independent, zero-mean, Gaussian noise processes for the process noise and the measurement noise, respectively.

Regarding the SOC-OCV curve alone, which is considered as the most critical influence factor [32,201], the drift in ECM could easily exceed 10 mV according to Section 4.1. Therefore, the model voltage drift is still the most challenging issue using the KF family based SOC estimation in all working conditions and full cycle life.

Fig. 7(D) demonstrates the influence of the model or measured voltage drift induced error on SOC estimation by KF family algorithm. The black circles indicate the model acknowledged SOC. When there is a model or measured voltage drift error, the model acknowledged SOC is larger or smaller than the real SOC. Fig. 7(D) arbitrarily takes the model acknowledged SOC smaller than the real SOC for an example. As depicted in the figure, the AHC prediction has zero error, but the Kalman correction will add additional error to the estimated SOC because the model acknowledged SOC is always smaller than the real SOC. Finally, the estimated SOC tends to be the model acknowledged SOC after several iterations.

4.3.3. EFC of the KF family based estimation method

Although the EFC of the AHC prediction can be given as shown in Fig. 5(A), the errors should be systematically considered for the KF family based estimation because of the Kalman correction. According to the aforementioned two sections, the error of the AHC prediction can be eliminated to some extent by the KF family algorithm. While the Kalman correction error has two parts, namely the measured voltage drift and the model voltage drift induced errors. Therefore, the EFC of the KF family based estimation method is shown in Fig. 5(C) according to the above analysis. The KF family algorithm in fact uses the predetermined SOC, the measured voltage and the battery voltage model. The predetermined SOC is calculated from the AHC estimation. Therefore, the EFC of the predetermined SOC is similar to that of the AHC estimation in Section 4.2. The only difference is that the initial SOC error is replaced by the estimated SOC error $e_{SOC,E}$ for every iteration. According to the analysis in Section 4.3.1, the influence of the predetermined SOC error on KF family estimation is fairly small, and therefore could be ignored.

Regarding the measured voltage, the error has three parts, i.e., the voltage drift $e_{U,D}$, noise $e_{U,N}$ and sampling frequency $e_{U,SF}$. According to Section 4.3.2, the noise and sampling frequency induced errors can be eliminated.

In addition to the adaptability of the model itself, ageing and temperature are the main factors influencing the model voltage error. Besides, the variation between the modeled and practically used LiBs is also an important factor. However, it is difficult to analyze the influences on the voltage errors for all the factors of every battery model and therefore little literature discussed this issue. Among the typical models like ECMs, machine learning models and electrochemical models, the accuracy of the machine learning model depends on the breadth and accuracy of the training data. And it is also difficult to analyze the battery voltage accuracy regarding each parameter due to the excessive parameters and possible over-fitting problems in the electrochemical model.

In contrast, some simple error flow analysis can be carried out for ECMs. The general ECMs have 3 parts: OCV, ohmic voltage and polarization voltage. The OCV error in the model has the same error as that in Section 4.1 which is influenced by the ageing, temperature and hysteresis. While the ohmic and polarization voltages are also affected by the temperature and ageing. Besides, cell inconsistency also influences the ohmic and polarization voltages. In addition, the ECM itself may ignore the Warburg and other effects so that the voltage error is inevitable when the ECM simulates the LiB dynamics. Hence, with the same conditions, the error of ECM + KF family based SOC estimation is undoubtedly larger than the OCV based estimation.

Without considering the details of models, the model voltage error has two parts: the model noise and drift. The model voltage drift is the main error source affecting KF family based SOC estimation according to Section 4.3.2. However, the model parameter optimization is always proceeded by minimizing the RMSE of the model voltage, but the model voltage drift should be further considered.

According to the whole EFC of the KF family based estimation method, the SOC error by the KF family estimation is principally influenced by the measured voltage drift and model voltage drift. He et al. [126] showed an average SOC estimation error of 1.5% with a mean 6 mV drift. Li et al. [35] also showed that 5 mV drift can result in an error of maximum 3% and average 0.5% in their applications. According to Section 4.3.2, the general SOC error is about $e_{SOC,E} \approx \frac{dSOC}{dOCV}(U_{k,drift} + \hat{U}^{-}_{k,drift})$.

5. Discussion

A number of SOC estimation methods are continually under investigation. Each has its merits and drawbacks. Therefore, some issues still need to be discussed in this section. The first issue is that which method is more reliable and applicable considering all working conditions and full cycle life. The second issue is that which method could be more promising with the rapid development of the battery chemistry, modeling and management as well as the calculation speed and requirements of the estimation accuracy. We are yet unable to give a perfect answer, but some suggestions might be made according to the aforementioned analysis.

5.1. Reliability of the methods

We may roughly give a comparison of the practical SOC estimation methods according to the aforementioned analysis, i.e. the full charge calibration has the highest estimation accuracy, with the OCV based estimation following behind, and the ECM + KF family based and the AHC estimation are the last. However, the problem lies that the full charge calibration and the OCV based estimation can only be used in some special working conditions. Though the full charge calibration has the best estimation accuracy, it can only be used in a standard full charge process theoretically. Under non-standard full charging (the charging rate or temperature is not as that defined in the nominal capacity test), experiments are required to get the relationship between the “full charge” SOC and the non-standard full charging rate and temperature in advance. However, the relationship is not reliable when SOH is considered. Hence, the accuracy of the full charge calibration is lower in non-standard full charging conditions. However, even if the full charge calibration is used in non-standard full charging conditions, we believe it to be an extremely high accuracy SOC estimation method if appropriate corrections are made according to the experimental results. Nevertheless, this method can only be applied in NEVs that may have chances to be fully charged, such as BEV or PHEV. For non-plugin HEVs and FCEVs, the full charge calibration provides no help.

The OCV based estimation also has a relatively high accuracy according to Section 4.1. However, it requires a sufficiently long time to rest in order to measure the terminal voltage as the OCV. Alternatively, the OCV may also be estimated through an empirical model with a short rest period. Nevertheless, the method is still under investigation and has a relatively low accuracy [5,56–58]. We refer the OCV based estimation here as the former method which requires a long rest. Though its accuracy is influenced by ageing and temperature, the OCV based SOC estimation with a sufficiently long time rest to measure the terminal voltage as the OCV has a better accuracy compared to the ECM + KF family based estimation, because the model voltage error is not involved. The OCV based SOC estimation also has a better accuracy than the AHC estimation if the initial SOC of the AHC estimation is calibrated by the OCV based estimation. Nonetheless, when the initial SOC is determined by the full charge calibration, the error of the OCV based SOC estimation may be larger than that of the AHC estimation in a short period. The length of the period is determined by the errors of the full charge calibration, the OCV based SOC estimation and as well as the

accumulative errors in AHC estimation. Nevertheless, the accuracy of the OCV based estimation is better than the AHC estimation and the ECM + KF family based estimation in general. The drawback of the OCV based estimation is also that it can only be used in some special working conditions. For NEVs, there could be opportunities to use the OCV based estimation immediately when the NEVs are started up before the main contactor is closed after a long time shutdown (such as more than 3 h). These conditions are frequently met in NEVs. However, for HEVs and FCEVs with LFP battery packs which often run in the SOC range where the SOC-OCV curve is very flat, the possible error of the OCV based estimation could be very large, and therefore the OCV based estimation is not suitable to be used.

Both the AHC estimation and the ECM + KF family based estimation can be applied in all working conditions, though the accuracies are not as good as the full charge calibration or the OCV based estimation. Obviously, when the full charge calibration could be applied, there is no doubt that the estimated SOC should use the SOC calibrated by the full charge calibration. When the OCV method could be applied, we should roughly evaluate the errors of the OCV based estimation and the current estimated SOC. Generally speaking, the OCV based estimation should be used. However, the problem lies that which method is more reliable considering the AHC estimation and the ECM + KF family based estimation. The ECM + KF family based estimation is generally considered to be more advantageous than the AHC method, but we see almost all references [8,29,30,43,114,145,156,165,178,275–283] used the SOC estimated by the AHC method in the experiments as the reference SOC or true SOC when evaluating the accuracy of the ECM + KF family based estimation. This at least shows that the AHC estimation could be more reliable than the ECM + KF family based estimation in some cases, e.g., in a relatively short experiment, when the initial SOC and the capacity are accurate and the current sensor has a high resolution.

To visually illustrate the reliability of the methods, we demonstrate scenarios that image the SOC errors using different methods in Fig. 8, where the ordinate represents the SOC estimation error and the abscissa indicates the time of a relatively long period. The red dash-dotted line represents the permissible SOC error in practical applications. Although we use one dotted line in the figure to stand for the permissible SOC error, it may be quite different in different applications. For the HEVs and FCEVs whose battery packs usually work in the middle SOC range, the permissible SOC error is allowed to be large. For BEVs and PHEVs, higher SOC accuracy is required due to the requirements of driving range estimation and SOP estimation.

The orange dashed line shows the OCV based SOC error, and the long dashed line indicates that the OCV based estimation cannot be used in all working conditions. Although a straight line is used in the figure, the real error may vary in different working conditions according to Section 4.1. Nevertheless, the relative error compared to the other methods is qualitatively fixed in the figure. The magenta long dashed line shows the full charge calibration based SOC error. Because the error is the lowest and quite stable, the straight line can represent the error very well.

The black curves represent the possible errors by the ECM + KF family estimation. The black short dashed curve indicates the possible SOC error trend by the ECM + KF family estimation. According to Section 4.3, the error showed with the black dashed curve is larger than the OCV based estimation. While in fact, a possible SOC error scene by the ECM + KF family estimation may be as shown with black solid curve, which stabilizes along the error trend curve with fluctuations if the model and measured voltage error maintains.

The blue and green short dashed curves stand for the possible SOC error trends by the AHC method. According to Fig. 6, we see that the trend of the possible SOC error by the AHC method gradually increases with time, and the error would be reset during a recalibration. However, SOC error trends are quite different for the AHC method between the HEVs/FCEVs and EVs/PHEVs applications. The blue and green solid lines respectively demonstrate possible SOC error scenes by the AHC method for HEVs/FCEVs and EVs/PHEVs. There are three main differences:

(1) LiBs in EVs/PHEVs will be frequently fully charged, and therefore have the opportunity to be recalibrated by the full charge calibration. Compared to the OCV based estimation that is the only recalibration method in HEVs/FCEVs, the full charge calibration has a higher accuracy.
(2) On the one hand, SOC of the LiBs in EVs/PHEVs may be recalibrated by the full charge calibration, and therefore could be recalibrated more frequently [20]. On the other hand, LiBs in EVs/PHEVs have almost a full SOC working range, and hence have more suitable SOCs for the OCV based recalibration because they may work in the SOC range where $\frac{dSOC}{dOCV}$ is small [20]. On the contrary, LiBs in HEVs/FCEVs work in a narrow SOC range due to the SOC maintaining strategies, so when the $\frac{dSOC}{dOCV}$ in the narrow working SOC range is large, the error of the OCV based estimation is large and even may not be suitable for an OCV based recalibration.
(3) The capacity induced SOC error will fluctuate with its net charge (discharge) electric quantity (see Fig. 6). Also because of the narrow SOC working range in HEVs/FCEVs, the capacity error has little effect on the SOC error by the AHC method because the net charge

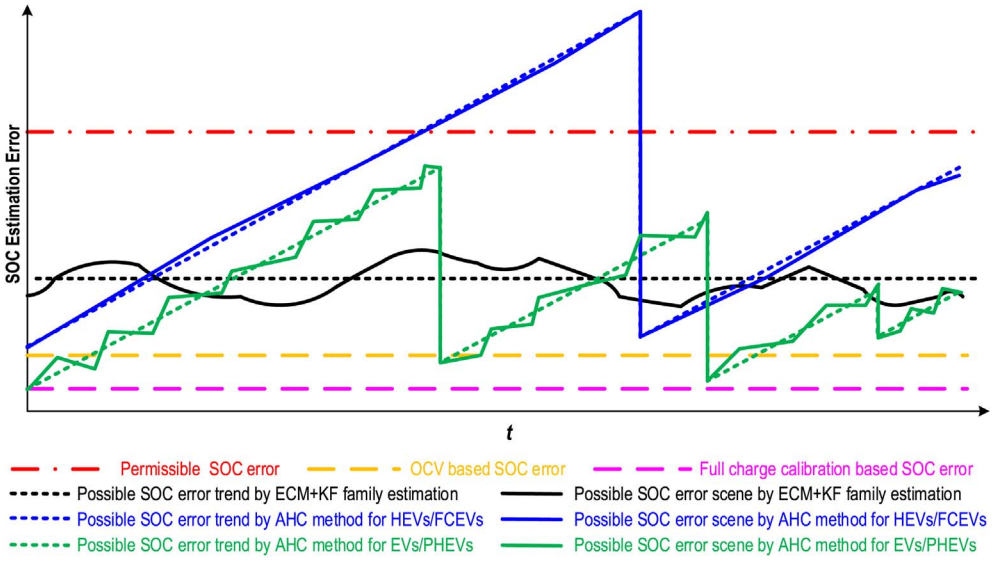

Fig. 8. Possible SOC errors by different online SOC estimation methods in different scenes.

(discharge) electric quantity is very small, which make the possible SOC error scene very close to its error trend. On the contrary, due to a full SOC working range for LiBs in EVs/PHEVs, the net charge (discharge) electric quantity could be as large as the battery capacity. Therefore, the possible SOC error scene by the AHC method for EVs/PHEVs could have a large fluctuation around its error trend. The fluctuation increases with the increasing capacity estimation error and the increasing working SOC range.

Among the three differences, the third one only affects the local SOC error, and the first two make SOC errors by the AHC method in EVs/PHEVs smaller than that in HEVs/FCEVs.

Because there might be a long time that SOC recalibration cannot be applied in HEVs/FCEVs, the SOC estimated by the AHC method is relatively unreliable. While the SOC error by the ECM + KF family estimation is quite stable, so SOC estimation in HEVs/FCEVs using the ECM + KF family estimation is more appropriate.

For LiBs in EVs/PHEVs, due to more frequent recalibration, the accumulated SOC error caused by the AHC method will be eliminated more frequently, and therefore, the accumulative error cannot be too large. In contrast, correcting the initial SOC is one of the important attributes of the ECM + KF family based estimation. When the initial SOC error is large, this attribute could be a benefit, but when the initial SOC is recalibrated by the full charge calibration, the ECM + KF family based estimation will also quickly force the SOC estimation error to its system error. It means that the relatively accurate initial SOC recalibrated by the full charge calibration is not utilized by the ECM + KF family based estimation. This phenomenon leads to a better accuracy for the AHC method than the ECM + KF family based estimation in a short period, so that the SOC estimation by the AHC method can be used as the reference for the evaluating the error of the ECM + KF family based estimation.

The ECM + KF family based estimation has a stable accuracy in the long term, but it cannot fully utilize the high accuracy initial SOC after recalibration. While the AHC method has a high accuracy in a short term after initial SOC recalibration, but the error will increase and exceed the stable error by the ECM + KF family based estimation if the recalibration is not in time. Therefore, a combination of the ECM + KF family based estimation and the AHC method seems a better solution for the SOC estimation in EVs/PHEVs [188]. The question is that how the ECM + KF family based estimation and the AHC method can be combined. A relatively direct method is to respectively estimate the SOC by both the ECM + KF family based estimation and the AHC method, and then choose one of the more reliable one as the combined SOC estimation result according to the actual SOC error [188]. Nevertheless, the problem lies that the online SOC error analysis can be very difficult. Another method is to choose a suitable SOC increment as demonstrated by equation (7).

$$SOC_{com}(k) = \begin{cases} SOC_{com}(k-1) + \Delta SOC_{AH}(k) & |\Delta SOC_{EKF}(k) - \Delta SOC_{AH}(k)| > \lambda \cdot |\Delta SOC_{AH}(k)| \\ SOC_{com}(k-1) + \Delta SOC_{EKF}(k) & |\Delta SOC_{EKF}(k) - \Delta SOC_{AH}(k)| \le \lambda \cdot |\Delta SOC_{AH}(k)| \end{cases} \quad (7)$$

where $SOC_{com}(k)$ is the combined SOC estimation at time k, $\Delta SOC_{AH}(k)$ and $\Delta SOC_{EKF}(k)$ are the SOC increments respectively by the AHC method and the ECM + KF family based estimation at time k, and λ is the coefficient. As discussed in Section 4.2, even if the errors from the current drift $e_{I,D}$, the balancing current e_{BC}, the self-discharge e_{SD}, and CE e_{CE} are very large and the capacity error is 20%, which is almost impossible in vehicle applications, the error of the SOC increment by the AHC method $\Delta SOC_{AH}(k)$ will not exceed 30%. Hence, we may take λ to be 0.3, and equation (7) means that when the SOC increment difference between $\Delta SOC_{AH}(k)$ and $\Delta SOC_{EKF}(k)$ is more than 30% of $\Delta SOC_{AH}(k)$, the SOC increment by the AHC method is used as the combined SOC increment. On the contrary, when the difference is small, we believe the SOC increment by the ECM + KF family based estimation is more reliable. This method cannot only effectively make use of the high accuracy initial SOC after the recalibration, but also inherits the advantage from the ECM + KF family based estimation, which has a stable SOC accuracy in the long term.

In conclusion, with consideration of the SOC estimation accuracy, we think the ECM + KF based SOC estimation is the most suitable in HEVs and FCEVs among the current practical online SOC estimation methods. Regarding LiBs in BEVs and PHEVs, if the full charge calibration and the OCV based estimation could be frequently used to recalibrate the initial SOC, a combination of the ECM + KF family based estimation and the AHC method seems a better solution.

5.2. Future of the methods

With the development of the voltage and current sensor technology, the increasing model accuracy, the reduction in time and space complexity of the algorithm, the improved robustness of the algorithm, and the fast upgrading of the hardware resources, the SOC estimation error will be undoubtedly reduced in the future. At the same time, the online feasible region in Fig. 3 will show a compression in the horizontal direction and extension in the vertical direction. The horizontal compression indicates the higher demands of the SOC estimation accuracy in vehicle applications, and the vertical extension allows more complex models and algorithms due to the progress of the hardware resources in BMSs.

In general, the current online feasible region has a low SOC accuracy demand, while the BMS hardware resources are also difficult to tackle the complex algorithms. Hence, the current online feasible SOC estimation method is dominated by the AHC method, with the full charge calibration and the OCV based estimation as the recalibration methods. Simple ECMs combined with simple algorithms such as EKF are currently the most popular candidate in the practical SOC estimation for online applications. In the future, we believe that the machine learning based SOC estimation will become a new practical SOC estimation method due to the fast development of the machine learning technology. While the electrochemical model based SOC estimation, in our opinion, still has a long way to go for online applications.

As suggested in Section 4.1, the voltage measurement accuracy, especially the voltage drift against the temperature, is very important to the SOC estimation accuracy. However, the voltage measurement drift is expected to be controlled in 1 mV in BMSs. Hence, further improvement of the voltage drift accuracy no longer seems attractive. On the contrary, the OCV estimation error caused by insufficient rest time e_t, and SOC-OCV curve errors caused by the temperature e_T, ageing e_A and hysteresis e_H are the dominate factors. For the current LiB system, SOC-OCV modeling considering all working conditions and full cycle life is rare. For possible newly developed LiB systems in vehicle applications, SOC-OCV modeling considering the errors from the temperature e_T, ageing e_A and hysteresis e_H in all working conditions and full cycle life will be the critical error sources in OCV based estimation. For example, the Si-C based anode LiB system, if successfully applied in NEVs due to its high energy density [284], may have obvious hysteresis [285,286]. Therefore, SOC-OCV modeling considering the hysteresis will be focused then. Nevertheless, after the ageing, temperature and hysteresis compensation, the OCV based estimation still has a high accuracy in most working conditions and is still suitable for SOC calibration in the future.

The initial SOC and the capacity induced SOC errors in the AHC method do not accumulate in the long term. Reducing the current drift error is the key solution for a long-term accurate SOC by the AHC estimation. The accuracies of the shunt resistance and the Hall sensor based current measurement cannot well satisfy the requirement of the current drift in AHC based SOC estimation. The fluxgate based current sensor at present has an accuracy of less than 50 ppm [234,235,287]. If

such types of current sensors could be universally used in BMS, the cumulative error by the AHC method will be greatly reduced. Therefore, in the near future, the current sensor drift may no longer be the main factor of the cumulative error in the AHC method. At the same time, high accuracy current sensors also improve the measurement accuracy of the CE, which will also reduce the error caused by the CE. However, CE and self-discharge rate will change with ageing, temperature and other factors. So, even if a measured CE has a high accuracy, CE induced error is unneglectable in real applications. High accurate current sensors reduce the current drift error so that the required recalibration time is extended, but CE and self-discharge rate induced errors will become the major error sources in AHC method. Especially for advanced battery systems such as LiS batteries, the self-discharge rate could be critical [288–292]. Hence, even with high accurate current sensors widely applied in the future, SOC estimation by the AHC method without recalibration in a long term will definitely exceed the error permitted for online applications.

ECM based estimation needs to combine algorithms to estimate SOC. In our opinion, in the near future, EKF and its derivatives will still dominate the online estimation algorithms in vehicle applications. Compared to more advanced and complex algorithms, EKF is simple and able to eliminate the SOC estimation error in case that the model voltage has zero error. The more advanced and complex algorithms have advantages on the convergence rate and robustness over the EKF algorithm [260], and hence, they perform better in details [15,36,141,178]. However, from the long-term error analysis, when there is some model or measured voltage error, any other more advanced algorithms have little advantage over the EKF algorithm [26,141,260,293]. Compared to the demerits of the EKF, the error induced by the model or measurement drift is more critical. Because the voltage measurement drift could be well controlled in the near further, we suggest that the model voltage drift should be focused in future research for ECM based estimation. RC structure based ECMs cannot well simulate the battery voltage. With additional pure mathematical components such as hysteresis, Warburg effects and fractional-order components adding into the current ECMs, the ECMs could better describe battery electrical characteristics. However, these models still have many questions such as parameter fitting with ageing and temperature change. In addition, LiBs in the low SOC range show very strong nonlinear performance that cannot be well simulated by ECMs [8,34,36,165]. However, the demand of the SOC accuracy is enhanced in the low SOC range because BEV users may suffer from “range anxiety” due to the low SOC accuracy in the low SOC range. Our previous work [8] proposed an enhanced ECM which used the concept of the surface SOC and based on the single particle (SP) model. The proposed model largely reduced the voltage error in the low SOC range. In the future, SOC estimation based on the combined voltage models may be a promising solution [153,159,294,295]. Zhou et al. [153] combined an ECM model and an electrochemical model with PF and showed a better result than the single ones. However, the accuracy of these models needs to be firstly examined before they can be fused.

With the fast development of the artificial intelligence and big data analysis in computer science, machine learning based SOC estimation may have a good prospect. Between the two phases of the machine learning based models, development of the learning phase seems easier to be implemented compared to other more complex artificial intelligence systems. While the training dataset phase may be a big challenge. Because the models based on machine learning strongly depend on the training dataset, the influence of partial data on model accuracy is critical. At present, most training data did not consider real vehicle applications in all working conditions and full cycle life. One problem is that a large number of vehicle test data are still difficult to obtain. This problem may be solved in the future with the development of the data store and transfer technology: the quality of the battery storage data would be improved with optimized sampling frequency, signal accuracy and synchronization [90,177]. The data can be transferred using the wireless technology and stored in the cloud [296,297]. While the other problem seems quite embarrassing. Because the machine learning based battery models are currently all based on the supervised machine learning, accurate SOC is required as the training data. However, SOC in real vehicle applications may have a large error, and if it is used as the training data, the machine learning based battery models obviously cannot achieve an accurate result. Perhaps, unsupervised machine learning may provide a solution. By using accurate SOC data from the experiments in the supervised machine learning, combined with real vehicle data in the unsupervised machine learning, machine learning based SOC may have a promising future.

6. Conclusion

The most important features for SOC estimation methods for LiBs in NEVs are the estimation accuracy and the computational complexity. Every effort is made for various online SOC estimation methods to reliably increase the estimation accuracy as much as possible within the limited on-chip resources. The commonly used SOC estimation methods are reviewed in this paper from a conventional classification, and their general merits and demerits are discussed.

Based on the generally introduced SOC estimation methods, a novel perspective focusing on the error analysis of the SOC estimation methods is proposed. The errors of the SOC estimation methods are analyzed from the views of the measured values, models, algorithms and state parameters. Technical routes of the SOC estimation methods are outlined. The estimation accuracy and the computational complexity are qualitatively compared.

According to the online feasible region, the OCV based estimation, the AHC method and the ECM + KF family based estimation methods are considered as the current online SOC estimation methods. Subsequently, EFCs are proposed to analyze the error sources for these methods. Error sources from the signal measurement to the models and algorithms are investigated. The main error sources of the OCV based estimation method are from the OCV estimation and the SOC-OCV curve. Its error is relatively small but could only be used when LiBs are not working. Therefore, it could be used as a reference or the initial SOC value. Error sources of the AHC method are mainly from the current sensor drift and as well as the inaccurate estimation of the CE and self-discharge. These cumulative errors will make the estimated SOC much deviate from the true value in a long term, but SOC estimation by the AHC method in a short time could still be used as a reference. The most significant error sources for ECM + KF family based estimation method are the model and voltage sensor drifts, which lead to a relatively stationary error compared to the AHC method. However, because of the ECM error, SOC error based on the ECM + KF family is larger than OCV based one.

Both the AHC method and the ECM + KF family based estimation method have their own merits and demerits considering their estimation errors. We suggest in the paper the ECM + KF family based estimation method is suitable for HEVs and FCEVs. While for BEVs and PHEVs, if full charge or the OCV based calibration could be regularly used to achieve an accurate initial SOC, a combination of the AHC method and the ECM + KF family based estimation method might be a better choice.

Finally, future development of the online SOC estimation methods is discussed. The OCV estimation should further focus on modeling the ageing, temperature and hysteresis induced SOC errors, but it will still be an accurate SOC reference for the other methods. The AHC method must firstly reduce the current sensor drift and also need to improve the estimation accuracy of the CE and self-discharge. However, occasional recalibration is still necessary, as the cumulative errors are not vanished. ECM + KF family based estimation method should pay more attention to improving the model voltage drift rather than using a more advanced estimation algorithm. The machine learning based estimation

method needs to further train the model with the real world data and maybe unsupervised machine learning is required because the accurate SOC can hardly be obtained in the real world data.

Acknowledgment

This research is supported by the National Natural Science Foundation of China (NSFC) under the Grant number of 51507102, "Chenguang Program" supported by Shanghai Education Development Foundation and Shanghai Municipal Education Commission under the Grant number of 16CG52, and the International Science & Technology Cooperation Program of China under contract No. 2016YFE0102200.

Abbreviations and nomenclature

AEKF	Adaptive Extended Kalman Filter
AHC	Ampere-hour Counting
ANN	Artificial Neural Network
BEV	Battery Electric Vehicle
BMS	Battery Management System
CDKF	Central Difference Kalman Filter
CE	Coulombic Efficiency
CPU	Central Processing Unit
ECM	Equivalent Circuit Model
EIS	Electrical Impedance Spectroscopy
EKF	Extended Kalman Filter
EMF	Electromotive Force
EMI	Electro Magnetic Interference
EV	Electric Vehicle
FCEV	Fuel Cell Electric Vehicle
FFT	Fast Fourier Transformation
FL	Fuzzy Logic
HEV	Hybrid Electric Vehicle
IRCL	Irreversible Capacity Loss
KF	Kalman Filter
Li	Lithium
LiB	Lithium-ion Battery
LiS	Lithium-Sulfur Battery
LFP	$LiFePO_4$
LS	Least Square
LTO	$Li_4Ti_5O_{12}$
NCM	$LiNi_xCo_yMn_{1-x-y}$
NEV	New Energy Vehicle
OCV	Open Circuit Voltage
PF	Particle Filter
PHEV	Plug-in Hybrid Electric Vehicle
RC	Resistance-Capacitance
RCL	Reversible Capacity Loss
RMSE	Root mean square error
SMC	Sequential Monte Carlo
SMO	Sliding-Mode Observer
SOC	Sate of Charge
SOH	State of Health
SOF	State of Function
SOP	State of Power
SP	Single Particle
SPKF	Sigma Point Kalman Filter
SVR	Support Vector Regression
UKF	Unscented Kalman Filter
C_N	Nominal capacity
C_k	The capacity at time k
I	Current
I_k	The current at time k
L_k	The Kalman gain at time k
$SOC0$	Initial SOC
$\hat{SOC}_k^+$	The estimated SOC at time k
$\hat{SOC}_k^-$	The SOC prediction by the AHC method at time k
$U_{1,k}$	The terminal voltage of the first RC
$U_{2,k}$	The terminal voltage of the second RC
$U_{3,k}$	The terminal voltage of the third RC
U_k	The measured voltage at time k
$\hat{U}_k^-$	The model voltage at time k
$\hat{U}_{k,drift}^-$	The model voltage drift at time k
$U_{k,drift}$	The measured voltage drift at time k
$U_{k,real}$	The real voltage at time k
Σ_w	Covariance matrix of the process noise
Σ_v	Covariance matrix of the measurement noise
e_{BC}	Balancing current estimation error
e_C	Capacity induced error
e_{CE}	CE induced error
$e_{I,D}$	Current drift error
$e_{I,N}$	Current noise error
$e_{I,SF}$	Current error due to signal distortion by the sampling frequency
$e_{M,D}$	Model voltage drift error
$e_{M,N}$	Model voltage noise error
$e_{O,E}$	OCV estimation error
e_{SD}	Self-discharge induced error
e_{SOC0}	Initial SOC induced error
$e_{SOC,E}$	Estimated SOC error
$e_{SOC,M,D}$	SOC error by model voltage drift
$e_{SOC,U,D}$	SOC error by measured voltage drift
$e_{U,D}$	Voltage drift error
$e_{U,N}$	Voltage noise error
$e_{U,SF}$	Voltage error due to signal distortion by the sampling frequency
e_t	OCV estimation error caused by insufficient rest time
h_k	Hysteresis voltage
x_k	Real SOC at time k
$\hat{x}_k^+$	Estimated SOC at time k
$\hat{x}_k^-$	Predetermined SOC at time k
η	Coulombic Efficiency
Δt	The time interval for each estimation iteration
Δx_k	Real SOC change at time k
$\Delta\hat{x}_k^-$	The modification from the AHC prediction at time k
$\Delta\hat{x}_k^+$	The modification from the Kalman correction at time k

References

[1] M. Contestabile, G.J. Offer, R. Slade, F. Jaeger, M. Thoennes, Battery electric vehicles, hydrogen fuel cells and biofuels. Which will be the winner? Energ Environ. Sci. 4 (2011) 3754.
[2] D.U. Eberle, D.R. von Helmolt, Sustainable transportation based on electric vehicle concepts: a brief overview, Energ Environ. Sci. 3 (2010) 689.
[3] L. Lu, X. Han, J. Li, J. Hua, M. Ouyang, A review on the key issues for lithium-ion battery management in electric vehicles, J. Power Sources 226 (2013) 272–288.
[4] Z. Li, J. Huang, B.Y. Liaw, J. Zhang, On state-of-charge determination for lithium-ion batteries, J. Power Sources 348 (2017) 281–301.
[5] W. Waag, C. Fleischer, D.U. Sauer, Critical review of the methods for monitoring of lithium-ion batteries in electric and hybrid vehicles, J. Power Sources 258 (2014) 321–339.
[6] J. Kalawoun, K. Biletska, F. Suard, M. Montaru, From a novel classification of the battery state of charge estimators toward a conception of an ideal one, J. Power Sources 279 (2015) 694–706.
[7] G. Lijun, L. Shengyi, R.A. Dougal, Dynamic lithium-ion battery model for system simulation, IEEE Trans. Compon. Packag. Technol. 25 (2002) 495–505.
[8] M. Ouyang, G. Liu, L. Lu, J. Li, X. Han, Enhancing the estimation accuracy in low state-of-charge area: a novel onboard battery model through surface state of charge determination, J. Power Sources 270 (2014) 221–237.
[9] A. Bartlett, J. Marcicki, S. Onori, G. Rizzoni, X.G. Yang, T. Miller, Electrochemical model-based state of charge and capacity estimation for a composite electrode lithium-ion battery, Ieee T Contr Syst. T 24 (2016) 384–399.
[10] J. Christensen, J. Newman, Cyclable lithium and capacity loss in Li-Ion cells, J. Electrochem Soc. 152 (2005) A818.
[11] D. Wang, J. Coignard, T. Zeng, C. Zhang, S. Saxena, Quantifying electric vehicle battery degradation from driving vs. vehicle-to-grid services, J. Power Sources 332 (2016) 193–203.
[12] M.A. Hannan, M.S.H. Lipu, A. Hussain, A. Mohamed, A review of lithium-ion

battery state of charge estimation and management system in electric vehicle applications: challenges and recommendations, Renew. Sustain. Energy Rev. 78 (2017) 834–854.
[13] J. Zhang, J. Lee, A review on prognostics and health monitoring of Li-ion battery, J. Power Sources 196 (2011) 6007–6014.
[14] M.U. Cuma, T. Koroglu, A comprehensive review on estimation strategies used in hybrid and battery electric vehicles, Renew. Sustain. Energy Rev. 42 (2015) 517–531.
[15] J. Li, J. Klee Barillas, C. Guenther, M.A. Danzer, A comparative study of state of charge estimation algorithms for LiFePO4 batteries used in electric vehicles, J. Power Sources 230 (2013) 244–250.
[16] J. Klee Barillas, J. Li, C. Günther, M.A. Danzer, A comparative study and validation of state estimation algorithms for Li-ion batteries in battery management systems, Appl. Energ 155 (2015) 455–462.
[17] S. Nejad, D.T. Gladwin, D.A. Stone, A systematic review of lumped-parameter equivalent circuit models for real-time estimation of lithium-ion battery states, J. Power Sources 316 (2016) 183–196.
[18] C. Campestrini, T. Heil, S. Kosch, A. Jossen, A comparative study and review of different Kalman filters by applying an enhanced validation method, J. Energy Storage 8 (2016) 142–159.
[19] X. Hu, F. Sun, Y. Zou, Estimation of state of charge of a lithium-ion battery pack for electric vehicles using an adaptive luenberger observer, Energies 3 (2010) 1586–1603.
[20] X. Hu, S. Li, H. Peng, F. Sun, Robustness analysis of State-of-Charge estimation methods for two types of Li-ion batteries, J. Power Sources 217 (2012) 209–219.
[21] Y. Hu, S. Yurkovich, Battery cell state-of-charge estimation using linear parameter varying system techniques, J. Power Sources 198 (2012) 338–350.
[22] L. Xu, J. Wang, Q. Chen, Kalman filtering state of charge estimation for battery management system based on a stochastic fuzzy neural network battery model, Energ Convers. Manage 53 (2012) 33–39.
[23] R. Xiong, X. Gong, C.C. Mi, F. Sun, A robust state-of-charge estimator for multiple types of lithium-ion batteries using adaptive extended Kalman filter, J. Power Sources 243 (2013) 805–816.
[24] J. Xu, C.C. Mi, B. Cao, J. Cao, A new method to estimate the state of charge of lithium-ion batteries based on the battery impedance model, J. Power Sources 233 (2013) 277–284.
[25] X. Chen, W. Shen, Z. Cao, A. Kapoor, A novel approach for state of charge estimation based on adaptive switching gain sliding mode observer in electric vehicles, J. Power Sources 246 (2014) 667–678.
[26] J. Du, Z. Liu, Y. Wang, State of charge estimation for Li-ion battery based on model from extreme learning machine, Control Eng. Pract. 26 (2014) 11–19.
[27] J. Li, J. Klee Barillas, C. Guenther, M.A. Danzer, Sequential Monte Carlo filter for state estimation of LiFePO4 batteries based on an online updated model, J. Power Sources 247 (2014) 156–162.
[28] X. Liu, Z. Chen, C. Zhang, J. Wu, A novel temperature-compensated model for power Li-ion batteries with dual-particle-filter state of charge estimation, Appl. Energ 123 (2014) 263–272.
[29] Y. Tian, B. Xia, W. Sun, Z. Xu, W. Zheng, A modified model based state of charge estimation of power lithium-ion batteries using unscented Kalman filter, J. Power Sources 270 (2014) 619–626.
[30] R. Xiong, F. Sun, X. Gong, C. Gao, A data-driven based adaptive state of charge estimator of lithium-ion polymer battery used in electric vehicles, Appl. Energ 113 (2014) 1421–1433.
[31] V.-H. Duong, H.A. Bastawrous, K. Lim, K.W. See, P. Zhang, S.X. Dou, Online state of charge and model parameters estimation of the LiFePO4 battery in electric vehicles using multiple adaptive forgetting factors recursive least-squares, J. Power Sources 296 (2015) 215–224.
[32] C. Zhang, L.Y. Wang, X. Li, W. Chen, G.G. Yin, J. Jiang, Robust and adaptive estimation of state of charge for lithium-ion batteries, Ieee T Ind. Electron 62 (2015) 4948–4957.
[33] Y. Zou, X. Hu, H. Ma, S.E. Li, Combined State of Charge and State of Health estimation over lithium-ion battery cell cycle lifespan for electric vehicles, J. Power Sources 273 (2015) 793–803.
[34] H. He, R. Xiong, J. Peng, Real-time estimation of battery state-of-charge with unscented Kalman filter and RTOS μCOS-II platform, Appl. Energ 162 (2016) 1410–1418.
[35] Y. Li, C. Wang, J. Gong, A combination Kalman filter approach for State of Charge estimation of lithium-ion battery considering model uncertainty, Energy 109 (2016) 933–946.
[36] F. Yang, Y. Xing, D. Wang, K.-L. Tsui, A comparative study of three model-based algorithms for estimating state-of-charge of lithium-ion batteries under a new combined dynamic loading profile, Appl. Energ 164 (2016) 387–399.
[37] B. Pattipati, B. Balasingam, G.V. Avvari, K.R. Pattipati, Y. Bar-Shalom, Open circuit voltage characterization of lithium-ion batteries, J. Power Sources 269 (2014) 317–333.
[38] M.A. Roscher, D.U. Sauer, Dynamic electric behavior and open-circuit-voltage modeling of LiFePO4-based lithium ion secondary batteries, J. Power Sources 196 (2011) 331–336.
[39] L. Zhu, Z. Sun, H. Dai, X. Wei, A novel modeling methodology of open circuit voltage hysteresis for LiFePO4 batteries based on an adaptive discrete Preisach model, Appl. Energ 155 (2015) 91–109.
[40] A. Marongiu, F.G.W. Nußbaum, W. Waag, M. Garmendia, D.U. Sauer, Comprehensive study of the influence of aging on the hysteresis behavior of a lithium iron phosphate cathode-based lithium ion battery – an experimental investigation of the hysteresis, Appl. Energ 171 (2016) 629–645.
[41] G. Dong, J. Wei, C. Zhang, Z. Chen, Online state of charge estimation and open circuit voltage hysteresis modeling of LiFePO4 battery using invariant imbedding method, Appl. Energ 162 (2016) 163–171.
[42] A. Barai, W.D. Widanage, J. Marco, A. McGordon, P. Jennings, A study of the open circuit voltage characterization technique and hysteresis assessment of lithium-ion cells, J. Power Sources 295 (2015) 99–107.
[43] T. Huria, G. Ludovici, G. Lutzemberger, State of charge estimation of high power lithium iron phosphate cells, J. Power Sources 249 (2014) 92–102.
[44] Z. Deng, L. Yang, Y. Cai, H. Deng, L. Sun, Online available capacity prediction and state of charge estimation based on advanced data-driven algorithms for lithium iron phosphate battery, Energy 112 (2016) 469–480.
[45] C. Zhang, K. Li, J. Deng, S. Song, Improved realtime state-of-charge estimation of LiFePO $_{\\\\\\\\\\\\\\\\\boldsymbol 4}$ battery based on a novel thermo-electric model, Ieee T Ind. Electron 64 (2017) 654–663.
[46] X. Han, M. Ouyang, L. Lu, J. Li, Y. Zheng, Z. Li, A comparative study of commercial lithium ion battery cycle life in electrical vehicle: aging mechanism identification, J. Power Sources 251 (2014) 38–54.
[47] Y. Zheng, M. Ouyang, L. Lu, J. Li, X. Han, L. Xu, H. Ma, T.A. Dollmeyer, V. Freyermuth, Cell state-of-charge inconsistency estimation for LiFePO4 battery pack in hybrid electric vehicles using mean-difference model, Appl. Energ 111 (2013) 571–580.
[48] C. Weng, Y. Cui, J. Sun, H. Peng, On-board state of health monitoring of lithium-ion batteries using incremental capacity analysis with support vector regression, J. Power Sources 235 (2013) 36–44.
[49] L. Lavigne, J. Sabatier, J.M. Francisco, F. Guillemard, A. Noury, Lithium-ion Open Circuit Voltage (OCV) curve modelling and its ageing adjustment, J. Power Sources 324 (2016) 694–703.
[50] M. Fleckenstein, O. Bohlen, M.A. Roscher, B. Bäker, Current density and state of charge inhomogeneities in Li-ion battery cells with LiFePO4 as cathode material due to temperature gradients, J. Power Sources 196 (2011) 4769–4778.
[51] Y. Xing, W. He, M. Pecht, K.L. Tsui, State of charge estimation of lithium-ion batteries using the open-circuit voltage at various ambient temperatures, Appl. Energ 113 (2014) 106–115.
[52] Y. Zhang, W. Song, S. Lin, Z. Feng, A novel model of the initial state of charge estimation for LiFePO4 batteries, J. Power Sources 248 (2014) 1028–1033.
[53] C. Unterrieder, C. Zhang, M. Lunglmayr, R. Priewasser, S. Marsili, M. Huemer, Battery state-of-charge estimation using approximate least squares, J. Power Sources 278 (2015) 274–286.
[54] Z. Yanhui, S. Wenji, X. Guoqing, Relaxation effect analysis on the initial state of charge for LiNi0.5Co0.2Mn0.3O2/graphite battery, Energy 74 (2014) 368–373.
[55] M. Petzl, M.A. Danzer, Advancements in OCV measurement and analysis for lithium-ion batteries, Ieee T Energy Conver 28 (2013) 675–681.
[56] L. Pei, T. Wang, R. Lu, C. Zhu, Development of a voltage relaxation model for rapid open-circuit voltage prediction in lithium-ion batteries, J. Power Sources 253 (2014) 412–418.
[57] L. Pei, R. Lu, C. Zhu, Relaxation model of the open-circuit voltage for state-of-charge estimation in lithium-ion batteries, IET Electr. Syst. Transp. 3 (2013) 112–117.
[58] W. Waag, D.U. Sauer, Adaptive estimation of the electromotive force of the lithium-ion battery after current interruption for an accurate state-of-charge and capacity determination, Appl. Energ 111 (2013) 416–427.
[59] H. Wenzl, Batteries and fuel cells, Efficiency, Encyclopedia of Electrochemical Power Sources, Elsevier, Amsterdam, 2009, pp. 544–551.
[60] C. Truchot, M. Dubarry, B.Y. Liaw, State-of-charge estimation and uncertainty for lithium-ion battery strings, Appl. Energ 119 (2014) 218–227.
[61] X. Tang, Y. Wang, Z. Chen, A method for state-of-charge estimation of LiFePO4 batteries based on a dual-circuit state observer, J. Power Sources 296 (2015) 23–29.
[62] M. Mastali, J. Vazquez-Arenas, R. Fraser, M. Fowler, S. Afshar, M. Stevens, Battery state of the charge estimation using Kalman filtering, J. Power Sources 239 (2013) 294–307.
[63] S.-L. Wu, H.-C. Chen, S.-R. Chou, Fast estimation of state of charge for lithium-ion batteries, Energies 7 (2014) 3438–3452.
[64] W. Huang, J.A.A. Qahouq, An online battery impedance measurement method using DC/DC power converter control, Ieee T Ind. Electron 61 (2014) 5987–5995.
[65] D.A. Howey, P.D. Mitcheson, V. Yufit, G.J. Offer, N.P. Brandon, Online measurement of battery impedance using motor controller excitation, Ieee T Veh. Technol. 63 (2014) 2557–2566.
[66] J.P. Schmidt, E. Ivers-Tiffée, Pulse-fitting – a novel method for the evaluation of pulse measurements, demonstrated for the low frequency behavior of lithium-ion cells, J. Power Sources 315 (2016) 316–323.
[67] D. Klotz, M. Schönleber, J.P. Schmidt, E. Ivers-Tiffée, New approach for the calculation of impedance spectra out of time domain data, Electrochim Acta 56 (2011) 8763–8769.
[68] W. Waag, S. Käbitz, D.U. Sauer, Experimental investigation of the lithium-ion battery impedance characteristic at various conditions and aging states and its influence on the application, Appl. Energ 102 (2013) 885–897.
[69] A. Eddahech, O. Briat, E. Woirgard, J.M. Vinassa, Remaining useful life prediction of lithium batteries in calendar ageing for automotive applications, Microelectron. Reliab 52 (2012) 2438–2442.
[70] T. Momma, M. Matsunaga, D. Mukoyama, T. Osaka, Ac impedance analysis of lithium ion battery under temperature control, J. Power Sources 216 (2012) 304–307.
[71] M. Ecker, J.B. Gerschler, J. Vogel, S. Käbitz, F. Hust, P. Dechent, D.U. Sauer, Development of a lifetime prediction model for lithium-ion batteries based on extended accelerated aging test data, J. Power Sources 215 (2012) 248–257.
[72] C. Huang, S. Zhuang, F. Tu, Electrode/electrolyte interfacial behaviors of LiCoO2/

mixed graphite Li-Ion cells during operation and storage, J. Electrochem Soc. 160 (2012) A376–A382.
[73] S.E. Li, B. Wang, H. Peng, X. Hu, An electrochemistry-based impedance model for lithium-ion batteries, J. Power Sources 258 (2014) 9–18.
[74] J.G. Zhu, Z.C. Sun, X.Z. Wei, H.F. Dai, A new lithium-ion battery internal temperature on-line estimate method based on electrochemical impedance spectroscopy measurement, J. Power Sources 274 (2015) 990–1004.
[75] P. Taheri, S. Hsieh, M. Bahrami, Investigating electrical contact resistance losses in lithium-ion battery assemblies for hybrid and electric vehicles, J. Power Sources 196 (2011) 6525–6533.
[76] T. Baumhöfer, M. Brühl, S. Rothgang, D.U. Sauer, Production caused variation in capacity aging trend and correlation to initial cell performance, J. Power Sources 247 (2014) 332–338.
[77] J. Gomez, R. Nelson, E.E. Kalu, M.H. Weatherspoon, J.P. Zheng, Equivalent circuit model parameters of a high-power Li-ion battery: thermal and state of charge effects, J. Power Sources 196 (2011) 4826–4831.
[78] C. Liu, W. Liu, L. Wang, G. Hu, L. Ma, B. Ren, A new method of modeling and state of charge estimation of the battery, J. Power Sources 320 (2016) 1–12.
[79] Y. Zou, S.E. Li, B. Shao, B. Wang, State-space model with non-integer order derivatives for lithium-ion battery, Appl. Energ 161 (2016) 330–336.
[80] F. Zhong, H. Li, S. Zhong, Q. Zhong, C. Yin, An SOC estimation approach based on adaptive sliding mode observer and fractional order equivalent circuit model for lithium-ion batteries, Commun. Nonlinear Sci. 24 (2015) 127–144.
[81] B. Wang, Z. Liu, S.E. Li, S.J. Moura, H. Peng, State-of-Charge estimation for lithium-ion batteries based on a nonlinear fractional model, Ieee T Contr Syst. T 25 (2017) 3–11.
[82] Y.-H. Chiang, W.-Y. Sean, J.-C. Ke, Online estimation of internal resistance and open-circuit voltage of lithium-ion batteries in electric vehicles, J. Power Sources 196 (2011) 3921–3932.
[83] T. Feng, L. Yang, X. Zhao, H. Zhang, J. Qiang, Online identification of lithium-ion battery parameters based on an improved equivalent-circuit model and its implementation on battery state-of-power prediction, J. Power Sources 281 (2015) 192–203.
[84] H. Dai, T. Xu, L. Zhu, X. Wei, Z. Sun, Adaptive model parameter identification for large capacity Li-ion batteries on separated time scales, Appl. Energ 184 (2016) 119–131.
[85] K. Lim, H.A. Bastawrous, V.-H. Duong, K.W. See, P. Zhang, S.X. Dou, Fading Kalman filter-based real-time state of charge estimation in LiFePO4 battery-powered electric vehicles, Appl. Energ 169 (2016) 40–48.
[86] Z. Wei, S. Meng, B. Xiong, D. Ji, K.J. Tseng, Enhanced online model identification and state of charge estimation for lithium-ion battery with a FBCRLS based observer, Appl. Energ 181 (2016) 332–341.
[87] S. Sepasi, R. Ghorbani, B.Y. Liaw, A novel on-board state-of-charge estimation method for aged Li-ion batteries based on model adaptive extended Kalman filter, J. Power Sources 245 (2014) 337–344.
[88] S. Sepasi, R. Ghorbani, B.Y. Liaw, Improved extended Kalman filter for state of charge estimation of battery pack, J. Power Sources 255 (2014) 368–376.
[89] B. Balasingam, G.V. Avvari, B. Pattipati, K.R. Pattipati, Y. Bar-Shalom, A robust approach to battery fuel gauging, part I: real time model identification, J. Power Sources 272 (2014) 1142–1153.
[90] X. Kong, Y. Zheng, M. Ouyang, X. Li, L. Lu, J. Li, Z. Zhang, Signal synchronization for massive data storage in modular battery management system with controller area network, Appl. Energ 197 (2017) 52–62.
[91] F. Sun, R. Xiong, H. He, W. Li, J.E.E. Aussems, Model-based dynamic multi-parameter method for peak power estimation of lithium–ion batteries, Appl. Energ 96 (2012) 378–386.
[92] R. Ahmed, M.E. Sayed, I. Arasaratnam, J. Tjong, S. Habibi, Reduced-order electrochemical model parameters identification and SOC estimation for healthy and aged Li-Ion batteries Part I: parameterization model development for healthy batteries, Ieee J. Em Sel. Top. P 2 (2014) 659–677.
[93] M. Doyle, J. Newman, A.S. Gozdz, C.N. Schmutz, J.M. Tarascon, Comparison of modeling predictions with experimental data from plastic lithium ion cells, J. Electrochem Soc. 143 (1996) 1890–1903.
[94] M. Doyle, T.F. Fuller, J. Newman, Modeling of galvanostatic charge and discharge of the lithium/polymer/insertion cell, J. Electrochem Soc. 140 (1993) 1526–1533.
[95] V. Ramadesigan, P.W.C. Northrop, S. De, S. Santhanagopalan, R.D. Braatz, V.R. Subramanian, Modeling and simulation of lithium-ion batteries from a systems engineering perspective, J. Electrochem Soc. 159 (2012) R31–R45.
[96] J. Marcicki, M. Canova, A.T. Conlisk, G. Rizzoni, Design and parametrization analysis of a reduced-order electrochemical model of graphite/LiFePO4 cells for SOC/SOH estimation, J. Power Sources 237 (2013) 310–324.
[97] E. Namor, D. Torregrossa, R. Cherkaoui, M. Paolone, Parameter identification of a lithium-ion cell single-particle model through non-invasive testing, J. Energy Storage 12 (2017) 138–148.
[98] J. Li, L. Wang, C. Lyu, H. Wang, X. Liu, New method for parameter estimation of an electrochemical-thermal coupling model for LiCoO2 battery, J. Power Sources 307 (2016) 220–230.
[99] N. Yang, X. Zhang, G. Li, State-of-charge estimation for lithium ion batteries via the simulation of lithium distribution in the electrode particles, J. Power Sources 272 (2014) 68–78.
[100] P. Tagade, K.S. Hariharan, P. Gambhire, S.M. Kolake, T. Song, D. Oh, T. Yeo, S. Doo, Recursive Bayesian filtering framework for lithium-ion cell state estimation, J. Power Sources 306 (2016) 274–288.
[101] J. Li, Q. Lai, L. Wang, C. Lyu, H. Wang, A method for SOC estimation based on simplified mechanistic model for LiFePO4 battery, Energy 114 (2016) 1266–1276.
[102] Y. Wang, H. Fang, Z. Sahinoglu, T. Wada, S. Hara, Adaptive estimation of the state of charge for lithium-ion batteries: nonlinear geometric observer approach, Ieee T Contr Syst. T 23 (2015) 948–962.
[103] J. Li, L. Wang, C. Lyu, M. Pecht, State of charge estimation based on a simplified electrochemical model for a single LiCoO2 battery and battery pack, Energy 133 (2017) 572–583.
[104] X. Han, M. Ouyang, L. Lu, J. Li, Simplification of physics-based electrochemical model for lithium ion battery on electric vehicle. Part II: pseudo-two-dimensional model simplification and state of charge estimation, J. Power Sources 278 (2015) 814–825.
[105] R. Ahmed, M.E. Sayed, I. Arasaratnam, J. Tjong, S. Habibi, Reduced-order electrochemical model parameters identification and state of charge estimation for healthy and aged Li-Ion Batteries-Part II: aged battery model and state of charge estimation, Ieee J. Em Sel. Top. P 2 (2014) 678–690.
[106] L. Kang, X. Zhao, J. Ma, A new neural network model for the state-of-charge estimation in the battery degradation process, Appl. Energ 121 (2014) 20–27.
[107] M. Charkhgard, M. Farrokhi, State-of-Charge estimation for lithium-ion batteries using neural networks and EKF, Ieee T Ind. Electron 57 (2010) 4178–4187.
[108] J.N. Hu, J.J. Hu, H.B. Lin, X.P. Li, C.L. Jiang, X.H. Qiu, W.S. Li, State-of-charge estimation for battery management system using optimized support vector machine for regression, J. Power Sources 269 (2014) 682–693.
[109] G. Bai, P. Wang, C. Hu, A self-cognizant dynamic system approach for prognostics and health management, J. Power Sources 278 (2015) 163–174.
[110] X. Dang, L. Yan, K. Xu, X. Wu, H. Jiang, H. Sun, Open-circuit voltage-based state of charge estimation of lithium-ion battery using dual neural network fusion battery model, Electrochim Acta 188 (2016) 356–366.
[111] X. Chen, W. Shen, M. Dai, Z. Cao, J. Jin, A. Kapoor, Robust adaptive sliding-mode observer using RBF neural network for lithium-ion battery state of charge estimation in electric vehicles, Ieee T Veh. Technol. 65 (2016) 1936–1947.
[112] H. Sheng, J. Xiao, Electric vehicle state of charge estimation: nonlinear correlation and fuzzy support vector machine, J. Power Sources 281 (2015) 131–137.
[113] J.C.Á. Antón, P.J.G. Nieto, C.B. Viejo, J.A.V. Vilán, Support vector machines used to estimate the battery state of charge, Ieee T Power Electr. 28 (2013) 5919–5926.
[114] J. Meng, G. Luo, F. Gao, Lithium polymer battery state-of-charge estimation based on adaptive unscented Kalman filter and support vector machine, Ieee T Power Electr. 31 (2016) 2226–2238.
[115] A. Alfi, M. Charkhgard, M.H. Zarif, Hybrid state of charge estimation for lithium-ion batteries: design and implementation, IET Power Electron. 7 (2014) 2758–2764.
[116] Z. Wei, T.M. Lim, M. Skyllas-Kazacos, N. Wai, K.J. Tseng, Online state of charge and model parameter co-estimation based on a novel multi-timescale estimator for vanadium redox flow battery, Appl. Energ 172 (2016) 169–179.
[117] S.J. Moura, N.A. Chaturvedi, M. Krstić, Adaptive partial differential equation observer for battery state-of-charge/state-of-health estimation via an electrochemical model, J. Dyn. Syst. Meas. Control 136 (2013) 011015.
[118] W. He, N. Williard, C. Chen, M. Pecht, State of charge estimation for Li-ion batteries using neural network modeling and unscented Kalman filter-based error cancellation, Electr. Power Energy Syst. 62 (2014) 783–791.
[119] X. Hu, S.E. Li, Y. Yang, Advanced machine learning approach for lithium-ion battery state estimation in electric vehicles, IEEE Trans. Transp. Electrification 2 (2016) 140–149.
[120] H. Sheng, J. Xiao, P. Wang, Lithium iron phosphate battery electric vehicle state-of-charge estimation based on evolutionary gaussian mixture regression, Ieee T Ind. Electron 64 (2017) 544–551.
[121] H. Rahimi-Eichi, F. Baronti, M.Y. Chow, Online adaptive parameter identification and state-of-charge coestimation for lithium-polymer battery cells, Ieee T Ind. Electron 61 (2014) 2053–2061.
[122] M.R. Khan, G. Mulder, J. Van Mierlo, An online framework for state of charge determination of battery systems using combined system identification approach, J. Power Sources 246 (2014) 629–641.
[123] J.C.Á. Antón, P.J.G. Nieto, E.G. Gonzalo, J.C.V. Pérez, M.G. Vega, C.B. Viejo, A new predictive model for the state-of-charge of a high-power lithium-ion cell based on a PSO-optimized multivariate adaptive regression spline approach, Ieee T Veh. Technol. 65 (2016) 4197–4208.
[124] W. Wang, H.S.-H. Chung, J. Zhang, Near-real-time parameter estimation of an electrical battery model with multiple time constants and SOC-dependent capacitance, Ieee T Power Electr. 29 (2014) 5905–5920.
[125] F. Feng, R. Lu, G. Wei, C. Zhu, Online estimation of model parameters and state of charge of LiFePO4 batteries using a novel open-circuit voltage at various ambient temperatures, Energies 8 (2015) 2950–2976.
[126] H. He, X. Zhang, R. Xiong, Y. Xu, H. Guo, Online model-based estimation of state-of-charge and open-circuit voltage of lithium-ion batteries in electric vehicles, Energy 39 (2012) 310–318.
[127] H. He, R. Xiong, H. Guo, Online estimation of model parameters and state-of-charge of LiFePO4 batteries in electric vehicles, Appl. Energ 89 (2012) 413–420.
[128] H. Dai, X. Wei, Z. Sun, J. Wang, W. Gu, Online cell SOC estimation of Li-ion battery packs using a dual time-scale Kalman filtering for EV applications, Appl. Energ 95 (2012) 227–237.
[129] X. Zhang, Y. Wang, D. Yang, Z. Chen, An on-line estimation of battery pack parameters and state-of-charge using dual filters based on pack model, Energy 115 (2016) 219–229.
[130] G. Dong, Z. Chen, J. Wei, C. Zhang, P. Wang, An online model-based method for state of energy estimation of lithium-ion batteries using dual filters, J. Power Sources 301 (2016) 277–286.
[131] C. Zou, C. Manzie, D. Nešić, A.G. Kallapur, Multi-time-scale observer design for state-of-charge and state-of-health of a lithium-ion battery, J. Power Sources 335 (2016) 121–130.

[132] A. Tulsyan, Y. Tsai, R.B. Gopaluni, R.D. Braatz, State-of-charge estimation in lithium-ion batteries: a particle filter approach, J. Power Sources 331 (2016) 208–223.
[133] L. Zheng, L. Zhang, J. Zhu, G. Wang, J. Jiang, Co-estimation of state-of-charge, capacity and resistance for lithium-ion batteries based on a high-fidelity electrochemical model, Appl. Energ 180 (2016) 424–434.
[134] S. Dey, B. Ayalew, P. Pisu, Nonlinear robust observers for state-of-charge estimation of lithium-ion cells based on a reduced electrochemical model, Ieee T Contr Syst. T 23 (2015) 1935–1942.
[135] G. Bai, P. Wang, C. Hu, M. Pecht, A generic model-free approach for lithium-ion battery health management, Appl. Energ 135 (2014) 247–260.
[136] M.A. Roscher, O.S. Bohlen, D.U. Sauer, Reliable state estimation of multicell lithium-ion battery systems, Ieee T Energy Conver 26 (2011) 737–743.
[137] Y. He, W. Liu, B.J. Koch, Battery algorithm verification and development using hardware-in-the-loop testing, J. Power Sources 195 (2010) 2969–2974.
[138] S. Wang, M. Verbrugge, J.S. Wang, P. Liu, Multi-parameter battery state estimator based on the adaptive and direct solution of the governing differential equations, J. Power Sources 196 (2011) 8735–8741.
[139] G.L. Plett, Extended Kalman filtering for battery management systems of LiPB-based HEV battery packs, J. Power Sources 134 (2004) 252–261.
[140] G.L. Plett, Sigma-point Kalman filtering for battery management systems of LiPB-based HEV battery packs, J. Power Sources 161 (2006) 1369–1384.
[141] D. Li, J. Ouyang, H. Li, J. Wan, State of charge estimation for LiMn2O4 power battery based on strong tracking sigma point Kalman filter, J. Power Sources 279 (2015) 439–449.
[142] H. He, Y. Zhang, R. Xiong, C. Wang, A novel Gaussian model based battery state estimation approach: state-of-Energy, Appl. Energ 151 (2015) 41–48.
[143] M. Partovibakhsh, G. Liu, An adaptive unscented Kalman filtering approach for online estimation of model parameters and state-of-charge of lithium-ion batteries for autonomous mobile robots, Ieee T Contr Syst. T 23 (2015) 357–363.
[144] Y. Ma, X. Zhou, B. Li, H. Chen, Fractional modeling and SOC estimation of lithium-ion battery, IEEE/CAA J. Automatica Sinica 3 (2016) 281–287.
[145] M.S.E. Din, M.F. Abdel-Hafez, A.A. Hussein, Enhancement in Li-Ion battery cell state-of-charge estimation under uncertain model statistics, Ieee T Veh. Technol. 65 (2016) 4608–4618.
[146] R. Xiong, H. He, F. Sun, X. Liu, Z. Liu, Model-based state of charge and peak power capability joint estimation of lithium-ion battery in plug-in hybrid electric vehicles, J. Power Sources 229 (2013) 159–169.
[147] W. Gao, Y. Zou, F. Sun, X. Hu, Y. Yu, S. Feng, Data pieces-based parameter identification for lithium-ion battery, J. Power Sources 328 (2016) 174–184.
[148] R. Xiong, F. Sun, H. He, T.D. Nguyen, A data-driven adaptive state of charge and power capability joint estimator of lithium-ion polymer battery used in electric vehicles, Energy 63 (2013) 295–308.
[149] S. Schwunk, N. Armbruster, S. Straub, J. Kehl, M. Vetter, Particle filter for state of charge and state of health estimation for lithium–iron phosphate batteries, J. Power Sources 239 (2013) 705–710.
[150] L. Zhong, C. Zhang, Y. He, Z. Chen, A method for the estimation of the battery pack state of charge based on in-pack cells uniformity analysis, Appl. Energ 113 (2014) 558–564.
[151] C. Burgos-Mellado, M.E. Orchard, M. Kazerani, R. Cárdenas, D. Sáez, Particle-filtering-based estimation of maximum available power state in Lithium-Ion batteries, Appl. Energ 161 (2016) 349–363.
[152] M. Ye, H. Guo, B. Cao, A model-based adaptive state of charge estimator for a lithium-ion battery using an improved adaptive particle filter, Appl. Energ 190 (2017) 740–748.
[153] D. Zhou, K. Zhang, A. Ravey, F. Gao, A. Miraoui, Online estimation of lithium polymer batteries state-of-charge using particle filter-based data fusion with multimodels approach, Ieee T Ind. Appl. 52 (2016) 2582–2595.
[154] X. Chen, W. Shen, Z. Cao, A. Kapoor, Adaptive gain sliding mode observer for state of charge estimation based on combined battery equivalent circuit model, Comput. Chem. Eng. 64 (2014) 114–123.
[155] Y. Tian, B. Xia, M. Wang, W. Sun, Z. Xu, Comparison study on two model-based adaptive algorithms for SOC estimation of lithium-ion batteries in electric vehicles, Energies 7 (2014) 8446–8464.
[156] D. Kim, T. Goh, M. Park, S. Kim, Fuzzy sliding mode observer with grey prediction for the estimation of the state-of-charge of a lithium-ion battery, Energies 8 (2015) 12409–12428.
[157] Q. Chen, J. Jiang, H. Ruan, C. Zhang, Simply designed and universal sliding mode observer for the SOC estimation of lithium-ion batteries, IET Power Electron. 10 (2017) 697–705.
[158] J. Li, J. Klee Barillas, C. Guenther, M.A. Danzer, Multicell state estimation using variation based sequential Monte Carlo filter for automotive battery packs, J. Power Sources 277 (2015) 95–103.
[159] C. Lin, H. Mu, R. Xiong, W. Shen, A novel multi-model probability battery state of charge estimation approach for electric vehicles using H-infinity algorithm, Appl. Energ 166 (2016) 76–83.
[160] J. Yan, G. Xu, H. Qian, Y. Xu, Robust state of charge estimation for hybrid electric vehicles: framework and algorithms, Energies 3 (2010) 1654–1672.
[161] F. Zhang, G. Liu, L. Fang, H. Wang, Estimation of battery state of charge with H-infinity observer: applied to a robot for inspecting power transmission lines, Ieee T Ind. Electron 59 (2012) 1086–1095.
[162] Y. Zhang, C. Zhang, X. Zhang, State-of-charge estimation of the lithium-ion battery system with time-varying parameter for hybrid electric vehicles, IET Control Theory & Appl. 8 (2014) 160–167.
[163] M. Charkhgard, M.H. Zarif, Design of adaptiveH ∞ filter for implementing on state-of-charge estimation based on battery state-of-charge-varying modelling, IET Power Electron. 8 (2015) 1825–1833.
[164] Y. Zhang, R. Xiong, H. He, W. Shen, Lithium-ion battery pack state of charge and state of energy estimation algorithms using a hardware-in-the-loop validation, Ieee T Power Electr. 32 (2017) 4421–4431.
[165] R. Xiong, F. Sun, Z. Chen, H. He, A data-driven multi-scale extended Kalman filtering based parameter and state estimation approach of lithium-ion olymer battery in electric vehicles, Appl. Energ 113 (2014) 463–476.
[166] C. Hu, B.D. Youn, J. Chung, A multiscale framework with extended Kalman filter for lithium-ion battery SOC and capacity estimation, Appl. Energ 92 (2012) 694–704.
[167] D. Andre, C. Appel, T. Soczka-Guth, D.U. Sauer, Advanced mathematical methods of SOC and SOH estimation for lithium-ion batteries, J. Power Sources 224 (2013) 20–27.
[168] T. Gallien, H. Krenn, R. Fischer, S. Lauterbach, B. Schweighofer, H. Wegleiter, Magnetism versus LiFePO4 Battery's state of charge: a feasibility study for magnetic-based charge monitoring, Ieee T Instrum. Meas. 64 (2015) 2959–2964.
[169] J. Cannarella, C.B. Arnold, State of health and charge measurements in lithium-ion batteries using mechanical stress, J. Power Sources 269 (2014) 7–14.
[170] H. Dai, C. Yu, X. Wei, Z. Sun, State of charge estimation for lithium-ion pouch batteries based on stress measurement, Energy 129 (2017) 16–27.
[171] A.G. Hsieh, S. Bhadra, B.J. Hertzberg, P.J. Gjeltema, A. Goy, J.W. Fleischer, D.A. Steingart, Electrochemical-acoustic time of flight: in operando correlation of physical dynamics with battery charge and health, Energ Environ. Sci. 8 (2015) 1569–1577.
[172] L. Gold, T. Bach, W. Virsik, A. Schmitt, J. Müller, T.E.M. Staab, G. Sextl, Probing lithium-ion batteries' state-of-charge using ultrasonic transmission – concept and laboratory testing, J. Power Sources 343 (2017) 536–544.
[173] C.Y. Chun, J. Baek, G.-S. Seo, B.H. Cho, J. Kim, I.K. Chang, S. Lee, Current sensorless state-of-charge estimation algorithm for lithium-ion batteries utilizing filtered terminal voltage, J. Power Sources 273 (2015) 255–263.
[174] Y. Zheng, L. Lu, X. Han, J. Li, M. Ouyang, LiFePO4 battery pack capacity estimation for electric vehicles based on charging cell voltage curve transformation, J. Power Sources 226 (2013) 33–41.
[175] M. Cacciato, G. Nobile, G. Scarcella, G. Scelba, Real-time model-based estimation of SOC and SOH for energy storage systems, Ieee T Power Electr. 32 (2017) 794–803.
[176] X. Hu, S. Li, H. Peng, A comparative study of equivalent circuit models for Li-ion batteries, J. Power Sources 198 (2012) 359–367.
[177] Y. Zheng, M. Ouyang, X. Li, L. Lu, J. Li, L. Zhou, Z. Zhang, Recording frequency optimization for massive battery data storage in battery management systems, Appl. Energ 183 (2016) 380–389.
[178] B. Xia, C. Chen, Y. Tian, W. Sun, Z. Xu, W. Zheng, A novel method for state of charge estimation of lithium-ion batteries using a nonlinear observer, J. Power Sources 270 (2014) 359–366.
[179] Y. Tian, D. Li, J. Tian, B. Xia, State of charge estimation of lithium-ion batteries using an optimal adaptive gain nonlinear observer, Electrochim Acta 225 (2017) 225–234.
[180] X. Lin, A.G. Stefanopoulou, Y. Li, R.D. Anderson, State of charge imbalance estimation for battery strings under reduced voltage sensing, Ieee T Contr Syst. T 23 (2015) 1052–1062.
[181] A. Jokar, B. Rajabloo, M. Désilets, M. Lacroix, Review of simplified Pseudo-two-Dimensional models of lithium-ion batteries, J. Power Sources 327 (2016) 44–55.
[182] K.A. Smith, C.D. Rahn, C.-Y. Wang, Control oriented 1D electrochemical model of lithium ion battery, Energ Convers. Manage 48 (2007) 2565–2578.
[183] T.-S. Dao, C.P. Vyasarayani, J. McPhee, Simplification and order reduction of lithium-ion battery model based on porous-electrode theory, J. Power Sources 198 (2012) 329–337.
[184] P. Kemper, S.E. Li, D. Kum, Simplification of pseudo two dimensional battery model using dynamic profile of lithium concentration, J. Power Sources 286 (2015) 510–525.
[185] S. Yuan, L. Jiang, C. Yin, H. Wu, X. Zhang, A transfer function type of simplified electrochemical model with modified boundary conditions and Padé approximation for Li-ion battery: Part 1. lithium concentration estimation, J. Power Sources 352 (2017) 245–257.
[186] P.P. Mishra, M. Garg, S. Mendoza, J. Liu, C.D. Rahn, H.K. Fathy, How does model reduction affect lithium-ion battery state of charge estimation Errors? Theory and experiments, J. Electrochem Soc. 164 (2017) A237–A251.
[187] A.M. Bizeray, S. Zhao, S.R. Duncan, D.A. Howey, Lithium-ion battery thermal-electrochemical model-based state estimation using orthogonal collocation and a modified extended Kalman filter, J. Power Sources 296 (2015) 400–412.
[188] S. Sepasi, R. Ghorbani, B.Y. Liaw, Inline state of health estimation of lithium-ion batteries using state of charge calculation, J. Power Sources 299 (2015) 246–254.
[189] http://www.analog.com/en/products/analog-to-digital-converters/integrated-special-purpose-converters/energy-metering-ics/ad7280a.html#product-overview [Accessed 08 January 2017].
[190] http://www.linear.com/product/LTC6804-1 [Accessed 08 January 2017].
[191] http://www.intersil.com/en/products/end-market-specific/automotive-ics/cell-balancing-and-safety/ISL78600.html [Accessed 08 January 2017].
[192] https://www.maximintegrated.com/en/products/power/battery-management/MAX14921.html [Accessed 08 January 2017].
[193] http://www.ti.com/product/bq76pl536a-q1 [Accessed 08 January 2017].
[194] W. Waag, C. Fleischer, D.U. Sauer, Adaptive on-line prediction of the available power of lithium-ion batteries, J. Power Sources 242 (2013) 548–559.
[195] T. Yue, L. Wu, X. Zhang, G. Tian, High-precision voltage measurement IP core for battery management SoC of electric vehicles, 2014 12th IEEE International Conference on Solid-state and Integrated Circuit Technology, ICSICT 2014,

October 28, 2014-October 31, 2014 Guilin, China.
[196] K.R. Hauser A, 11-High-voltage battery management systems (BMS) for electric vehicles A2-Scrosati, Bruno, in: J. Garche, W. Tillmetz (Eds.), Advances in Battery Technologies for Electric Vehicles, Woodhead Publishing, 2015, pp. 265–282.
[197] http://www.ime-actia.de/download/IR14069_Slave_6_EN.pdf [Accessed 08 January 2017].
[198] http://www.digatron.com/en/automotive-battery/universal-battery-tester/ [Accessed 08 January 2017].
[199] http://www.arbin.com/products/battery-testing/cell-testing/ [Accessed 08 January 2017].
[200] X. Li, J. Jiang, C. Zhang, L.Y. Wang, L. Zheng, Robustness of SOC estimation algorithms for EV lithium-ion batteries against modeling errors and measurement noise, Math. Probl. Eng. 2015 2015 (2015) 1–14 (2015-10-19).
[201] C. Campestrini, S. Kosch, A. Jossen, Influence of change in open circuit voltage on the state of charge estimation with an extended Kalman filter, J. Energy Storage 12 (2017) 149–156.
[202] A.E. Mejdoubi, A. Oukaour, H. Chaoui, H. Gualous, J. Sabor, Y. Slamani, State-of-Charge and state-of-health lithium-ion batteries' diagnosis according to surface temperature variation, Ieee T Ind. Electron 63 (2016) 2391–2402.
[203] G. Liu, M. Ouyang, L. Lu, J. Li, X. Han, Analysis of the heat generation of lithium-ion battery during charging and discharging considering different influencing factors, J. Therm. Anal. Calorim. 116 (2014) 1001–1010.
[204] H. Chaoui, H. Gualous, Adaptive state of charge estimation of lithium-ion batteries with parameter and thermal uncertainties, Ieee T Contr Syst. T 25 (2017) 752–759.
[205] H. Chaoui, A.E. Mejdoubi, H. Gualous, Online parameter identification of lithium-ion batteries with surface temperature variations, Ieee T Veh. Technol. 66 (2017) 2000–2009.
[206] K. Wu, J. Yang, Y. Zhang, C.Y. Wang, D.Y. Wang, Investigation on Li4Ti5O12 batteries developed for hybrid electric vehicle, J. Appl. Electrochem 42 (2012) 989–995.
[207] X.B. Han, M.G. Ouyang, L.G. Lu, J.Q. Li, Cycle life of commercial lithium-ion batteries with lithium titanium oxide anodes in electric vehicles, Energies 7 (2014) 4895–4909.
[208] N. Takami, H. Inagaki, Y. Tatebayashi, H. Saruwatari, K. Honda, S. Egusa, High-power and long-life lithium-ion batteries using lithium titanium oxide anode for automotive and stationary power applications, J. Power Sources 244 (2013) 469–475.
[209] N. Nitta, F. Wu, J.T. Lee, G. Yushin, Li-ion battery materials: present and future, Mater Today 18 (2015) 252–264.
[210] A. Farmann, W. Waag, A. Marongiu, D.U. Sauer, Critical review of on-board capacity estimation techniques for lithium-ion batteries in electric and hybrid electric vehicles, J. Power Sources 281 (2015) 114–130.
[211] H. Chaoui, N. Golbon, I. Hmouz, R. Souissi, S. Tahar, Lyapunov-based adaptive state of charge and state of health estimation for lithium-ion batteries, Ieee T Ind. Electron 62 (2015) 1610–1618.
[212] S. Tong, M.P. Klein, J.W. Park, On-line optimization of battery open circuit voltage for improved state-of-charge and state-of-health estimation, J. Power Sources 293 (2015) 416–428.
[213] G. Pérez, M. Garmendia, J.F. Reynaud, J. Crego, U. Viscarret, Enhanced closed loop State of Charge estimator for lithium-ion batteries based on Extended Kalman Filter, Appl. Energ 155 (2015) 834–845.
[214] C. Weng, J. Sun, H. Peng, A unified open-circuit-voltage model of lithium-ion batteries for state-of-charge estimation and state-of-health monitoring, J. Power Sources 258 (2014) 228–237.
[215] M. Ouyang, S. Gao, L. Lu, X. Feng, D. Ren, J. Li, Y. Zheng, P. Shen, Determination of the battery pack capacity considering the estimation error using a Capacity–Quantity diagram, Appl. Energ 177 (2016) 384–392.
[216] Z. Chen, Y. Fu, C.C. Mi, State of charge estimation of lithium-ion batteries in electric drive vehicles using extended Kalman filtering, Ieee T Veh. Technol. 62 (2013) 1020–1030.
[217] J. Gallardo-Lozano, E. Romero-Cadaval, M.I. Milanes-Montero, M.A. Guerrero-Martinez, A novel active battery equalization control with on-line unhealthy cell detection and cell change decision, J. Power Sources 299 (2015) 356–370.
[218] M.M. Hoque, M.A. Hannan, A. Mohamed, A. Ayob, Battery charge equalization controller in electric vehicle applications: a review, Renew. Sustain. Energy Rev. 75 (2017) 1363–1385.
[219] T.A. Stuart, W. Zhu, Modularized battery management for large lithium ion cells, J. Power Sources 196 (2011) 458–464.
[220] H.S. Park, C.E. Kim, C.H. Kim, G.W. Moon, J.H. Lee, A modularized charge equalizer for an HEV lithium-ion battery string, Ieee T Ind. Electron 56 (2009) 1464–1476.
[221] C.H. Kim, M.Y. Kim, H.S. Park, G.W. Moon, A modularized two-stage charge equalizer with cell selection switches for series-connected lithium-ion battery string in an HEV, Ieee T Power Electr. 27 (2012) 3764–3774.
[222] X. Cui, W. Shen, Y. Zhang, C. Hu, J. Zheng, Novel active LiFePO4 battery balancing method based on chargeable and dischargeable capacity, Comput. Chem. Eng. 97 (2017) 27–35.
[223] X. Liu, H. Wang, Y. Bian, The quantitative control strategy research for battery equalization circuits, 2016 19th International Conference on Electrical Machines and Systems (ICEMS), 2016, pp. 1–5.
[224] S. Yuan, H. Wu, X. Ma, C. Yin, Stability analysis for Li-Ion battery model parameters and state of charge estimation by measurement uncertainty consideration, Energies 8 (2015) 7729–7751.
[225] Y. Zheng, M. Ouyang, L. Lu, J. Li, Understanding aging mechanisms in lithium-ion battery packs: from cell capacity loss to pack capacity evolution, J. Power Sources 278 (2015) 287–295.
[226] A. Barré, B. Deguilhem, S. Grolleau, M. Gérard, F. Suard, D. Riu, A review on lithium-ion battery ageing mechanisms and estimations for automotive applications, J. Power Sources 241 (2013) 680–689.
[227] M. Broussely, S. Herreyre, P. Biensan, P. Kasztejna, K. Nechev, R.J. Staniewicz, Aging mechanism in Li ion cells and calendar life predictions, J. Power Sources 97 (2001) 13–21.
[228] S.E. Sloop, J.B. Kerr, K. Kinoshita, The role of Li-ion battery electrolyte reactivity in performance decline and self-discharge, J. Power Sources 119–121 (2003) 330–337.
[229] J. Vetter, P. Novák, M.R. Wagner, C. Veit, K.C. Möller, J.O. Besenhard, M. Winter, M. Wohlfahrt-Mehrens, C. Vogler, A. Hammouche, Ageing mechanisms in lithium-ion batteries, J. Power Sources 147 (2005) 269–281.
[230] R.P. Ramasamy, J.-W. Lee, B.N. Popov, Simulation of capacity loss in carbon electrode for lithium-ion cells during storage, J. Power Sources 166 (2007) 266–272.
[231] M. Kassem, J. Bernard, R. Revel, S. Pélissier, F. Duclaud, C. Delacourt, Calendar aging of a graphite/LiFePO4 cell, J. Power Sources 208 (2012) 296–305.
[232] M. Safari, C. Delacourt, Aging of a commercial graphite/LiFePO4 cell, J. Electrochem Soc. 158 (2011) A1123.
[233] C. Huang, K. Huang, S. Liu, Y. Zeng, L. Chen, Storage behavior of LiNi1/3Co1/3Mn1/3O2/artificial graphite Li-ion cells, Electrochim Acta 54 (2009) 4783–4788.
[234] R. Weiss, R. Makuch, A. Itzke, R. Weigel, Crosstalk in circular arrays of magnetic sensors for current measurement, Ieee T Ind. Electron 64 (2017) 4903–4909.
[235] N. Wang, Z.H. Zhang, Z.K. Li, Q. He, F.P. Lin, Y.F. Lu, Design and characterization of a low-cost self-oscillating fluxgate transducer for precision measurement of high-current, Ieee Sens. J. 16 (2016) 2971–2981.
[236] K.S. Ng, C.-S. Moo, Y.-P. Chen, Y.-C. Hsieh, Enhanced coulomb counting method for estimating state-of-charge and state-of-health of lithium-ion batteries, Appl. Energ 86 (2009) 1506–1511.
[237] M.-H. Chang, H.-P. Huang, S.-W. Chang, A new state of charge estimation method for LiFePO4 battery packs used in robots, Energies 6 (2013) 2007–2030.
[238] H. Wenzl, Batteries and fuel cells | Efficiency A2-Garche, Jürgen, Encyclopedia of Electrochemical Power Sources, Elsevier, Amsterdam, 2009, pp. 544–551.
[239] J. Xia, M. Nie, L. Ma, J.R. Dahn, Variation of coulombic efficiency versus upper cutoff potential of Li-ion cells tested with aggressive protocols, J. Power Sources 306 (2016) 233–240.
[240] P. Kurzweil, K. Brandt, Secondary batteries – lithium rechargeable systems | Overview A2-Garche, Jürgen, Encyclopedia of Electrochemical Power Sources, Elsevier, Amsterdam, 2009, pp. 1–26.
[241] J. Wang, B. Cao, Q. Chen, F. Wang, Combined state of charge estimator for electric vehicle battery pack, Control Eng. Pract. 15 (2007) 1569–1576.
[242] A.J. Smith, J.C. Burns, S. Trussler, J.R. Dahn, Precision measurements of the coulombic efficiency of lithium-ion batteries and of electrode materials for lithium-ion batteries, J. Electrochem Soc. 157 (2010) A196–A202.
[243] T.M. Bond, J.C. Burns, D.A. Stevens, H.M. Dahn, J.R. Dahn, Improving precision and accuracy in coulombic efficiency measurements of Li-Ion batteries, J. Electrochem Soc. 160 (2013) A521–A527.
[244] S. Torai, M. Nakagomi, S. Yoshitake, S. Yamaguchi, N. Oyama, State-of-health estimation of LiFePO 4/graphite batteries based on a model using differential capacity, J. Power Sources 306 (2016) 62–69.
[245] C. Weng, X. Feng, J. Sun, H. Peng, State-of-health monitoring of lithium-ion battery modules and packs via incremental capacity peak tracking, Appl. Energ 180 (2016) 360–368.
[246] C. Hu, G. Jain, P. Tamirisa, T. Gorka, Method for estimating capacity and predicting remaining useful life of lithium-ion battery, Appl. Energ 126 (2014) 182–189.
[247] C. Hu, G. Jain, C. Schmidt, C. Strief, M. Sullivan, Online estimation of lithium-ion battery capacity using sparse Bayesian learning, J. Power Sources 289 (2015) 105–113.
[248] J.L. Torres, R. Gonzalez, A. Gimenez, J. Lopez, Energy management strategy for plug-in hybrid electric vehicles. A comparative study, Appl. Energ 113 (2014) 816–824.
[249] S. Beninati, L. Damen, M. Mastragostino, Fast sol–gel synthesis of LiFePO4/C for high power lithium-ion batteries for hybrid electric vehicle application, J. Power Sources 194 (2009) 1094–1098.
[250] G. Li, J. Zhang, H. He, Battery SOC constraint comparison for predictive energy management of plug-in hybrid electric bus, Appl. Energ 194 (2017) 578–587.
[251] G.L. Plett, Extended Kalman filtering for battery management systems of LiPB-based HEV battery packs, J. Power Sources 134 (2004) 262–276.
[252] G.L. Plett, Sigma-point Kalman filtering for battery management systems of LiPB-based HEV battery packs, J. Power Sources 161 (2006) 1356–1368.
[253] F. Sun, R. Xiong, H. He, A systematic state-of-charge estimation framework for multi-cell battery pack in electric vehicles using bias correction technique, Appl. Energ 162 (2016) 1399–1409.
[254] F. Sun, R. Xiong, A novel dual-scale cell state-of-charge estimation approach for series-connected battery pack used in electric vehicles, J. Power Sources 274 (2015) 582–594.
[255] G. Dong, J. Wei, Z. Chen, Kalman filter for onboard state of charge estimation and peak power capability analysis of lithium-ion batteries, J. Power Sources 328 (2016) 615–626.
[256] Q. Wang, J. Wang, P. Zhao, J. Kang, F. Yan, C. Du, Correlation between the model accuracy and model-based SOC estimation, Electrochim Acta 228 (2017) 146–159.
[257] H. Aung, K.S. Low, Temperature dependent state-of-charge estimation of lithium ion battery using dual spherical unscented Kalman filter, IET Power Electron. 8 (2015) 2026–2033.

[258] B. Fridholm, T. Wik, M. Nilsson, Robust recursive impedance estimation for automotive lithium-ion batteries, J. Power Sources 304 (2016) 33–41.
[259] C. Zhang, K. Li, J. Deng, Real-time estimation of battery internal temperature based on a simplified thermoelectric model, J. Power Sources 302 (2016) 146–154.
[260] F. Sun, X. Hu, Y. Zou, S. Li, Adaptive unscented Kalman filtering for state of charge estimation of a lithium-ion battery for electric vehicles, Energy 36 (2011) 3531–3540.
[261] B. Xia, H. Wang, Y. Tian, M. Wang, W. Sun, Z. Xu, State of charge estimation of lithium-ion batteries using an adaptive cubature Kalman filter, Energies 8 (2015) 5916–5936.
[262] Y. He, X. Liu, C. Zhang, Z. Chen, A new model for State-of-Charge (SOC) estimation for high-power Li-ion batteries, Appl. Energ 101 (2013) 808–814.
[263] H. He, R. Xiong, X. Zhang, F. Sun, J. Fan, State-of-Charge estimation of the lithium-ion battery using an adaptive extended Kalman filter based on an improved thevenin model, Ieee T Veh. Technol. 60 (2011) 1461–1469.
[264] D.B.W. Abeywardana, B. Hredzak, V.G. Agelidis, Single-phase grid-connected LiFePO4 battery - supercapacitor hybrid energy storage system with interleaved boost inverter, Ieee T Power Electr. 30 (2015) 5591–5604.
[265] S. Yuan, H. Wu, C. Yin, State of charge estimation using the extended Kalman filter for battery management systems based on the ARX battery model, Energies 6 (2013) 444–470.
[266] C. Campestrini, M.F. Horsche, I. Zilberman, T. Heil, T. Zimmermann, A. Jossen, Validation and benchmark methods for battery management system functionalities: state of charge estimation algorithms, J. Energy Storage 7 (2016) 38–51.
[267] S. Mendoza, J. Liu, P. Mishra, H. Fathy, On the relative contributions of bias and noise to lithium-ion battery state of charge estimation errors, J. Energy Storage 11 (2017) 86–92.
[268] M. Corno, N. Bhatt, S.M. Savaresi, M. Verhaegen, Electrochemical model-based state of charge estimation for Li-Ion cells, Ieee T Contr Syst. T 23 (2015) 117–127.
[269] Y. Hu, S. Yurkovich, Y. Guezennec, B.J. Yurkovich, Electro-thermal battery model identification for automotive applications, J. Power Sources 196 (2011) 449–457.
[270] B. Xia, X. Zhao, R. de Callafon, H. Garnier, T. Nguyen, C. Mi, Accurate Lithium-ion battery parameter estimation with continuous-time system identification methods, Appl. Energ 179 (2016) 426–436.
[271] S. Yuan, L. Jiang, C. Yin, H. Wu, X. Zhang, A transfer function type of simplified electrochemical model with modified boundary conditions and Padé approximation for Li-ion battery: Part 2. Modeling and parameter estimation, J. Power Sources 352 (2017) 258–271.
[272] Y. Wang, C. Zhang, Z. Chen, On-line battery state-of-charge estimation based on an integrated estimator, Appl. Energ 185 (2017) 2026–2032.
[273] V. Klass, M. Behm, G. Lindbergh, A support vector machine-based state-of-health estimation method for lithium-ion batteries under electric vehicle operation, J. Power Sources 270 (2014) 262–272.
[274] S.F. Schuster, M.J. Brand, P. Berg, M. Gleissenberger, A. Jossen, Lithium-ion cell-to-cell variation during battery electric vehicle operation.pdf, J. Power Sources 297 (2015) 242–251.
[275] Z. Yu, R. Huai, L. Xiao, State-of-Charge estimation for lithium-ion batteries using a Kalman filter based on local linearization, Energies 8 (2015) 7854–7873.
[276] Z. Wei, J. Zhao, D. Ji, K.J. Tseng, A multi-timescale estimator for battery state of charge and capacity dual estimation based on an online identified model, A multi-timescale estimator for battery state of charge and capacity dual estimation based on an online identified model. Applied Energy. 10.1016/j.apenergy.2017.02.016.
[277] H. Aung, K.S. Low, S.T. Goh, State-of-Charge estimation of lithium-ion battery using square root spherical unscented Kalman filter (Sqrt-UKFST) in nanosatellite, Ieee T Power Electr. 30 (2015) 4774–4783.
[278] G. Liu, M. Ouyang, L. Lu, J. Li, J. Hua, A highly accurate predictive-adaptive method for lithium-ion battery remaining discharge energy prediction in electric vehicle applications, Appl. Energ 149 (2015) 297–314.
[279] B. Xia, C. Chen, Y. Tian, M. Wang, W. Sun, Z. Xu, State of charge estimation of lithium-ion batteries based on an improved parameter identification method, Energy 90 (2015) 1426–1434.
[280] G. Liu, M. Ouyang, L. Lu, J. Li, X. Han, Online estimation of lithium-ion battery remaining discharge capacity through differential voltage analysis, J. Power Sources 274 (2015) 971–989.
[281] R. Xiong, F. Sun, X. Gong, H. He, Adaptive state of charge estimator for lithium-ion cells series battery pack in electric vehicles, J. Power Sources 242 (2013) 699–713.
[282] Z. Zou, J. Xu, C. Mi, B. Cao, Z. Chen, Evaluation of model based state of charge estimation methods for lithium-ion batteries, Energies 7 (2014) 5065–5082.
[283] B. Xia, H. Wang, M. Wang, W. Sun, Z. Xu, Y. Lai, A new method for state of charge estimation of lithium-ion battery based on strong tracking cubature Kalman filter, Energies 8 (2015) 13458–13472.
[284] M.L. Terranova, S. Orlanducci, E. Tamburri, V. Guglielmotti, M. Rossi, Si/C hybrid nanostructures for Li-ion anodes: an overview, J. Power Sources 246 (2014) 167–177.
[285] L.-b. Chen, X.-h. Xie, K. Wang, J.-y. Xie, Study on preparation and property of carbon-coated silicon/carbon composite, Chin. J. Power Sources 31 (2007) 34–37.
[286] Z.S. Wen, X.H. Xie, K. Wang, J. Yang, J.Y. Xie, High capacity SiAl/C anode material for lithium-ion batteries, J. Inorg. Mater 20 (2005) 139–143.
[287] http://www.lem.com/hq/en/component/option[287],com_catalog/task,displayserie/serie,IN%20Series/output_type,/ [Accessed 08 January 2017].
[288] K. Propp, D.J. Auger, A. Fotouhi, S. Longo, V. Knap, Kalman-variant estimators for state of charge in lithium-sulfur batteries, J. Power Sources 343 (2017) 254–267.
[289] V.S. Kolosnitsyn, E.V. Karaseva, Lithium-sulfur batteries: problems and solutions, Russ. J. Electrochem+ 44 (2008) 506–509.
[290] S.H. Chung, P. Han, A. Manthiram, Quantitative analysis of electrochemical and electrode stability with low self-discharge lithium-sulfur batteries, Acs Appl. Mater Inter 9 (2017) 20318–20323.
[291] W.T. Xu, H.J. Peng, J.Q. Huang, C.Z. Zhao, X.B. Cheng, Q. Zhang, Towards stable lithium-sulfur batteries with a low self-discharge rate: ion diffusion modulation and anode protection, Chemsuschem 8 (2015) 2892–2901.
[292] J.Q. Huang, T.Z. Zhuang, Q. Zhang, H.J. Peng, C.M. Chen, F. Wei, Permselective graphene oxide membrane for highly stable and anti-self-discharge lithium-sulfur batteries, Acs Nano 9 (2015) 3002–3011.
[293] X. Hu, F. Sun, Y. Zou, Comparison between two model-based algorithms for Li-ion battery SOC estimation in electric vehicles, Simul. Model Pract. Th 34 (2013) 1–11.
[294] H. Fang, X. Zhao, Y. Wang, Z. Sahinoglu, T. Wada, S. Hara, R.A. de Callafon, Improved adaptive state-of-charge estimation for batteries using a multi-model approach, J. Power Sources 254 (2014) 258–267.
[295] Y. Wang, C. Zhang, Z. Chen, A method for state-of-charge estimation of Li-ion batteries based on multi-model switching strategy, Appl. Energ 137 (2015) 427–434.
[296] S. Chen, C.C. Chen, Intelligent power management of electric vehicle with Li-Ion battery, in: C.K. Wang, J. Guo (Eds.), Mechatronics and Applied Mechanics Ii, Pts 1 and 2, Trans Tech Publications Ltd, Durnten-Zurich, 20131558-+.
[297] T. Tanizawa, T. Suzumiya, K. Ikeda, Cloud-connected Battery Management System Supporting e-Mobility, Fujitsu Sci. Tech. J. 51 (2015) 27–35.